NTNU
Norwegian University of
Science and Technology

Modelling and Optimization of a Process from Biomass to Liquid Fuels via Fischer-Tropsch Synthesis

Helene Florence Amndine Bour

Master's Thesis
Submission date: June 2016
Supervisor: Magne Hillestad, IKP

Norwegian University of Science and Technology
Department of Chemical Engineering

Abstract

The global energy demand is expected to increase by almost 50% by 2040. Simultaneously, fossil energy reserves are threatened to disappear. Thus it is imperative to development renewable technologies such as Biomass-To-Liquid process. This work investigates the performances of a Biomass-To-Liquid process involving a Fischer-Tropsch synthesis and the performances of a hybrid hydrogen-carbon process including hydrogen supply for a biomass feedstock of 20 000 tonnes per day. The processes have been simulated using the software Aspen Hysys and Aspen Properties. The impact of several parameters such as the water and oxygen content in the gasifier as well as the influence of the recycle rate on the Biomass-To-Liquid-Fischer-Tropsch process has been explored. The syngas production reaches a maximum for an oxygen supply into the gasifier of 42.4 tonnes per hour. It has been found that the addition of steam into the gasifier is not beneficial when having a fixed gasifier temperature and that recycling 90% of the tail gas into the Fischer-Tropsch gives the best performances. An optimal configuration of the BTL process which maximizes the carbon and energy efficiencies has been determined. It gives an energy efficiency of 56.55% and a carbon efficiency of 40.23% with a production of 4 257 barrel per day. Results are improved when using the hybrid hydrogen-carbon process and when the gasifier inlets are pre-heated. The highest performances have been found when the feedstock is pre-heated at 100°C and the oxygen supply at 1600°C. It gives an energy efficiency of 63.09% and a carbon efficiency of 79.4%. Greenhouse emissions have been divided by 12 and the production of hydrocarbons has doubled when using the hybrid process. The simulation for the hybrid process requires an important amount of hydrogen which compensates the economic benefit generated by the production rise. An increase in the pre-heating of the gasifier inlet must enhance this aspect.

Preface

This master thesis has been written as part of the subject “TKP4900 Environmental Engineering and Reactor Technology” at the Department of Chemical Engineering at NTNU for the final master degree during spring 2016. The thesis has been supervised by Professor Magne Hillestad.

I declare that this is an independent work according to the exam regulations of the Norwegian University of Science and Technology (NTNU).

Bour Hélène

Trondheim, 07/06/2016

Acknowledges

I would like to thank my thesis advisor Professor Magne Hillestad of the Department of Chemical Engineering at The Norwegian University of Science and Technology (NTNU) for his patience and his pedagogic supervision.

I would also like to thank the PhD student Mohammad Ostadi and my fellow student Tor Olav Høva Erevik. I am gratefully indebted for their precious advices and explanations, as well as for their pleasant conversations. I would also like to acknowledge the PhD student Koteswara Rao Putta for his interest in my thesis and for his advices.

I would like to show my gratitude to the postdoctoral researcher William Thomas Sanders who tirelessly offers me coffee, support and good humour.

I thank the university canteen for cooking good vegetarian dished which warmed my heart when I needed it.

Finally, I thank my family for providing me with unfailing support throughout my years of study. This accomplishment would not have been possible without them.

Table of content

List of Tables

List of figures

Nomenclature

α	growth factor (-)
Λ	Annualization factor
ΔHr	Enthalpy of reaction (KJ/mol)
ΔH°298	Standard enthalpy of formation at 298°K (KJ/Kmol)
ΔH_{vap}	Enthalpy of vaporization
ΔTmin	Global minimum approach temperature (°C)
ΔP	Difference of pressure (bar)
ΔT	Difference of temperature (°C)
λ	O2 stoichiometric ratio (-)
$\lambda_{optimal}$	Optimal O2 stoichiometric ratio (-)
ρ	density (lb/ft3)
τ	residence time (s, min)
μ	oil viscosity (cP)
A	Area (m^2)
Aw	Area occupied by water (m^2)
API	American Petroleum Institute gravity (°)
C	Total purchased cost (USD)
CC	Installed capital cost (USD)
C_{cu}	utility cost for cold utility ($/KW.yr)
C_{hu}	utility cost for hot utility ($/KW.yr)
CD	drag coefficient (-)
Ce	purchased equipment cost (USD)
C_{eff}	Carbon efficiency (mol%)
C_{ISBL}	Inside battery cost (USD)
C_{loss}	Carbon loss (mol%)
C_{FC}	Total fixed capital (USD)
C_1	Inside battery cost for the plant of capacity S1
C_2	Inside battery cost for the plant of capacity S2
d	Inside vessel diameter (in)
dm	Diameter of liquid droplet (μm)
Di	Internal diameter (m)
E	welded-joint efficiency (-)
E_{eff}	Energy efficiency (mol%)
$E_{eff\ mod}$	Modified energy efficiency (mol%)
F	Molar flow (Kmole/h)
fx	Installation factor (-)

$\mathbf{f_{ISBL}}$	ISBL factor
H	Height (m)
Ki	Equilibrium constant (-)
$\mathbf{L_{eff}}$	Vessel effective length (ft)
Lss	Seam-to-seam length (ft)
M	Mass flow (tonnes/h)
P	Pressure (bar)
Pi	Internal design pressure (Kpa)
Q	Volumetric flow (m3/h)
$\mathbf{Q_{hu,min}}$	energy target of the hot utility (KW)
$\mathbf{Q_{cu,min}}$	energy target of the cold utility (KW)
$\mathbf{q_{in}}$	Gas velocity (m/s)
$\mathbf{r_{FT}}$	Paraffin reaction rate (mol/g-cat.h)
r1	Paraffin reaction rate (mol/g-cat.h)
r2	Olefin reaction rate (mol/g-cat.h)
S	maximal allowable stress (KPa)
SR	Slenderness Ratio (-)
T	Temperature (°C)
t	Vessel thickness (m)
ut	Settling velocity of liquid droplet (m/s)
V	Volume (m3)
X	Contingency (-)
$\mathbf{X_{CO}}$	CO conversion in the Fischer-Tropsch reactor
Z	gas compressibility (-)

Acronyms

ACCR	Annual capital charge ratio
ASF	Anderson-Schulz-Flory
ACM	Aspen custom modeler
Aspen EA	Aspen Energy Analyser
BTL-FT	Biomass-To-Liquid-Fischer-Tropsch
CRV	Conversion reactor vessel
CSTR	Continuous stirred-tank reactor
CEPCI	Chemical Engineering Plant Cost Index
D&E	Design and Engineering costs
ERV	Equilibrium reactor vessel
FT	Fischer-Tropsch
GBR	Gibbs reactor
HHV	High heating value
HI	Heat integration
HTWGS	High temperature Water-gas-shift
HX	Heat exchanger
ISBL	Inside battery limit
LHV	Low heating value
LTWGS	Low temperature Water-gas-shift
MP	Medium pressure
NREL	National Renewable Energy Laboratory
OS	Offsite investment
OC	Operating costs
PL	Plant life
SG	Specific gravity
ROR	Rate on return
TAC	Total annual cost
WGS	Water gas shift

1. Introduction

1.1. Project objective

Biomass-to-Liquid process via Fischer-Tropsch (BTL-FT) synthesis is a recent and promising solution for biofuel production. Several former studies investigate the performance of a BTL-FT process for various configurations with or without unconverted syngas recycle. Some researchers have studied hybrid process involving a second feedstock such as natural gas or coal (1), (2), (3). In any case, the process displays a potential for reducing net carbon emission, but it is not economically viable in the current context of oil prices. The main focus of this report is to find a method to maximize the crude oil production from biomass while minimizing the greenhouse emissions.

1.2. Background

The global energy demand is expected to increase by almost 50% by 2040. The 2015 OPEC world Oil Outlook estimates fossil fuels as main source of energy with covering 78% of the energy needs (4). However, fossil fuels, which include oil, natural gas and coal, are finite resources which threaten to exhaust in a near future. Thus, it is crucial to develop technologies based on renewable feedstocks. A renewable production method of fuel for transportation is investigated in this document: The Biomass-to-liquid (BtL) process using Fischer-Tropsch synthesis. Liquid hydrocarbons are mainly used in the transportation sector ahead of electricity and hydrogen because of their high volumetric energy density and of their convenience (5). It is then interesting to find renewable technologies to produce them. The biomass is a non-depleting resource which offers the advantage of being easily accessible and low cost. Moreover, the BTL-FT process is more environmentally friendly than traditional technology since biomass contains much less sulfur and other contaminant compounds (6) and emits less CO_2 than crude oil during its treatment (7). The BTL process has become especially attractive after the Copenhagen Accord (8) which established new emission reduction targets. However, such process exists only at a pilot scale. The gasification remains a challenge since stable gasifier performances depend on a homogeneous feedstock. Another important limitation is the needed quantity of biomass. It requires a large production of biomass per year, high transportation costs and high storage costs. But the main limitation is the high breakeven manufacturing cost which is around 120$/bbl (1), (2).

1.3. Overview of the process

The objective of a Biomass-to-Liquids process is to produce synthetic fuels from biomass. The process is composed of a pre-treatment stage for making a suitable feed to the gasifier which produced the syngas. For kinetic reasons, a $\frac{H2}{CO}$ ratio slightly below two must be set at the Fischer Tropsch (FT) inlet by a water-gas-shift. The gas is then purified to remove impurities which poison the FT catalyst. Finally, the FT unit produces the hydrocarbons by polymerization. The following conceptual flow-sheet summarizes the procedure:

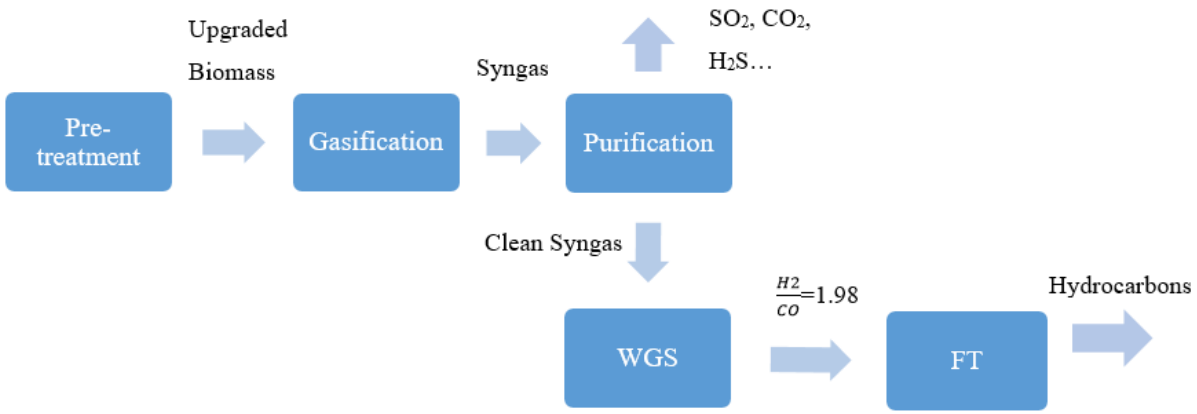

Figure 1 : The Biomass-to-Liquids process

The source material is the below flowsheet:

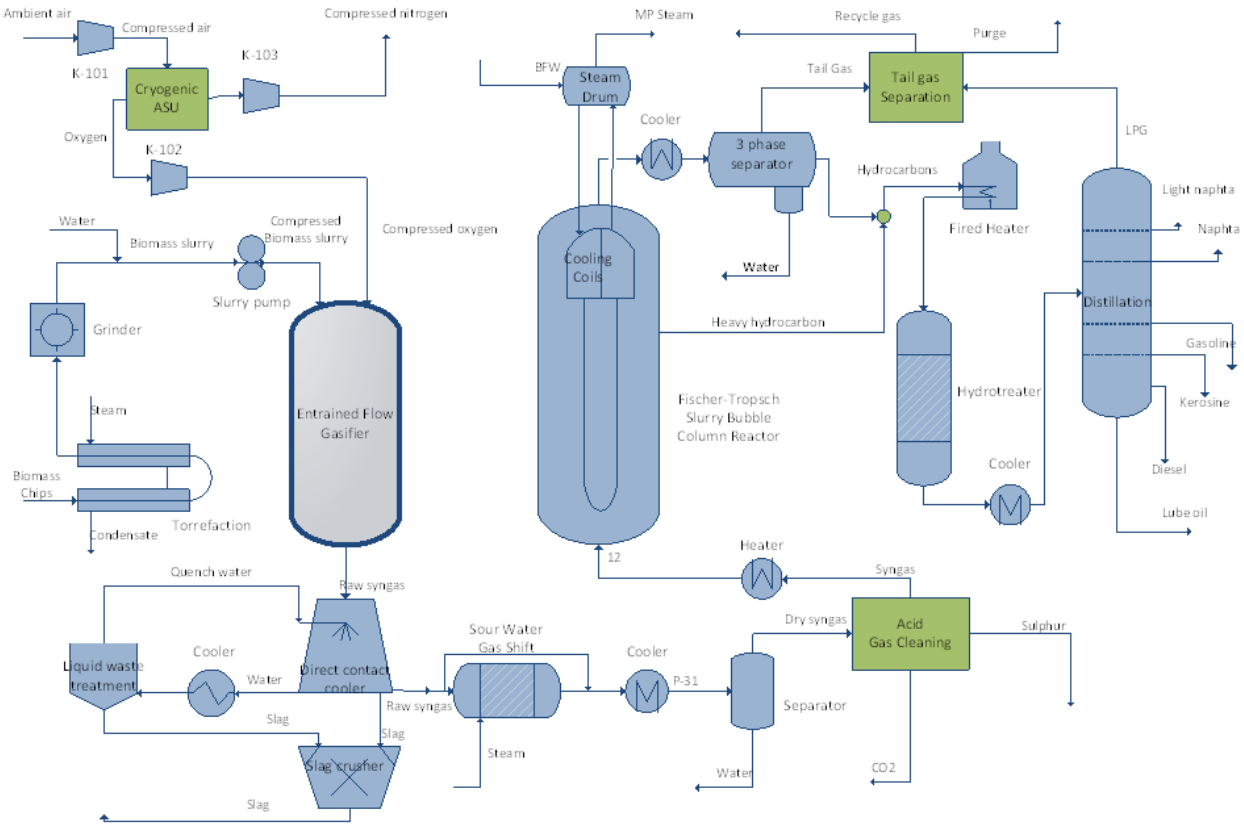

Figure 2 : Original flowsheet provided by the advisor

The process has been centered on the gasification and the polymerization of hydrocarbons. Thus, the hydrotreatment and the distillation are not considered. A recycling loop has been added and technologies have been selected for reactors and separation units from literature data. The resulting flowsheet is presented Figure 17. The simulation of the BtL process was done using Aspen Hysys and Aspen Properties. In both case, the thermodynamic package “Peng Robinson” is used. The elements before the ACM model, which includes the gasifier, the water-shift reactor, the separator and the scrubber, are modeled by Hysys. The ACM model uses the data base of Aspen properties. A stream cutter ensures the connection. In Chapter 2, the type of biomass for the feedstock is chosen and described. Chapter 3 investigates the gasification performances under several operating conditions. Syngas treatment and the kinetic model used for the polymerization are described in Chapter 4. The two following sections presents and discuss the simulation

results: Chapter 5 deals with the results for the standard BTL-FT process and Chapter 6 with results when using a hybrid hydrogen-carbon process. Heat integration and economical evaluation were performed for the traditional BTL-FT process and for the hybrid configuration, and are presented in Chapter 7 and Chapter 8. Chapter 9 is dedicated to the conclusion. The last Chapter contains the advices for further work.

2. Feedstocks

2.1. Biomass

Several biomass sources can be used such as wood, plant from energy crops, agricultural and forest residues as well as food waste. The choice for the biomass is discussed in this section. Controlling the available quantity of biomass is an important aspect if once wants biofuel to make an important contribution to the oil market. In this way, energy crops are appealing. However, they present the drawback to compete with crops dedicating to food production, which leads to an ethical problem. Using food waste seems to be an interesting sustainable solution, since it enables the people to satisfy the energy needs while getting rid of their waste. Unfortunately, food waste are not homogeneous feedstocks and contain a high percentage of moisture and impurities like soluble heavy metal (9). Agricultural and forestry residues are a potential choice. Both have an important role in soil fertility but they are not entirely used and a large part remain available. For instance, $3\ 10^{12}$ t/y of agricultural residues are unused and 15 tons of non-valuated forest residues are generated for each 100 tons of roundwood produced (10). The heating value of the biomass is an important quality parameter for biomass. The excel sheet called "Heat content ranges for various biomass fuels" presents the heating value for different biomass (confer appendix A). On average, forest residues have the greatest calorific value. Hence, forest residues are finally chosen as biomass in this report. As other woody biomass, it contains less amount of sulfur as well as heavy metals than fossil fuels and it is cheaper. Forestry residues are biogenic waste which come from thinning and logging. They consist of small trees, branches and un-marketable wood. The ultimate analysis given by the NREL report (11) (Table 1) is used in this study. Ashes are metals present in the biomass. For simplicity, we assume a dry feedstock with no ash content. The ash percentage involved in the NREL report is replaced by a carbon percentage in this study since no ash are assumed (51.8 wt% is considered instead of 50.88%). The influence of this modification on the heating value is neglected.

Component	C	H	N	S	O
Wt% dry basis	51.8	6.04	0.17	0.09	41.9
Heating value (Btu/lb):	8 671 HHV	8 060 LHV			

Table 1: Ultimate analysis of hybrid popular feed (wt%, dry basis)

The chemical formula is determined thanks to the ultimate analysis. In 100g of biomass, 51.8g of carbon are found. Divided by the carbon molar weight (12.01 g/mol), it gives a result of 4.32 carbon

moles contained in 100g of biomass. The same is applied to other atoms which leads to the following chemical formula: $C_{4.31}H_{6.04}O_{2.62}N_{0.012}S_{0.003}$.

2.2. Feedstock pretreatment

Size reduction and drying are needed before gasification and the specifications depend on the type of the gasifier. For an entrained-flow gasifier, the typical range of the particles is 0.1 to 1 mm which is very consuming. Besides, pretreatment reduces the cost of the transportation in the case where the torrefaction process is chosen to be operated next to a forest and not on the BtL plant. Pyrolysis and torrefaction are two options. Pyrolysis has the advantages to be a well-known technology widely used at a large scale and shows good performances. Although its immaturity, torrefaction has interesting benefits. It is a mild pyrolysis which operates only between 200 and 300°C and attests the same efficiency than the pyrolysis. Furthermore, torrefaction prevents from agglomeration which can occur during high pressure feeding. Torrefied biomass is then assumed in the current study which justify the use of a dry biomass as feedstock since very low moisture content can be reached (12).

3. Syngas Production

3.1. Gasifier and modelling

Several kind of gasifier have been developed. The advantages and disadvantages for the various technologies are summarized in the table below (13), (14):

Advantages	Disadvantages
Fixed/moving bed, updraft	
Simple, inexpensive process	Large tar production
Operates satisfactorily under pressure	Potential channelling
High carbon conversion efficiency	Potential bridging
High thermal efficiency	Small feed size
Low dust levels in gas	Potential clinkering
Fixed/moving bed, downdraft	
Simple process	Minimum feed size
Only traces of tar in product gas	Limited ash content allowable in feed
Good compactness	Low operating pressure
	Potential for bridging and clinkering
Fluidized-bed	
Flexible feed rate and composition	
High ash fuels acceptable	Operating temperature limited by ash clinkering
Able to pressurize	High tar and fines content in gas
High volumetric capacity	Possibility of high C content in fly ash
Easy temperature control	
Circulating fluidized-bed	
Up to 850 °C operating temperature	Corrosion and attrition problems
Flexible process	Poor operational control using biomass
Entrained bed	
Flexible to feedstock	Extreme feedstock size reduction required
Exit gas temperature	Complex operational control
Very low in tar and CO_2	Carbon loss with ash
	Ash slagging

Table 2 : Table of advantages and disadvantages of different types of gasifiers

The entrained flow gasification has been chosen among the available technologies as it presents good performances and reliability (15) and enables one to produce a clean syngas at high pressure. It has the advantages to operate at high temperature which means little methane and tar production

(14). Higher is the pressure in the gasifier, smaller is the volume equipment but higher is the wall thickness. Both volume and thickness have an influence on the price. Gasification at 20 bars can often be read in literature (2) and has then be chosen. Besides, it enables the process to reach a high pressure in the FT without using a compressor. The equilibrium is assumed for the gasification. The O_2 stoichiometric ratio is adjusted to reach the desired temperature. The gasification is modeled in two part in Aspen Hysys. The biomass is first entirely decomposed in a conversion reactor by pyrolysis. Then, oxygen, water and the decomposed biomass react in a Gibbs reactor. In practice, only one adiabatic device would be used, that is why the duty of the second reactor is set as the opposite of the conversion reactor duty (-5.5 10^5 KJ/Kmole). Modeling the gasifier with two reactors is acceptable since the pyrolysis takes place before the oxidation in a entrained-flow gasifier (16). However, it is considered that 100% of the biomass is decomposed in the conversion reactor which is a non-realistic assumption. Indeed, some char and soot remain after gasification (17).

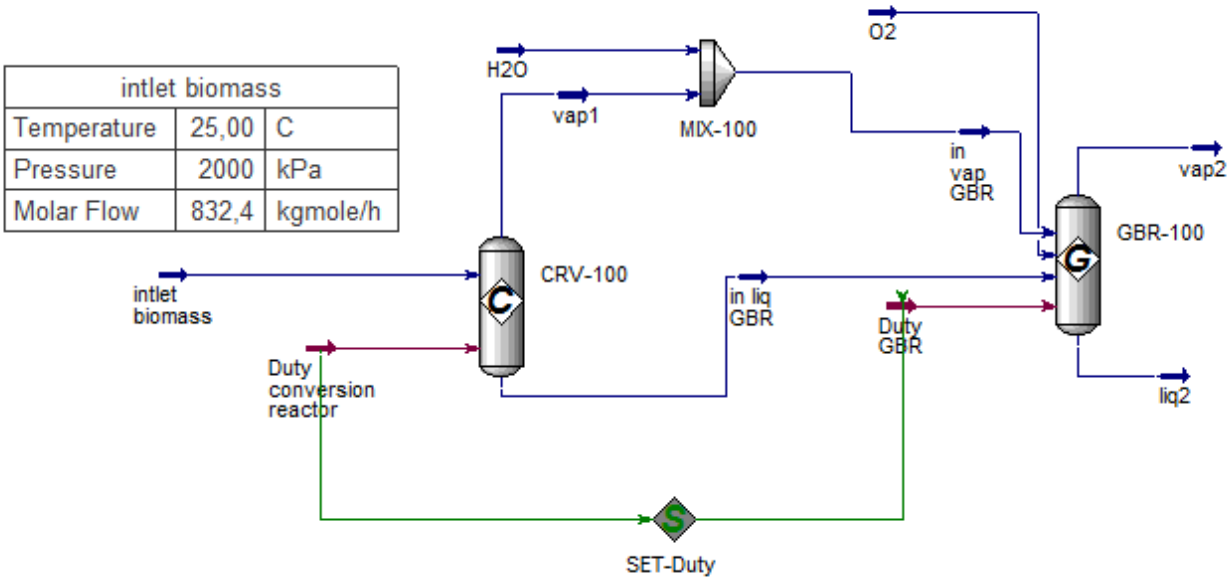

Figure 3 : Modelling of the entrained-flow gasifier with Aspen Hysys

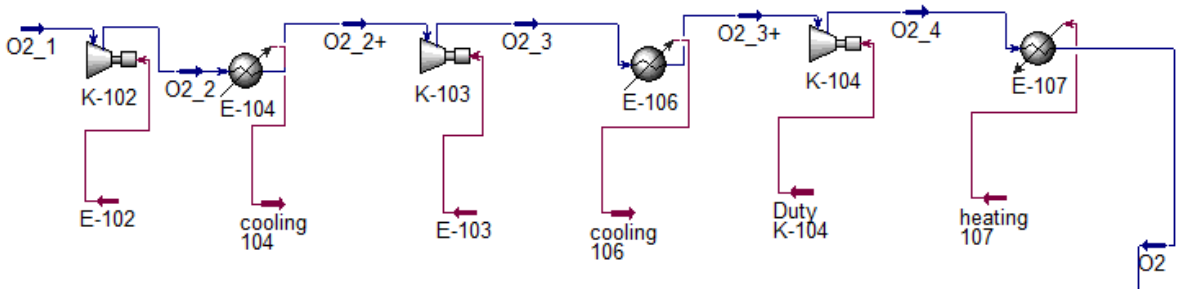

Figure 4 : Isothermal compression of the oxygen

The steam is inputted at 800°C and the pure oxygen at 600°C. Both streams are at 20 bar. Isothermal compressing requires less working energy than a simple compressing. Then, 3 compressors with a pressure ratio of 2.7 are used and 2 coolers ensures the refrigeration of the gas. A heater brings the compressed oxygen to 600°C. Some assumptions are made; the procedure operates under steady state conditions, chemical equilibrium is established during the gasification, the device is adiabatic (no heat loss) and the formation of tars is neglected.

3.2. Chemical reactions

The biomass particles quickly undergo pyrolysis in the gasifier:

$C_{4.31}H_{6.04}O_{2.62}N_{0.012}S_{0.003} = 4.31C(s) + 3.02H_2 + 0.006N_2 + 0.003S + 1.31O_2$	$\Delta H°_{298} = +5.510^5$ KJ/Kmol	R1

The resulting compounds subsequently react in the gasifier by the followings (17):

$H_2 + ½\ O_2 = H_2O$	ΔHr = -242 KJ/mol	R2
$CO + ½\ O_2 = CO_2$	ΔHr = -283 KJ/mol	R3
$CH_4 + ½\ O_2 = CO + 2H_2$	ΔHr = -36 KJ/mol	R4
$CH_4 + 2O_2 = CO_2 + 2H_2O$	ΔHr = -803 KJ/mol	R5
$CO + H_2O = CO_2 + H_2$	ΔHr = -41 KJ/mol	R6
$CH_4 + H_2O = CO + 3H_2$	ΔHr = +206 KJ/mol	R7
$C(s) + CO_2 = 2CO$	ΔHr = +172 KJ/mol	R8
$C(s) + H_2O = H_2 + CO$	ΔHr = +131 KJ/mol	R9
$C(s) + 2H_2 = CH_4$	ΔHr = -75 KJ/mol	R10
$C(s) + O_2 = CO_2$	ΔHr = -394 KJ/mol	R11
$C(s) + ½\ O_2 = CO$	ΔHr = -111 KJ/mol	R12

The gasification is simulated with a conversion (CRV) and a Gibbs reactor (GBR). The latter minimizes the Gibbs free energy in the GBR. The above list presents the main reactions involved

in the gasification but the list is non-exhaustive. The water gas shift reaction R6 has a fast reaction rate unlike R7, the steam-methane reforming, which has a slow kinetic. Those two reactions are assumed to determine the bulk gas composition (17). Char, represented by solid carbon particles C(s), are fully consumed during the gasification. The reaction R12 is known to have a faster reaction rate than R8, R10 and R11 (18). Methane formation is not wanted since it contains carbon atoms which are automatically not used to form CO and since it is a too light hydrocarbons to be in the final products.

3.3. Influence of the reactor temperature on the syngas production

The temperature was varied from 1064 to 1415°C keeping a constant pressure (P = 20bar), constant O_2 inlet flowrate (λ=0.6) and constant H_20 inlet flowrate (S/C=0.2). To do this, the "SET-duty" (see Figure 3) has been ignored and the "Duty-GBR" has been manually set. The results are presented in Figure 5. "Stream (1)" stands for the gasifier outlet stream. The sum of the CO and H_2 molar flowrate is called "syngas" as they are the compounds of interest.

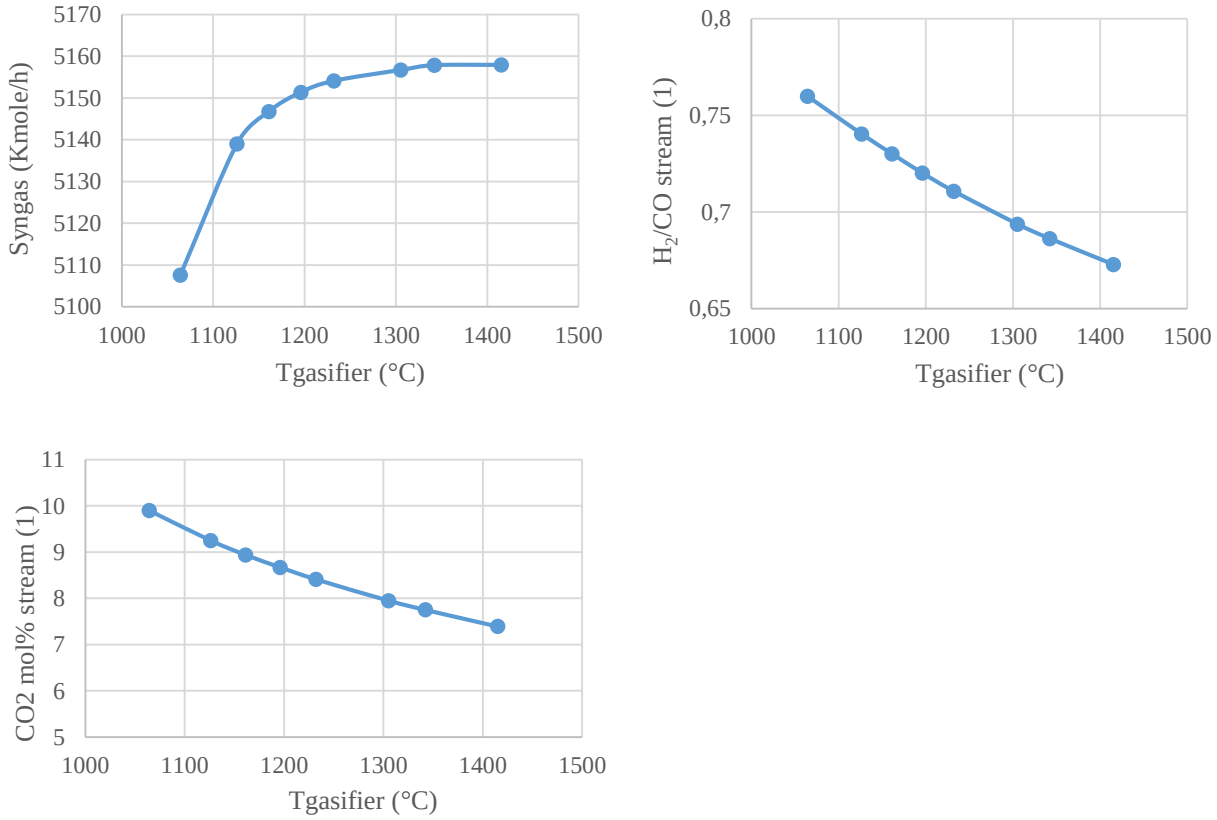

Figure 5 : Simulation results as function of the gasifier temperature for λ=0.6 and S/C=0.2

The yield of syngas increases with the reactor temperature and reaches a stability zone above 1300°C. This effect is predictable from the thermodynamic. Indeed, high temperature favors endothermic reactions (R7, R8 and R9) which produce the syngas (CO and H_2) according to the "Le Châtelier's principle". Above a certain temperature, the equilibrium constants $K_i(T)$ changes very little and then, the syngas yield does as well. At higher temperature, the H_2/CO ratio becomes somewhat lower, but a high temperature variation is needed to bring a small change to the ratio. The inert concentration is broadly constant (Table 3). A 3 mol% change in CO_2 is noticed while the temperature increases by around 400°C.

T (°C)	CH4 mol%	duty (KJ/h)
1064	0,19	-5,89E+08
1126	0,07	-5,70E+08
1161	0,04	-5,60E+08
1196	0,03	-5,50E+08
1232	0,02	-5,40E+08
1305	0,01	-5,20E+08
1342	0	-5,10E+08
1415	0	-4,90E+08

Table 3 : Table of the simulation results for different temperatures in the gasifier at lambda = 0,6 and at S/C = 0,2

NB: (1) stands for the outlet gasifier stream

Hence, high temperature improves the quantity and the quality of syngas by reducing the CO_2 generation. In the further study, an auto-thermal and adiabatic gasifier is assumed, and the temperature is modified by changing the amount of oxygen.

3.4. Influence of H_2O on the syngas production

The ratio stream-to-carbon (S/C) defines an important parameter for the gasification.

$$S/C = \frac{\text{Molar flow of the steam inlet in the gasifier } (\frac{\text{Kgmole}}{\text{h}})}{\text{Molar flow of the inlet carbon in the gasifier } (\frac{\text{Kgmole}}{\text{h}})} \quad (1)$$

Its impact has been investigated by varying it between 0.01 to 2 and keeping a constant lambda (λ=0.6) and a constant pressure.

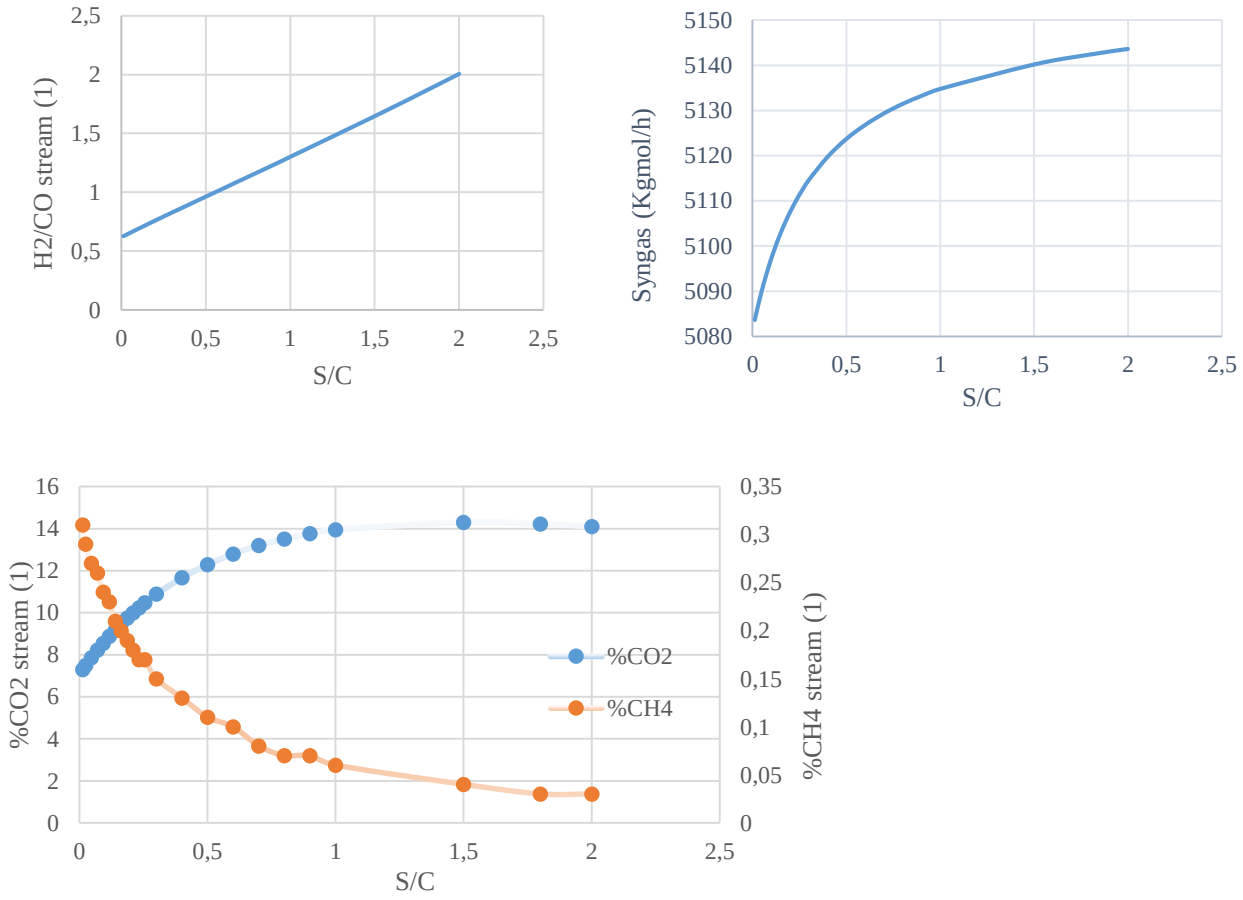

Figure 6 : Simulation results as function of the Steam-to-Carbon ratio at lambda=0.6

The main impact of the water steam inlet is to enrich the syngas with hydrogen which leads to an improved H_2/CO ratio (confer Figure 6). This result comes from that the water-gas-shift reaction, R6. It is enhanced by the high concentration of water. which is one of the two equations governing the syngas composition (17).

Simultaneously, the same reaction conducts to the reduction of the CO content (Table 4) and increase the CO_2 formation, which is not favorable in this case. Conversely, the methane is consumed by the reforming reaction R7. Above S/C=1, the change in the gas composition is less important. Similarly, the rise of the syngas production slows down. This is attributed to the thermodynamic. The addition of steam enhances the reactions R6, R7 and R9 but it also decreases the temperature (Table 4). Indeed, the steam is introduced at moderate temperature (800°C) and then takes heat to the system to warm it up. In this way, the endothermic reactions R7, R8 and R9 are disfavored which slows down the syngas production.

S/C	H20 (kg/h)	Syngas (kmol/h)	CO (Kmol/h)	%CH_4	%CO_2	H_2/CO (1)	T (°C)
0,01	7,49E+02	5,08E+03	3,12E+03	0,31	7,29	0,63	1073
0,05	3,00E+03	5,09E+03	3,08E+03	0,27	7,86	0,65	1071
0,12	7,49E+03	5,10E+03	3,00E+03	0,23	8,87	0,70	1068
0,16	1,05E+04	5,10E+03	2,94E+03	0,2	9,46	0,73	1066
0,23	1,50E+04	5,11E+03	2,87E+03	0,17	10,24	0,78	1063
0,40	2,58E+04	5,12E+03	2,70E+03	0,13	11,66	0,90	1056
0,50	3,23E+04	5,12E+03	2,61E+03	0,11	12,29	0,96	1051
0,70	4,52E+04	5,13E+03	2,45E+03	0,08	13,2	1,10	1043
0,80	5,17E+04	5,13E+03	2,37E+03	0,07	13,51	1,17	1039
0,90	5,81E+04	5,13E+03	2,30E+03	0,07	13,76	1,23	1035
1,00	6,46E+04	5,13E+03	2,23E+03	0,06	13,95	1,30	1030
1,50	9,69E+04	5,14E+03	1,94E+03	0,04	14,3	1,65	1011
1,80	1,16E+05	5,14E+03	1,80E+03	0,03	14,22	1,86	1001
2,00	1,29E+05	5,14E+03	1,71E+03	0,03	14,1	2,01	994,6

Table 4 : Table of the simulation results for different steam-to-carbon ratio in the gasifier at lambda = 0,6

According to the simulation results, a high value of the S/C ratio rise the syngas production and improves the H_2/CO ratio. Besides, the formation of unwanted methane is limited by the attendance of steam. However, the steam converts CO in CO_2, thus generating carbon loss.

3.5. Influence of the oxygen content on the syngas production

The quantity of oxygen inside the gasifier is quantified by the O_2 stoichiometric ratio λ :

$$\lambda = \frac{\text{Actual O2 inlet in the gasifier } (\frac{kg}{h})}{\text{O2 inlet for stoichiometric combustion in the gasifier } (\frac{kg}{h})}$$

The stoichiometric quantity of oxygen has been determined with Aspen Hysys by increasing progressively the oxygen inlet in the gasifier for a ratio S/C=0. Stoichiometric combustion is reached right before the gasifier outlet contains oxygen. The result is an inlet mass flow of 6.23 10^4 Kg/h. A lambda below 1 is here desired since the interest is to have an incomplete combustion to produce CO. The oxygen inlet is at 20 bar and 600°C. The impact of oxygen on the gasifier temperature, the syngas flowrate and on the outlet gas composition have been investigated with 2 different water flow inlet.

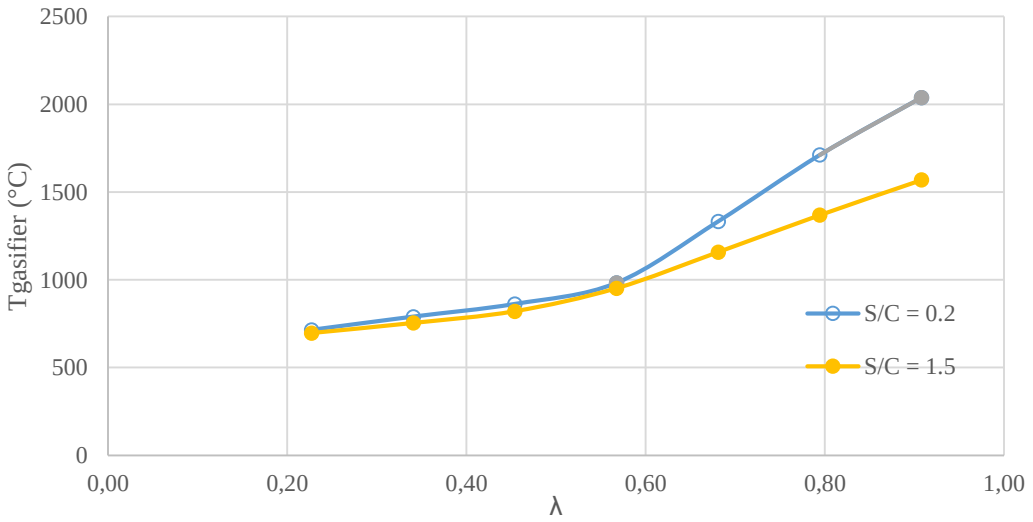

Figure 7 : Temperature profile in the entrained flow gasifier versus λ for a steam-to-carbon ratio (S/C) of 0.2 and of 0.5

For the two steam-to-carbon ratio, a breakpoint is noticeable on the curve of the temperature versus λ. The temperature increases faster for a lambda above around 0.57. Indeed, below the breakpoint, an increase in lambda of 0.1 leads to a temperature increase between 55 and 65 °C while the rise is between 182 and 313°C beyond the breaking point. The increase in temperature lies in the fact that the oxygen takes part in the exothermic equation R2, R3, R4, R5, R11 and R12 which release heat in the adiabatic system. The linear relation between the gasifier temperature and λ suggests that one chemical equation is mainly responsible for the heat released. The change in the slope before and after the breaking point indicates that the global equilibrium changes in the gasifier. An explanation for this phenomena is here proposed: The oxygen first reacts with the compound which attracts it the most. After the breaking point, the oxygen amount in the gasifier is high enough to enable oxygen to take part in the others reaction. Thus, several reactions release heat after the breaking point (λ=0.57) and not just one anymore, which leads to a higher slope.

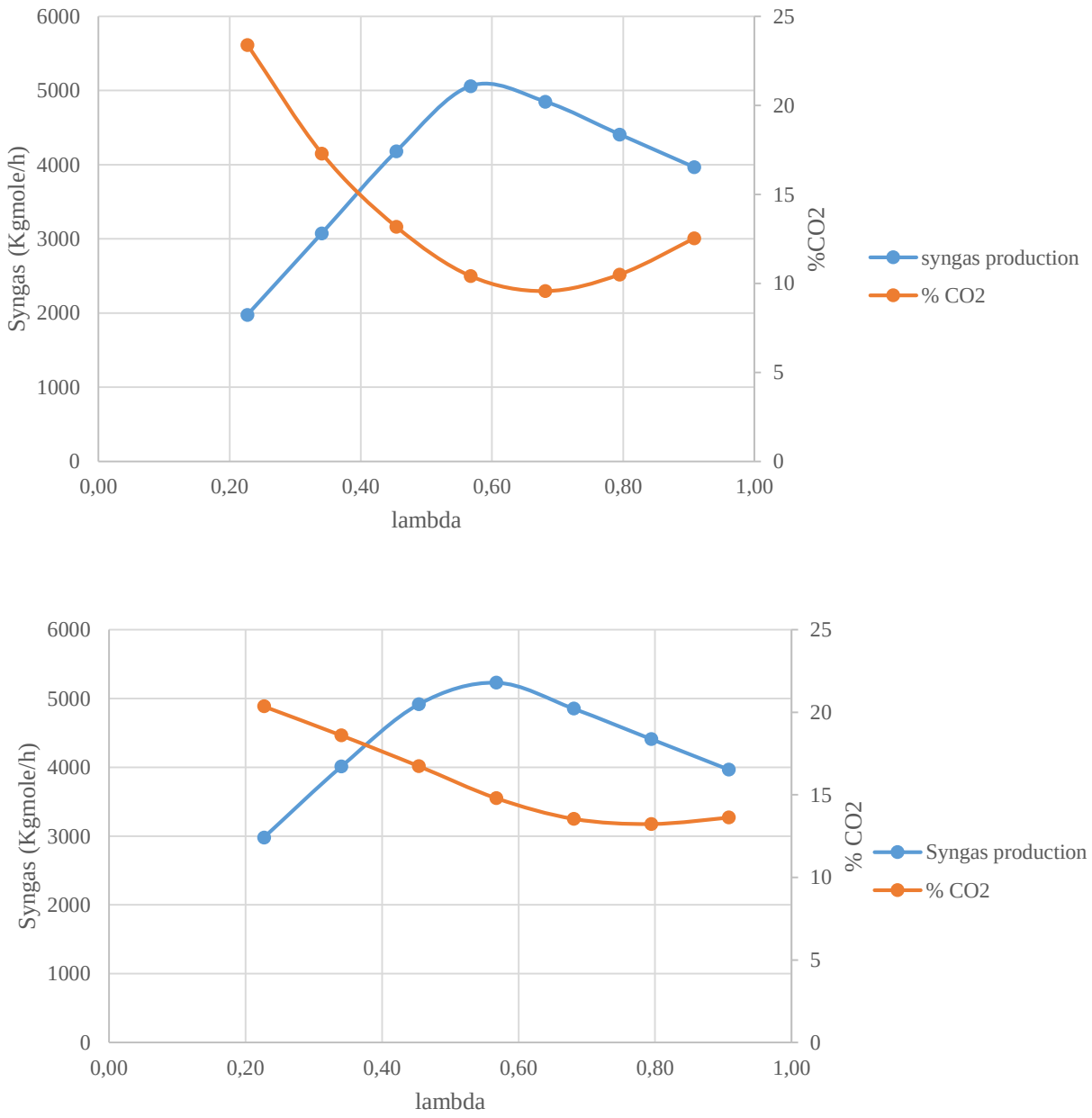

Figure 8 : Molar flowrate of the syngas and concentration in percentage of the carbon dioxide in function of lambda for S/C=0.2 (on the top) and of S/C=1.5 (below)

The syngas production flowrate reaches an optimum for a lambda around 0.57 for the two different S/C values. Weiland et al (17) have also noted an optimal λ which maximize the syngas production. The study uses an entrained flow gasifier at 2-7 barA with pure oxygen. A maximal CO production is observed at λ= 0.425. The difference between the λ found in the literature and the λ in the current study can have several reasons: the difference of pressure, of water content or

of inert content. Simultaneously, the CO_2 formation is considered. A minimal production of carbon dioxide is desired since it means less carbon loss for the process. For S/C=0.2, the minimum is reached at λ=0.689 and at λ=0.796 for S/C=1.5. The trend line equation can be found in Table 5 and Table 6. As explain above, oxygen makes the temperature increase and high temperature improves the syngas yield (confer 3.3). However, it means that CO and H_2 are oxidized which is translated into a drop of the syngas (CO and H_2) amount. The optimum corresponds to the operating point where the incidence of the temperature and the incidence of the oxygen concentration on the syngas formation are equally important.

λ	O_2 (Kg/h)	T gasifier (°C)	Syngas (kmol/h)	% CO_2	% CH_4	H2/CO (1)
0,23	1,41E+04	714,2	1,98E+03	23,40	25,79	0,44
0,34	2,12E+04	789,6	3,08E+03	17,30	14,70	0,62
0,45	2,83E+04	861,7	4,18E+03	13,18	6,42	0,74
0,57	3,54E+04	981,8	5061,71	10,41	0,85	0,79
0,68	4,24E+04	1332	4851,363	9,57	0,00	0,65
0,79	4,95E+04	1711	4408,52	10,50	0,00	0,54
0,91	5,66E+04	2038	3967,954	12,53	0,00	0,45

Trend line (Syngas)	$y = 110597x^4 - 251240x^3 + 184107x^2 - 44130x + 5158,3$	$R^2 = 0,9965$
Trend line (CO_2 mol%)	$y = 64,486x^2 - 88,859x + 40,178$	$R^2 = 0,9994$

Table 5 : Table of the simulation results for different lambda values in the gasifier at S/C = 0,2

λ	O_2 (Kg/h)	T gasifier (°C)	Syngas (kmol/h)	% CO_2	% CH_4	H_2/CO (1)
0,23	1,41E+04	696,2	2,98E+03	20,35	9,42	3,194
0,34	2,12E+04	753,7	4,01E+03	18,59	5,21	2,606
0,45	2,83E+04	820,7	4,92E+03	16,73	1,84	2,214
0,57	3,54E+04	951,9	5,23E+03	14,79	0,13	1,784
0,68	4,24E+04	1158	4,85E+03	13,54	0	1,386
0,79	4,95E+04	1369	4,41E+03	13,23	0	1,132
0,91	5,66E+04	1569	3,97E+03	13,62	0	0,959

Trend line (Syngas)	$y = 69572x^4 - 145435x^3 + 90254x^2 - 12751x + 2728,4$	$R^2 = 0,9962$
Trend line (CO2 mol%)	$y = 34,592x^3 - 40,507x^2 - 1,2931x + 22,345$	$R^2 = 0,9991$

Table 6 : Table of the simulation results for different λ values in the gasifier at S/C = 1,5

NB: (1) stands for the outlet gasifier stream

CH_4 is an unwanted by product. Its production decreases the energy efficiency of fuel since it is a hydrocarbon too light to be in the fuel. Furthermore, the methane does not react much in the process and then, it accumulates if once set a recycling loop. The simulation results give a significant concentration of methane at a lambda below 0.5 which corresponds to a temperature below 950 °C. Thus, a temperature above 1000°C seems to improve the syngas quality by reducing the methane concentration. An optimal lambda ($\lambda_{optimal} = 0.57$) which maximizes the syngas production has been determined and seems to remain constant for different water inlet. This value is found again below in the study. O_2 has a linear relationship with the gasifier temperature which enables one to control the vessel temperature by setting the oxygen inlet.

3.6. Influence of the pressure on the syngas production

The incidence of the pressure has been investigated in the interval from 15 bar to 80 bar for λ=0.6 and S/C=0.23. It is interesting to study the pressure impact as high pressure allows to reduce the size, and thus, the price of the reactor. The amount of syngas formed, the H_2/CO ratio and the CO_2 concentration remain roughly constant. The pressure has only an interesting impact on the methane concentration. The increase of methane is slight (around 0.15% every 10 bar). The rise of the CH_4 content is derived from the steam-methane equilibrium reaction R7. Increasing the pressure leads to shift the reaction towards the formation of methane and water. Weiland and al (17) have come to the same observation.

P (bar)	%CH_4	%CO_2	T	CO (Kmol/h)	H_2/CO (1)	Syngas (Kmol/h)
15	0,12	9,8	1060	2,91E+03	0,76	5,13E+03
20	0,19	9,82	1064	2,90E+03	0,76	5,10E+03
25	0,27	9,84	1069	2,90E+03	0,75	5,09E+03
30	0,35	9,87	1074	2,90E+03	0,75	5,06E+03
35	0,44	9,89	1078	2,89E+03	0,74	5,04E+03
40	0,52	9,91	1083	2,89E+03	0,74	5,02E+03
50	0,68	9,95	1092	2,87E+03	0,73	4,98E+03
60	0,83	10	1100	2,86E+03	0,72	4,94E+03
70	0,97	10,04	1108	2,85E+03	0,72	4,90E+03
80	1,1	10,08	1115	2,84E+03	0,71	4,87E+03

Table 7 : Table of the simulation results for different pressure in the gasifier at lambda = 0,6 and S/C = 0,23

3.7. Concurrent variation of the steam-to-carbon ratio and lambda

The simultaneous variation of the two parameters S/C and λ has been studied. The aim is to obtain a constant temperature of 1300°C for different S/C ratio by changing the oxygen inlet i.e. λ.

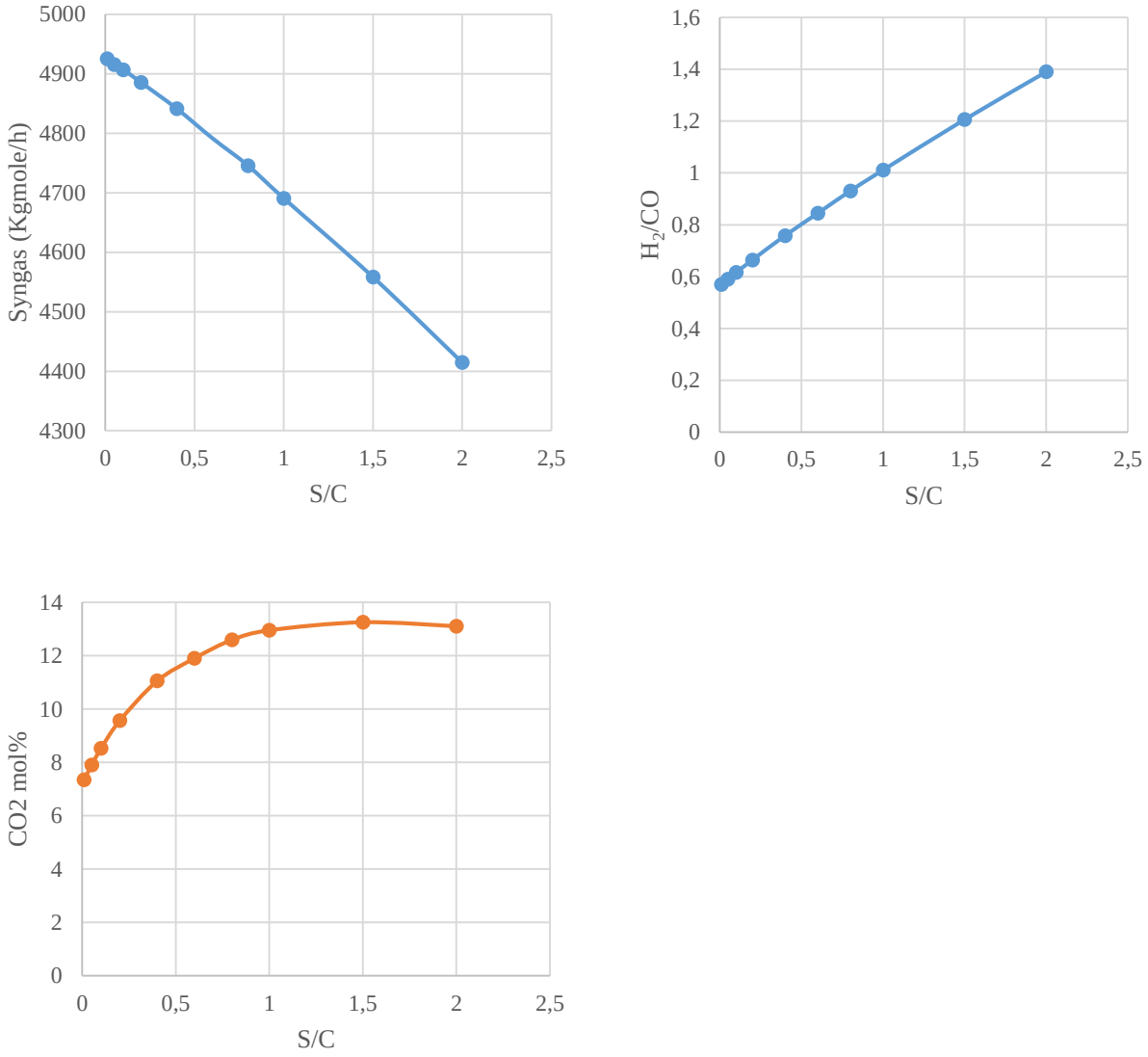

Figure 9 : Simulation results versus the steam-to-carbon ratio for a gasifier temperature of 1300°C

When more steam is introduced; more oxygen is needed to keep a high temperature which leads to higher λ than the optimal λ previously found. It results to a decrease of the syngas amount. Thus, the oxygen seems to have a higher impact on the syngas production than the S/C ratio. This was

predictable. Indeed, when going from S/C = 0.2 to S/C= 0.4 (+0.2), λ increases by +0.1. According to the previous results, an increase by 0.1 for λ makes drop the syngas by around 440 Kmol/h (above the optimum). On the other hand, an increase by +0.2 for S/C at constant λ makes only rise the syngas production by 10 Kmol/h. Oxygen influences then more the syngas production than water. However, the steam still governs the evolution of the H_2/CO ratio and of the CO_2 concentration as they evolve in the same way than shown in 3.4.

S/C	H_20 (kg/h)	O_2 (kg/h)	λ	Syngas (kmole/h)	CH_4 mol%	CO_2 mol%	H_2/CO (1)
0,01	6,46E+02	4,12E+04	0,66	4,93E+03	0,01	7,34	0,57
0,05	3,23E+03	4,14E+04	0,66	4,92E+03	0,01	7,9	0,59
0,1	6,46E+03	4,15E+04	0,67	4,91E+03	0,01	8,52	0,62
0,2	1,29E+04	4,19E+04	0,67	4,89E+03	0	9,56	0,66
0,4	2,58E+04	4,27E+04	0,68	4,84E+03	0	11,05	0,76
0,6	3,87E+04	4,34E+04	0,70	4,79E+03	0	11,9	0,84
0,8	5,17E+04	4,41E+04	0,71	4,75E+03	0	12,59	0,93
1	6,46E+04	4,50E+04	0,72	4,69E+03	0	12,95	1,01
1,5	9,69E+04	4,71E+04	0,76	4,56E+03	0	13,25	1,21
2	1,29E+05	4,94E+04	0,79	4,41E+03	0	13,1	1,39

Table 8 : Table of the simulation results for different S/C values in the gasifier at T = 1300° C

To conclude, adding steam in the gasifier would be beneficial if the gasifier temperature was not fixed at 1300°C, since water improves the syngas production and the H_2/CO ratio as seen in 3.4. However, to avoid tar formation, high temperature for the gasifier is needed. Then, to maximize the syngas production, no additional water in the gasifier is suggested.

4. Production of hydrocarbons

4.1. Treatment of the syngas

4.1.1. Water-gas-shift reactor

The Fischer-Tropsch synthesis is carried out in the presence of a catalyst which implies a cleanup of the input to avoid the catalyst poisoning. Furthermore in our case, the FT reactor is the most effective when the inlet has a ratio $\frac{H2}{CO}$ slightly below 2 (14). A ratio of 1.98 has been chosen for the study. After gasification, the first stage is to adjust the ratio $\frac{H2}{CO}$ using a Water-Gas-Shift (WGS) reactor:

$$CO + H_2O = CO_2 + H_2 \qquad \Delta Hr = -41\ KJ/mol \qquad (2)$$

An equilibrium reactor is used for modelling the WGS reactor and the amount of provided steam is set to obtain a ratio $\frac{H2}{CO}$ = 1.98 at the Fischer-Tropsch inlet using an "Adjust" tool in Aspen Hysys. High or low-temperature WGS can be used. The reaction is thermodynamically fostered by low temperature as shown on the below figure (19):

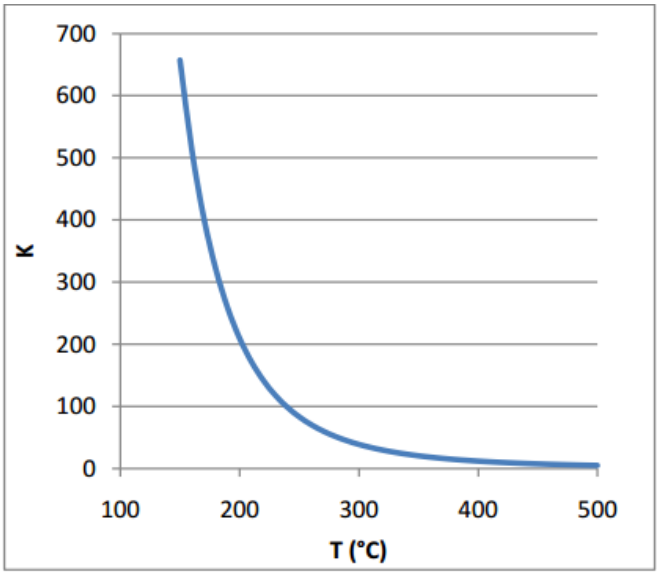

Figure 10: Effect on the temperature on the equilibrium constant of the WGS reaction

The catalysts for low-temperature WGS (LTWGS) are based on Cu-ZnO/Al_2O_3 and the operating temperature is in the range 190-250°C. The conversion is then higher when using a LTWGS but a high-temperature WGS kinetically favors the water gas shift reaction, which means a greater reaction rate. As the aim of the WGS reactor in the process is not to convert all the CO which is a valuable compound, HTWGS is chosen which makes increase the kinetic. High-temperature WGS typically use catalysts based on Fe_2O_3-Cr_2O_3 and operate at temperature between 300°C and 450°C. The WGS reactor in the simulation operates at 400°C. The sulfur resistance is assumed for the catalyst.

4.1.2. Discussion about the influence of water supply on the system "Gasifier and Water-Gas-Shirt reactor"

The WGS reactor enables one to set the hydrogen-carbon monoxide ration but also consumes CO and produces CO_2. More hydrogen is produced in the gasifier when adding water according to the equations R6, R7 and R9 which suggests that adding water in the gasifier could reduce the carbon loss which occurring in the WGS reactor. Indeed, if the H_2/CO is improved at the gasifier outlet, less CO has to be consume in the WGS reactor to adjust the H_2/CO ratio. The impact of the water inlet in the gasifier has been investigated for a constant lambda ($\lambda = 0.601$). It is recalled that a constant lambda does not mean a constant temperature in the gasifier and that "stream (1) is the outlet of the gasifier.

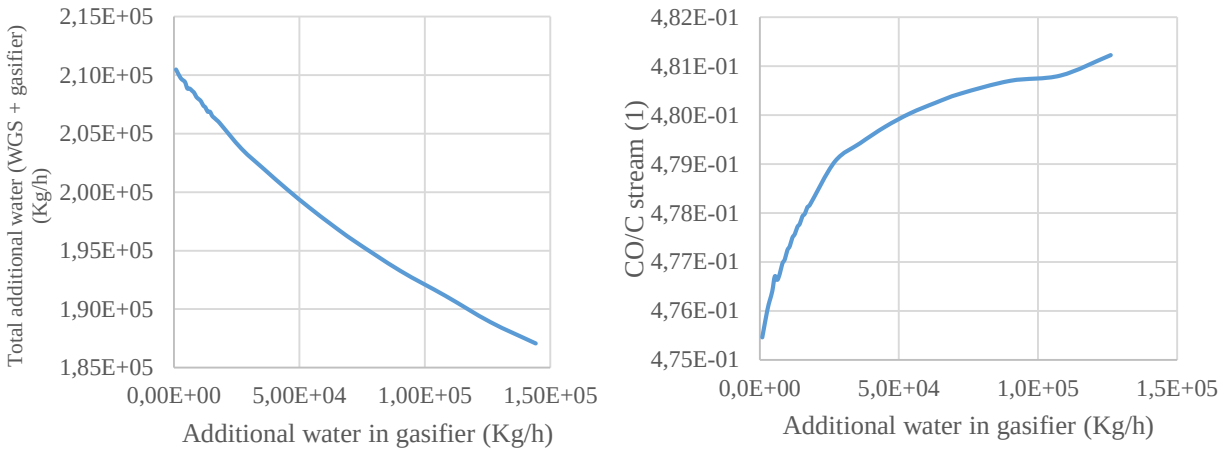

Figure 11 : Simulation results at λ=0.601 for different water inlet in the gasifier

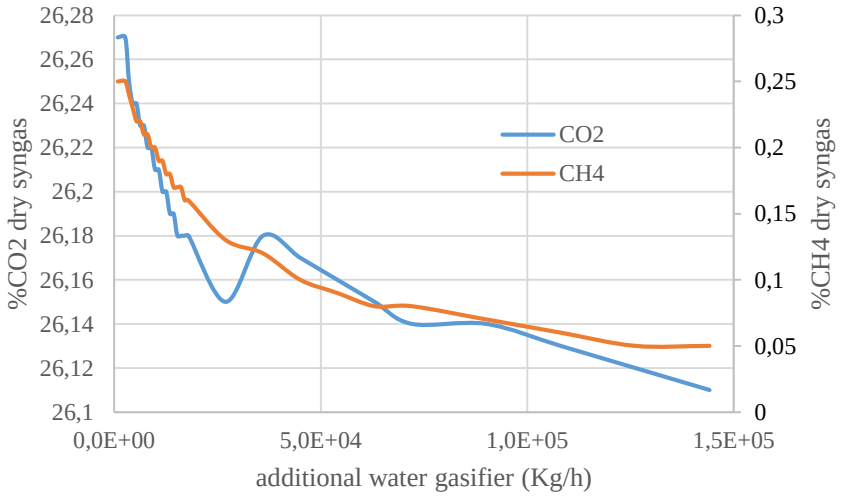

Figure 12 : Inerts concentration in dry syngas at λ=0.601 for different water inlet in the gasifier

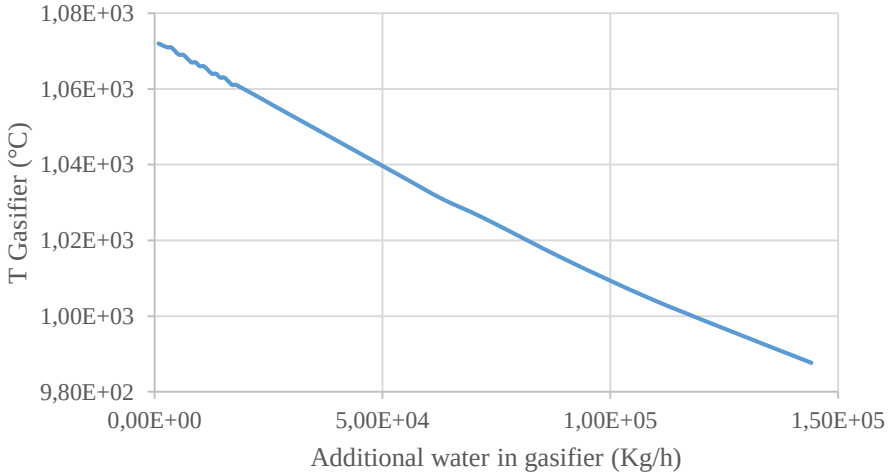

Figure 13 : Temperature of the gasifier at λ=0.601 for different water inlet in the gasifier

The discontinuities on the plots are due to the fact that each experimental points are connected and the experience has been realized with a point spacing really small for small values of additional water (see appendix B). It can be fixed by using a trend line. The increase in water at the gasifier inlet does decrease the needed amount of steam in the WGS reactor as expected. Multiplying the steam inlet in the gasifier by 160 (from 50 Kmole/h to 800 Kmole/h) permits to spare 11% of the total needed water ($1.17x10^4$ Kmole/h needed steam for an inlet of 50 Kmole/h and $1.04x10^4$ Kmole/h for an inlet of 800 Kmole/h). Less steam in the WGS reactor leads to less conversion of CO and then to less carbon loss. The carbon loss generates by the gasifier and the WGS reactor are calculated using the following equation. The molar flows are taken at the outlet of the WGS reactor (stream (2)).

$$\%\text{Carbon loss at the WGS reactor outlet} = \frac{\text{Fcarbon in CO2} + \text{Fcarbon in CH4}}{\text{Fcarbon in Biomass}} \quad (3)$$

Fcarbon in "compound": Molar flow of carbon contained in the compound (Kmole/h)

It is noticed that the carbon loss has not been improved even though less CO is consumed when increasing the water inlet in the gasifier (see appendix B). It is due to the fact that the CO consummation does not change enough to influence the carbon loss. For the same reason, the CO_2 percentage in the dry syngas remains quite constant. Indeed, a decrease of only 0.18 points is noticed when the water inlet in the gasifier is multiplied by 160. The gasifier temperature drops when water is added, which leads to the production of tars. This comes from the fact that the water is introduced at 800°C and thus, the water captures a part of the heat released by the exothermic reaction. To maintain the temperature of the gasifier, extra oxygen should be added, which moves one from the optimal λ.

In sum, increasing the water inlet in the gasifier does not improve the performance (amount of CO and CO_2 almost constant) but permit to spare water. However, it makes the gasifier temperature drop. The optimal water inlet in the gasifier is discussed later in the study.

4.1.3. Acid gas cleaning

The FT reactor uses a catalyzer (cobalt) which poisoning is likely to occur. A clean up system is then used to remove the sulfur compounds and water. Indeed, sulfur compounds and water deactivate the catalyst by blocking the cobalt surface sites (14) (p15). CO_2 is removed as well since it does not react in the FT reactor and then, just make increase the FT volume. A dryer and a scrubber are set after the WGS reactor. A separator simulates the dryer and a component splitter is used for the scrubber. 1 mol% of water is tolerated in the dry syngas. The performances of the amine scrubber used in the simulation are summarized in the below table, assuming the use of ethanolamine (MEA) (20) (p837), the NO_2 removal is fixed at 0.7. The CO_2 and H_2S are assumed at 0.9 and 1 for the purpose of the simulation.

Component	Removal in mol% of each component	Component	Removal in mol% of each component
CO_2	0.9	Dry biomass*	1
H_2O	1	CO	0
H_2S	1	H_2	0
SO2	1	NO	0
C	1	NO_2	0.25
S-rhombic	1	COS	1
NH_3	1	Hydrocarbons	1
HCN	1		

Table 9 : Separation performances of the amine scrubber

Finally, a heat exchanger warms up the syngas at the FT operating temperature (220°C) (see Figure 17).

4.2. Kinetic

The Fischer-Tropsch synthesis converts synthesis gas to liquid hydrocarbons using a set of polymerization reactions in the presence of a catalyst. It was introduced by Han Fischer and Franz Tropsch in 1923. The FT kinetic over a cobalt catalyst have been studied by Magne Hillestad (21) and results are here used. Hydrogenation of CO takes place to produce n-paraffins, 1-olefins and some oxygenates. The production of oxygenates are here neglected since they are produced in a small amount and the water gas shift reaction is not considered here since we use a cobalt catalyst which are known not to be shift active.

Then, we consider the two following equations (21):

$$nCO + (2n+1)H_2 \rightarrow C_nH_{2n+2} + nH_2O \quad n = 1,2,\ldots,\infty \qquad (4)$$

$$nCO + 2nH_2 \rightarrow C_nH_{2n} + nH_2O \quad n = 2,3,\ldots,\infty \qquad (5)$$

The kinetic results of Ma et al (22) given for a FT synthesis under 220°C using a continuously stirred tank reactor (CSTR) over a 25%Co/Al_2O_3 catalyst are here used. The empirical CAER kinetic model have been employed. After determination of the parameter values, the resultant model is:

$$r_{FT} = \frac{kP_{CO}^{a}P_{H_2}^{b}}{1 + mP_{H_2O}/P_{H_2}}. \qquad (6)$$

r_{FT} : Paraffin reaction rate in mol/g-cat.h (cf reaction $nCO + (2n+1)H2 \rightarrow CnH2n+2 + nH2O \quad n = 1,2,\ldots,\infty$ *(4), $r_{FT} = r_1$)*

k = 0.0133

a= -0.31

b= 0.88

m= -0.24

Olefin reaction rate is assumed to be 8% of the paraffin reaction rate : $r_2 = 0.08r_1$.
In the aspen ACM model, the paraffin reaction rate r_1 is multiplied by a coefficient called

"Paraffin_rate_adjuster" (value=0.6) to take into account the catalyst loading as well as the catalyst deactivation.

Generally, the products from Fischer-Tropsch synthesis follow the Anderson-Schulz-Flory (ASF) distribution. This states that the ratio of two consecutive reactions is given by the growth factor α which can be used to determine the product distribution. The Anderson-Schulz-Flory distribution is here applied, therefore no chain limitation and a constant growth factor α are assumed even though α can change from one reaction to another due to differences in temperature and concentration. The chain growth probability is defined by the below equation:

$$\alpha=\frac{rp}{rp+rt} \quad (7)$$

rp : reaction rate for propagation

rt: reaction rate for termination

α can be expressed in function of partial pressure:

$$\alpha = \frac{1}{1 + K_1 \frac{P_{H2}^{1.45}}{P_{CO} P_{H2O}^{0.228}}} \quad (8)$$

The instantaneous molar fraction is given as the probability to produce a molecule with *i* carbon atoms.

$$x_i = (1-\alpha)\alpha^{i-1} \quad (9)$$

The expression of the instantaneous weight fraction is:

$$w_i = i(1-\alpha)^2\alpha^{i-1} \quad (10)$$

From experiences, once observe a high selectivity of methane. Indeed, the plot of log(xi) in function of i (the number of carbon) gives a slope equals to log(α) according to equation (6). However, the plot log(xi)=f(i) obtained by experimental results from FT synthesis shows two slopes (21):

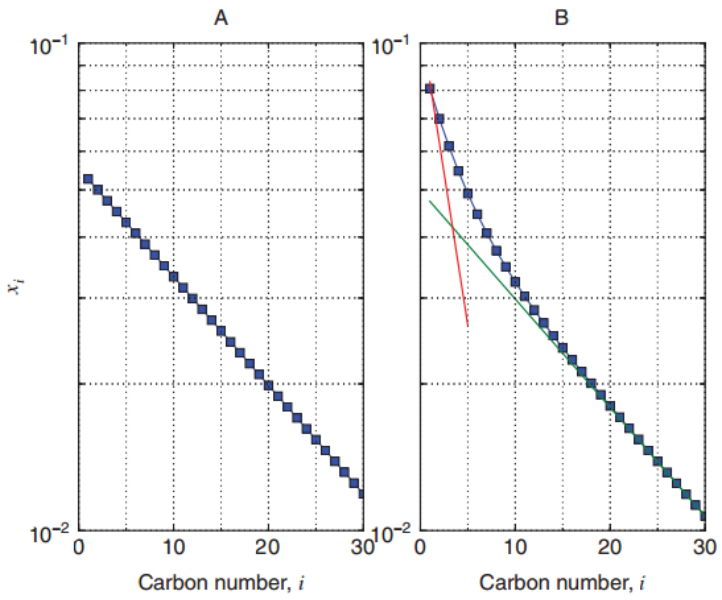

Figure 14 :(A) plot of molar distribution obtained by the ASF model considering one constant propagation probability α =0.95, and (B) plot based on experimental results where the red line has a slope of logα1 with α1= 0.95 and the red line has a slope of logα2 with α2= 0.75

Possible reasons for the double-α behavior are the existence of two types of active Fischer-Tropsch sites as decribed by Huff and Satterfield (23) and/or two separate reaction pathways (24). Two constant growth factor are then taken in account, α_1 for paraffin production and α_2 for 1-olefin formation. Figure 14 brings to light that the selectivity of CH_4 is higher and C_2H_4 selectivity is lower than predicted by ASF distribution. To fit more properly to the experimental results, the cleavage of ethylene (5) and an additional methanation reaction (6) are introduced:

$$C_2H_4 + 2H_2 \rightarrow 2CH_4 \quad (11)$$

$$CO + 3H_2 \rightarrow CH_4 + H_2O \quad (12)$$

The summation of all the reactions in the equation $nCO + (2n+1)H_2 \rightarrow C_nH_{2n+2} + nH_2O$ n = 1,2,…,∞ (4) and $nCO + 2nH_2 \rightarrow C_nH_{2n} + nH_2O$ n = 2,3,…,∞ (5) leads to the following equations:

$$CO + U1\ H_2 \rightarrow \sum v_{i,1}\ C_iH_{2i+2} + H_2O \quad (13)$$

$$CO + U2\ H_2 \rightarrow v_{1,2}\ CH_4 + \sum v_{i,2}\ C_iH_{2i} + H_2O \quad (14)$$

U : stoichiometric usage of hydrogen

v : Stoichiometric coefficient

$$U1 = \sum_{i=1}^{\infty}(i+1)vi, 1 + 1 = 3 - \alpha_1 \quad (15)$$

$$U2 = 2v_{1,2} + \sum_{i=2}^{\infty} ivi, 2 + 1 = (1-\alpha_2)^2 + 2 \quad (16)$$

$$vi,1 = (1-\alpha_1)^2\alpha_1^{i-1} \quad (17)$$

$$vi,2 = (1-\alpha_2)^2\alpha_2^{i-1} \quad (18)$$

No chain limitation is assumed which means that an infinite number of components are formed. Lumps of components are introduced to model the infinity of compound. Two lumps are considered in the study, $C5+^{olefin}$ and $C11+^{paraffin}$. According to Hillestad (21), the finite sum of the molar fraction S, the stoichiometric coefficient v, the average carbon number and the weight average carbon number of the lumps are defined as follows:

$$S|5,\infty] = \sum_{i=5}^{\infty} xi = (1-\alpha_2)\sum_{i=5} \alpha_2^{i-1} = \alpha_2^{5-1} \quad (19)$$

$$S|11,\infty] = \sum_{i=11}^{\infty} xi = (1-\alpha_1)\sum_{i=11} \alpha_1^{i-1} = \alpha_1^{11-1} \quad (20)$$

$$v[5,\infty] = \sum_{i=5}^{\infty} vi = (1-\alpha_2)\alpha_2^{5-1} \quad (21)$$

$$v[11,\infty] = \sum_{i=11}^{\infty} vi = (1-\alpha_1)\alpha_1^{11-1} \quad (22)$$

$$n_n[5,\infty] = 5 + \frac{\alpha 2}{1-\alpha 2} \quad (23)$$

$$n_n[11,\infty] = 11 + \frac{\alpha 1}{1-\alpha 1} \quad (24)$$

$$n_w[5,\infty] = \frac{\left(5-1+\frac{1+\alpha 2}{1-\alpha 2}\right)*5+\frac{(1+\alpha 2)\alpha 2}{(1-\alpha 2)^2}}{5+\frac{\alpha 2}{1-\alpha 2}} \quad (25)$$

$$n_w[11,\infty] = \frac{\left(5-1+\frac{1+\alpha 1}{1-\alpha 1}\right)*5+\frac{(1+\alpha 1)\alpha 1}{(1-\alpha 1)^2}}{5+\frac{\alpha 1}{1-\alpha 1}} \quad (26)$$

With α1 the paraffin growth factor and α2 the olefin growth factor.

The lumps are defined as hypothetical compounds in the simulation software. However, a hypothetical component needs a constant molecular weight to be properly described which doesn't correspond to the lumps. To represent the changing molecular weight of the lumps, it is the α which is changed, since nw depends on α as seen above. Thus, two lumps $C5+^{OL}$ and $C5+^{OH}$ with respectively a constant low α_L and a constant high α_H, are now considered instead of $C5+^{O}$. The same reasoning is applied to $C11+^{P}$.

4.3. Modeling of the Fischer-Tropsch reactor

The Fischer-Tropsch reactor is considered as a perfectly mixed reactor (CSTR). Then, the temperature and concentrations are assumed uniform. The reactions which take place in the FT reactor are highly exothermic. A high temperature fosters the production of lighter hydrocarbons, which is not the aim. This entails that the capability to evacuate heat is a major characteristic. Hence, a low temperature Fischer-Tropsch reactor is the best option, which leads to choose between a fixed bed reactor and a slurry reactor. For maintenance issues, we choose the slurry reactor and fixed the cooling temperature at 220°C. The cooling is assured by a U-tube where boiling water at 220°C goes. Once set the pressure at 20 bars, knowing that a high pressure decreases the price of the unit and increases the solubility of gas in the liquid. The FT reactor is modeled in Aspen as a CSTR using a ACM model. The main parameters are summarized below. The ACM model does not represent the separation between liquid hydrocarbons and the slurry. The FT outlet is composed of both vapor and liquid products. An external separator vessel is then added to separate liquid hydrocarbons and vapor products. The pressure drop in the reactor is estimated at 1 bar and it is simulated by setting ΔP = 1bar in the heat exchanger following the reactor.

Parameters (unit)	Value	Parameters (unit)	Value
T (°C)	220	Phi (mass fraction of catalyst in slurry)	0.2
P (bar)	19.5	α1 high	0.97
Specific area of heat transfer (m^{-1})	40	α1 low	0.7
ρcat (Kg/m^3)	3000	α2 high	0.74
ρliq (Kg/m^3)	700	α1 low	0.6

Table 10 : Main parameters used in the ACM model

The CO conversion is fixed at 65% (+/- 0.5), since it gives the maximum C5+ selectivity (25) as shows below.

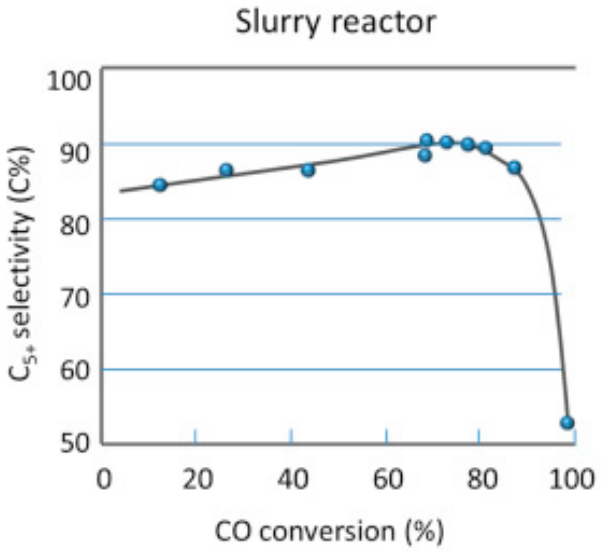

Figure 15 : C5+ selectivity versus CO conversion in the FT reactor

To obtain a conversion of 65%, the volume of the CSTR is modified. Indeed, the volume is the higher, the higher the CO conversion.

$$V_{CSTR}\ (L) = \frac{CO_{in}.X_{CO}}{r_{CO}} \quad (27)$$

r_{co}: reaction rate ($mol/s.dm^3$)

X_{CO}: CO conversion

Co_{in} : inlet flowrate of CO (mol/s)

When handling, it is noticed that there is a lack of robustness for the ACM model. First, the model difficultly reaches convergence for high values of reactor volume. This is due to two equations (6) and (8). Indeed, the CO partial pressure stands in the denominator of the FT rate which make the FT rate tends to infinity when the conversion is too high. In the equation (7), it is noted that α tends towards 1 for low value of P_{CO} and H_2/CO. A α equals to 1 means infinite carbon chain (rt=0), which leads to instability. Secondly, the FT results are not reproducible. Concretely, the FT outlet results depend on the data history which means on the previous results. This is due to the fact that the ACM modeler uses the previous results to converge. Then, the results have some imprecision.

As $C5+^{OL}$, $C5+^{OH}$, $C11+^{PL}$ and $C11+^{PH}$ are hypothetical compounds, the heating value are unknown. The heating of combustion or low heating value (LHV) is proportional to the carbon number as shown on the below figure:

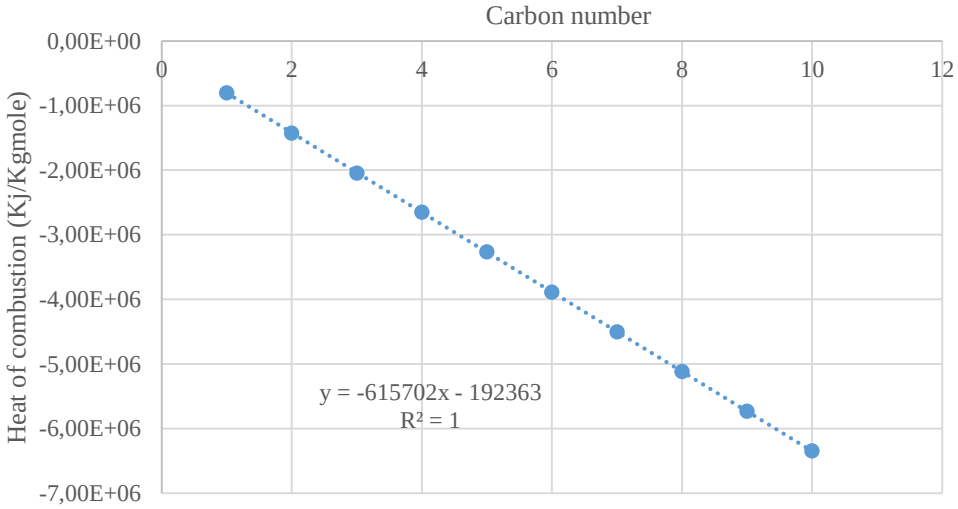

Figure 16 : Heat of combustion of hydrocarbons versus the carbon number

Using equation (23) and (24) with the appropriate α and the relation between carbon number and LHV, the following results are obtained:

Lumps	α	Carbon number	Heat of combustion (Kj/Kmole)
$C5+^{OL}$	0.6	6.5	$-4{,}19.10^{6}$
$C5+^{OH}$	0.74	7.846	$-5{,}02.10^{6}$
$C11+^{PL}$	0.7	13.334	$-8{,}40.10^{6}$
$C11+^{PH}$	0.97	43.334	$-2{,}69.10^{7}$

Table 11 : determination of lumps LHV

5. Biomass-to-Liquid process with recycle

5.1. Process description

The FT products are separated thanks to a three phases separator. The heaviest hydrocarbons are the interest product. The water byproduct might be reused in the process and the lightest products are recycled. Some streams are assigned to a number:

stream	name	number
Gasifier outlet	Out GBR	(1)
Water gas shift outlet	In E-101	(2)
Byproducts removed by the scrubber	CO_2 and H_2S	(3)
Fischer-Tropsch inlet	Inlet FT	(4)

Table 12: Assigned number for stream identification

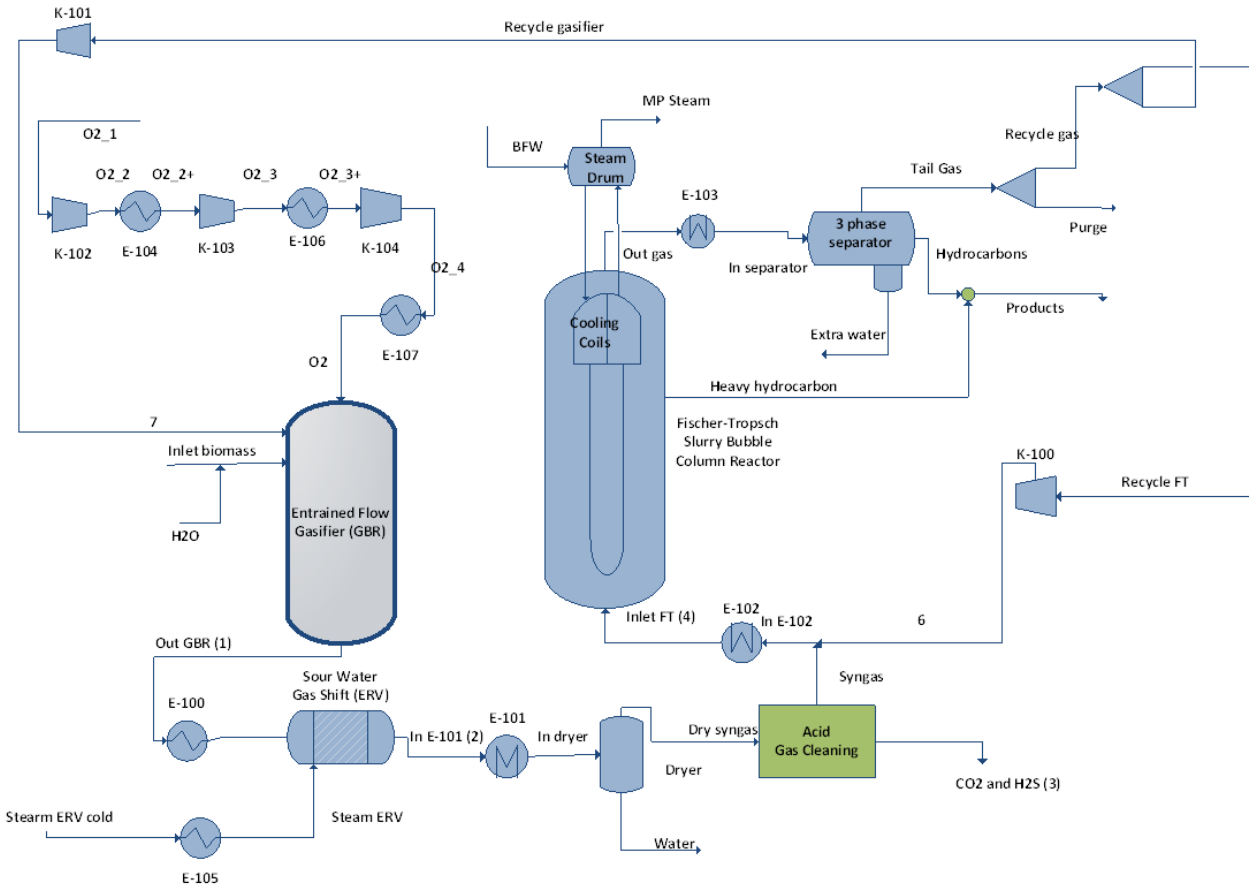

Figure 17 : Process flow diagram with recycle

A more detailed description of the flowsheet (including all the streams and the stream cutters) is available in appendix C.

5.2. Purge and recycle split

N_2, CH_4 and CO_2 are the inert in this process. The nitrogen is produced in the gasifier when decomposing the biomass and does not react in the process. CH_4 and CO_2 are "pseudo-inert" since they react at some point in the process but they are more produced than consumed which leads to their accumulation. They are both produced and consumed in the gasifier but are produces in large quantities in the WGS reactor (for CO_2) and in the FT reactor (for CH_4). Then, a purge is needed. The recycling can be carried out on the gasifier or on the FT reactor. The accumulation of inert is investigated for different value of the purge split at a fixed recycle split. The recycle split represents the fraction of recycled gas (after the purge has occurred) which is recycle into the Fischer-Tropsch. Concretely, take 100 Kmol/h of tail gas outgoing from the three phase separator. The first utility split is called "the purge utility split". If 10mol% is purged, 90 Kmol/h of gas remain and the stream is named "recycle gas". The second split utility is the "recycle split utility" and a value of 10mol% for the recycle split means that 81 Kmol/h feeds the gasifier and 9 Kmol/h go into the FT reactor.

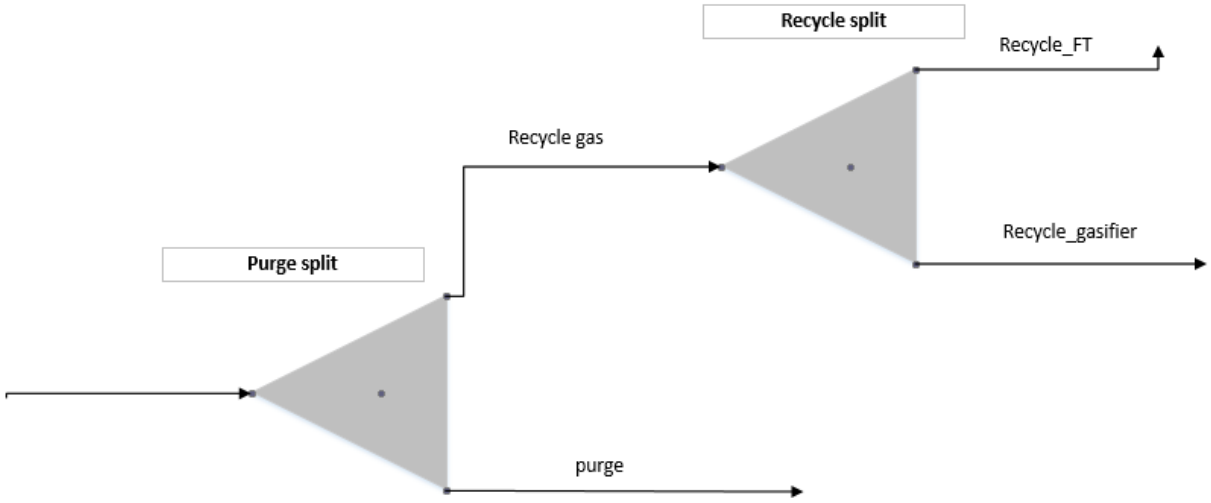

Figure 18 : Explanatory diagram of the splitting system

The recycle split is fixed at 0.5 to have an equal inlet in the FT reactor and in the gasifier. The purge split goes from 0.1 to 0.5. Upper values have not been studied since important purge is not

favorable as it represents carbon loss. The gasifier temperature has been maintained at 1200°C and CO conversion in the Fischer-Tropsch at 65% (+/- 0.5%). The inert concentration is collected at the inlet of the FT reactor.

split	0,1	0,2	0,3	0,4	0,5
mol% CH_4 in FT	0,4	0,3	0,26	0,21	0,17
mol% CO_2 in FT	5,44	5,13	4,9	4,71	4,54
mol% N_2 in FT	0,66	0,35	0,25	0,19	0,16
mol% total inert	6,5	5,78	5,41	5,11	4,87
V_{CSTR} (m^3)	322	303,5	288	273	261
O_2 inlet (Kg/h)	4,70E+04	4,60E+04	4,54E+04	4,51E+04	4,46E+04
λ	0,66	0,65	0,64	0,64	0,63
hydrocarbons (kg/h)	1,97E+04	1,87E+04	1,79E+04	1,69E+04	1,62E+04

Table 13 : Simulation results table of the process included a recycling loop for different purge values at a recycling spit of 0.5

As expected, the inert concentration decreases when higher purge occurs. Ranging a purge split from 0.1 to 0.5, one purges 25mol% more inert (calculation detail : $100*(1-\frac{4.87}{6.5}) = 25\%$). More purge leads to a smaller FT reactor volume and then to a cheaper one, since less gases are introduced. Similarly, less oxygen supply for the gasifier is needed as less gases need to be warm up. However, 17.8 mol% of the hydrocarbons production is waived if 50% of tail gas is purged instead of 10%. As the aim is to optimize the production, the purge is tried to be minimized in the rest of the study.

Simulations results are now studied for different recycle split at a fixed purge rate of 20 mol% and at two gasifier temperature (1200 °C and 1300 °C). 20% of purge has been chosen for practical reason. Indeed, the convergence is more difficult to reach when the purge is small, especially under 10 mol% (see the discussion about the ACM model robustness in 4.3). The target set in the study is to maximize the carbon efficiency and the energy efficiency.

$$C_{eff}\ (mol\%) = 100.\frac{Cbiomass - Cpurge - Cscrubber}{Cbiomass} \quad (28)$$

$C_{biomass}$, C_{purge} and $C_{scrubber}$ are respectively the molar flow of carbon contained in the biomass stream, in the purge and the carbon molar flow evacuated by the scrubber.

$$E_{eff}\ (\%) = 100.\frac{\sum LHV(i).F(i)}{LHVbiomass.Fbiomass} \quad (29)$$

LHV(i) : Low heating value of the compound i (KJ/Kgmole)
F(i) : Molar flow of the compound i (Kmole/h)

The optimal recycle split is then defined by the split which maximize both carbon and energy efficiency. It is recalled that higher the split recycle, higher the Fischer-Tropsch inlet. The results summarized in Table 14 have been obtained with a CO conversion in the FT reactor fixed at 65mol%, a specific area fixed at 40 m^{-1}, a gasifier temperature at 1300°C (+/- 5 °C) and a steam-to-carbon ratio at 1.5.

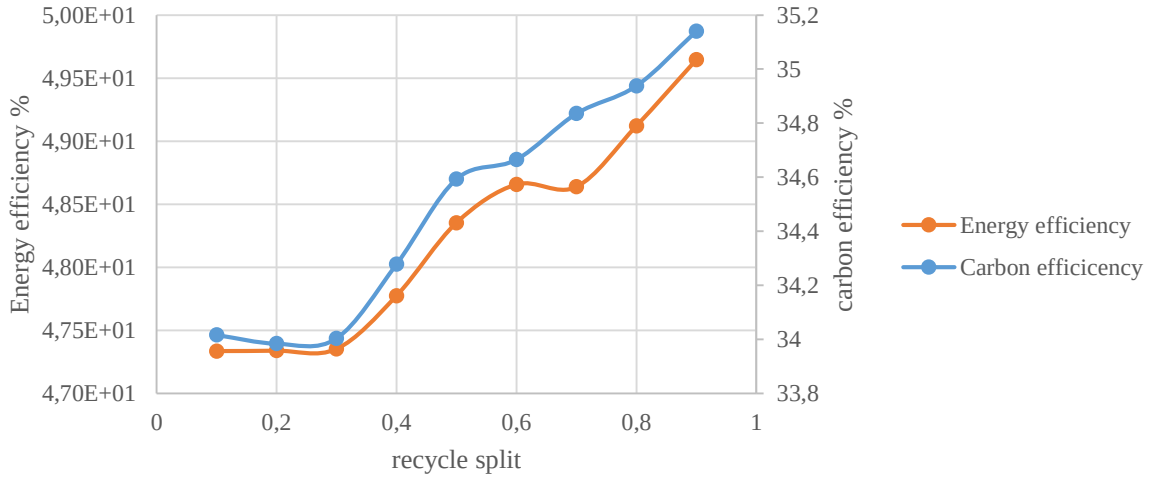

Figure 19: Energy and carbon efficiency versus recycle split at 20% purge, at TGBR=1300°C and at S/C = 1.5

Erling Rytter et al (14) (p 40) reports similar value for Eeff and Ceff originating from existing BTL-FT processes, as well as Kreutz et al (1) (p 24) who has simulated a BTL process. Regarding the above figure, it is noticed that the carbon efficiency slightly rises with the recycle split: it goes from 34% to 35%. The change in the energy efficiency is a bit stronger and goes from 47% to 49.6%. Both efficiencies increase when more tail gas is recycled in the FT reactor. The recycle stream is mainly composed of H_2, CO and CO_2. An important recycle in the FT reactor increases the hydrocarbons production since it increases the amount of reagents (H_2 and CO) and then their partial pressure. Introducing H_2 and CO in the gasifier does not improve the gasifier performance. On the contrary, H_2 and CO are the gasifier products and adding them shift the equilibrium towards the consumption of the products. However, recycling in the gasifier has the advantage to consume the CO_2 byproduct as it is seen in the table 13. It leads to less inerts and to more CO produced.

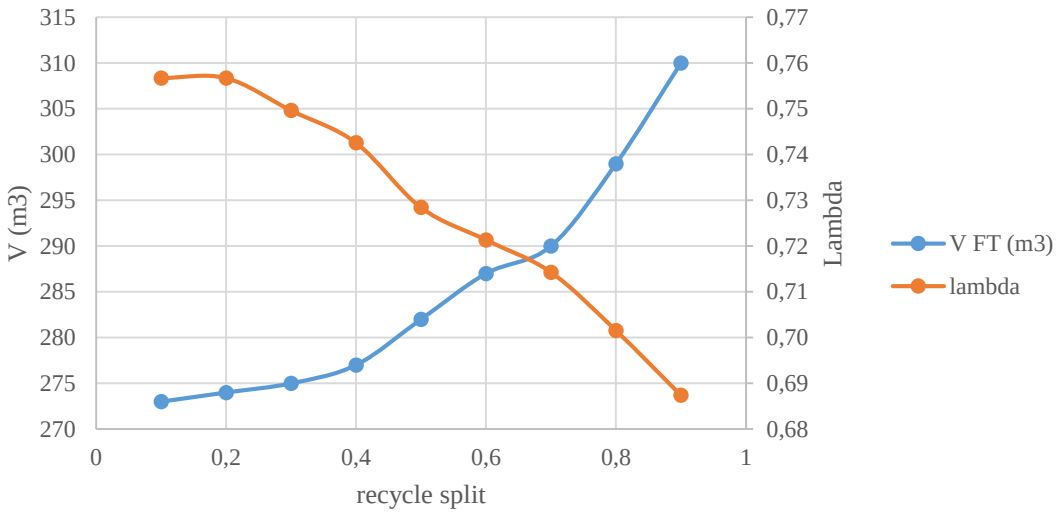

Figure 20 : Fischer-Tropsch volume and lambda ratio versus recycle split at 20% purge, at TGBR = 1300°C and at S/C= 1.5

To maintain the gasifier temperature at 1300°C, the oxygen inlet shall be increased when more gases are recycled into the gasifier reactor as the recycle stream temperature is at 40°C. The lambda moves then away from its optimal λ value (see 3.5 and 5.5) thus decreasing the gasifier performance. One of the advantage to recycle in the gasifier is that the CO_2 and the steam contained in the recycle stream are largely diminished since a part react in the gasifier and the

rest is eliminated by the dryer and the scrubber. Hence, less non-reagents enter in the FT reactor which make drops the volumetric flow, thus decreasing the FT volume and then the vessel cost.

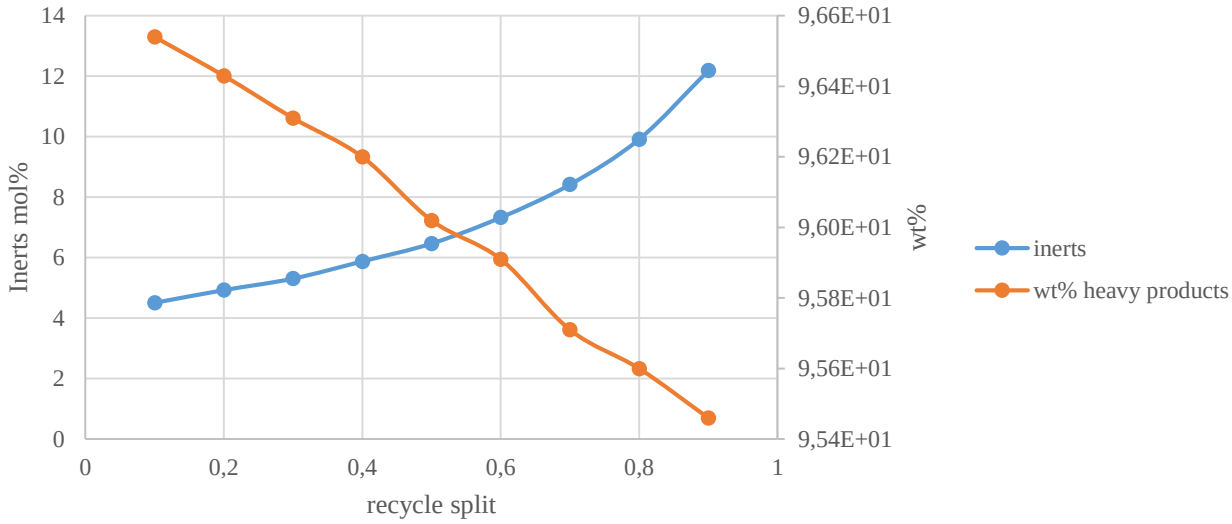

Figure 21 : : Inerts content of FT inlet (mol%) and percentage of heavy hydrocarbons produced versus recycle split at 20% purge, at TGBR = 1300°C and at S/C = 1.5

As said previously, the "semi-inerts" (CH_4 and CO_2) react in the gasifier but not in the Fischer-Tropsch reactor which explains the important rise of inert content (double between split=0.1 and split=0.9) with high recycling split values. The quality of the production is also considered. To get an idea of the hydrocarbons composition, the wt% of heavy hydrocarbons is determined. Heavy hydrocarbons term assigns here $C11+^{PH*}$, $C11+^{PL*}$, $C5+^{OH*}$ and decane. It is noticed that less heavy compounds are produced when more gas is recycled into the Fischer-Tropsch.

recycle split	Products (Kgmole/h)	%CO2	%CH4	%N2	Sum inerts	ERV CO conversion	λ	V FT (m3)	%wt heavy products	% Eeff	% Ceff
0,1	1,69E+04	4,08	0,04	0,39	4,51	27,11	0,76	273	96,54	47,34	34,02
0,2	1,69E+04	4,45	0,09	0,39	4,93	27,78	0,76	274	96,43	47,34	33,98
0,3	1,69E+04	4,77	0,16	0,38	5,31	27,85	0,75	275	96,31	47,35	34,00
0,4	1,71E+04	5,27	0,23	0,38	5,88	28,22	0,74	277	96,20	47,77	34,28
0,5	1,73E+04	5,77	0,33	0,37	58,4	27,82	0,73	282	96,02	48,35	34,59
0,6	1,74E+04	6,52	0,44	0,37	7,33	28,07	0,72	287	95,91	48,66	34,67
0,7	1,74E+04	7,46	0,6	0,36	8,42	28,38	0,71	290	95,71	48,64	34,84
0,8	1,76E+04	8,77	0,79	0,36	9,92	28,34	0,70	299	95,60	49,12	34,94
0,9	1,78E+04	10,76	1,08	0,35	12,19	28,2	0,69	310	95,46	49,65	35,14

Table 14 : Investigation of the recycle split for a 20% purge at TGBR = 1300°C and at S/C= 1.5

The same experiment has been made for a gasifier temperature T_{GBR}=1200°C to see if it has an important impact on the efficiencies.

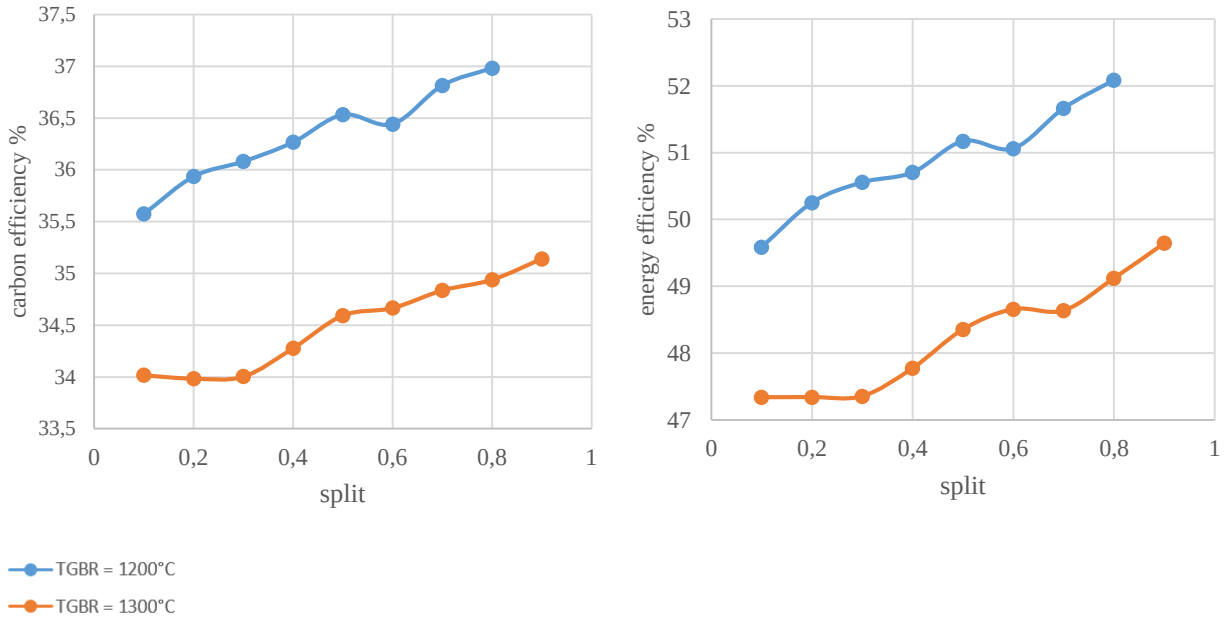

Figure 22 : Carbon and energy efficiency versus recycle split at 20% purge, at TGBR = 1200°C and S/C = 1.5

The gasifier temperature seems to have an important impact on the efficiencies of the plant. Indeed, E_{eff} and C_{eff} are 2 points higher at T_{GBR}=1200°C than at 1300°C for each value of the split.

recycle split	products (Kgmole/h)	%CO2	%CH4	%N2	Sum inerts %	CO conversion in WGS %	λ	V FT (m3)	Eeff %	Ceff %
0,1	17700	3,73	0,05	0,37	4,15	23.25	0,71	284	49,59	35,57
0,2	17900	4,07	0,1	0,37	4,54	23.61	0,7	289	50,25	35,94
0,3	18100	4,37	0,16	0,36	4,89	23.38	0,69	292,5	50,55	36,08
0,4	18100	4,83	0,24	0,36	5,43	23.9	0,69	292	50,7	36,27
0,5	18300	5,3	0,32	0,35	5,97	23.61	0,67	299	51,17	36,53
0,6	18300	6,03	0,45	0,35	6,83	24.3	0,67	299	51,06	36,44
0,7	18500	6,89	0,6	0,35	7,84	23.99	0,66	305,5	51,67	36,81
0,8	18600	8,17	0,79	0,34	9,3	24.04	0,65	314	52,09	36,98

Table 15 : Investigation of the recycle split for a 20% purge at TGBR = 1200°C and at S/C= 1.5

The results at 1200°C are similar to those obtain at 1300°C. It is noticed that the hydrocarbons production is more significant at 1200°C which is consistent with the highest value of E_{eff} and C_{eff}. The influence of the gasifier temperature on the process performances is studied in the next subsection.

Higher recycle split leads to higher efficiencies but also to higher FT volume. The increase of the FT volume is all the more important as the recycle split is large, especially for split higher than 0.8. A recycle split of 0.9 is selected for the moment.

5.3. Gasifier temperature

The influence of the gasifier temperature on the process performances is here investigated. The results are obtained for 20% purge, a recycle split of 0.9 and a S/C ratio of 1.5. The gasifier temperature is adjusted by changing the oxygen concentration. It is seen that the carbon efficiency and the energy efficiency decrease when the temperature of the gasifier increases as shown in the below figure.

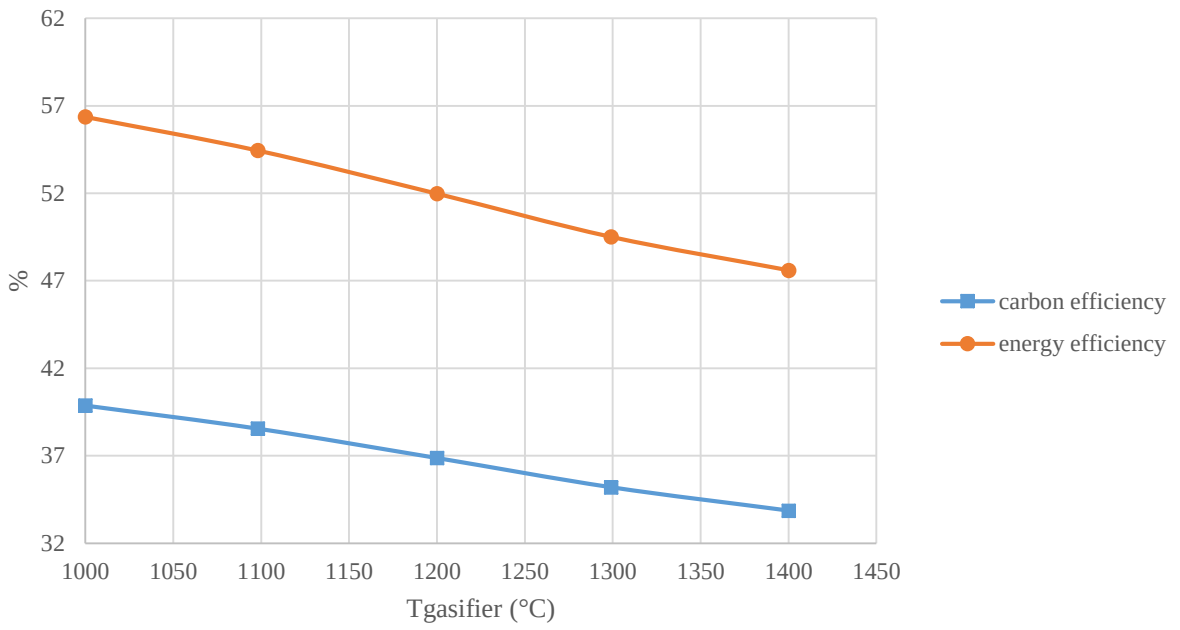

Figure 23 : Energy and carbon efficiencies versus the gasifier temperature at 20% purge, S/C =1.5 and recycle split = 0.9

This decline is explained by the $\frac{H2}{CO}$ ratio at the outlet of the gasifier which decreases when more oxygen is added. Indeed, a decrease of the ratio leads to more converted CO in the WGS reactor which means more CO_2 produced (see next figure). The process has a total inlet carbon flow of 3.59 10^3 Kmole Carbons/h. At 1000 °C, 282.79 Kmole/h of CO are converted into CO_2 in the Water Gas Shift reactor. Thus, 282.76 Kmole/h of carbons are lost by producing the byproduct CO_2 which represents 7.88% of carbon loss. For 400 more degrees, a total of 691.19 Kmole/h of CO are shifted, which generates a carbon loss of 19.27%.

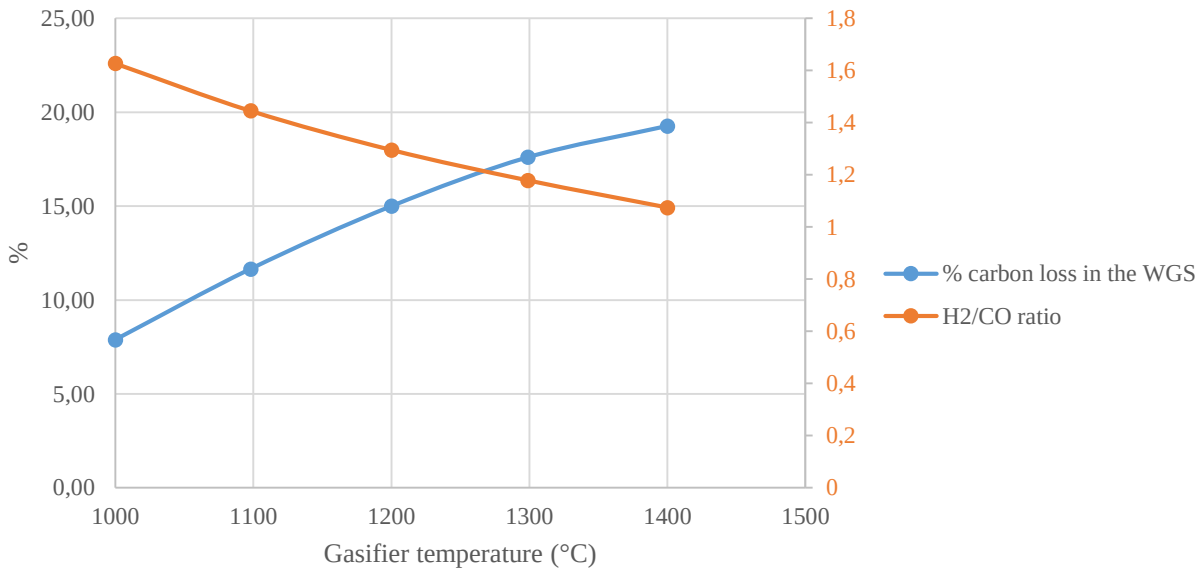

Figure 24 : Percentage of the carbon loss in the WGS and of the H2/CO ratio versus the gasifier temperature at 20% purge, S/C =1.5 and recycle split = 0.9

Higher gasifier temperature implies higher oxygen content which explains why the carbon capture of the process decreases. However, a high temperature enables the entrained flow gasifier to be prevented from tars. Qin et al. (26) has proved that above 1350°C, a tar free gasification can be obtained. For the rest of the study, we choose to use a temperature of 1300°C and we assume no tar production. As the temperature is closed to 1350°C, the assumption of no tar formation is acceptable.

Tgasifier (°C)	**1000**	**1098**	**1200**	**1299**	**1400**
λ	0,55	0,60	0,65	0,70	0,74
V CSTR (m^3)	334,5	327	314	300,1	298,5
$\%_{mol}CO_2$ out gasifier	14,26	13,71	13,37	13,23	13,32
H_2/CO GBR	1,63	1,45	1,30	1,18	1,07
% Co conversion WGS	13,24	18,99	24,00	27,99	30,81
Carbon loss in ERV %	7,88	11,65	14,99	17,60	19,27
C_{eff} %	39,88	38,56	36,87	35,20	33,87
E_{eff} %	56,37	54,45	51,98	49,51	47,60
Syngas (Kmole/h)	5,61E+03	5,38E+03	5,14E+03	4,91E+03	4,65E+03

Table 16 : Simulation results for different gasifier temperature at 20% purge, S/C=1.5 and recycle split=0.9

The ratio called "H_2/CO GBR" stands for the ratio at the gasifier outlet. The H_2/CO at the FT inlet is always fix at 1.98 by adjusting the steam in the WGS reactor.

5.4. Influence of lambda

Now that the recycling loop has been introduced, the influence of the quantity of O_2 introduced in the gasifier on the process is studied. The recycle split is fixed at 0.9, the purge at 20% and the CO conversion in the FT reactor at 65%. The λ parameter is ranged from 0.3 to 0.9 for two value of the steam-to-carbon ration, S/C = 1.5 and S/C = 0.5.

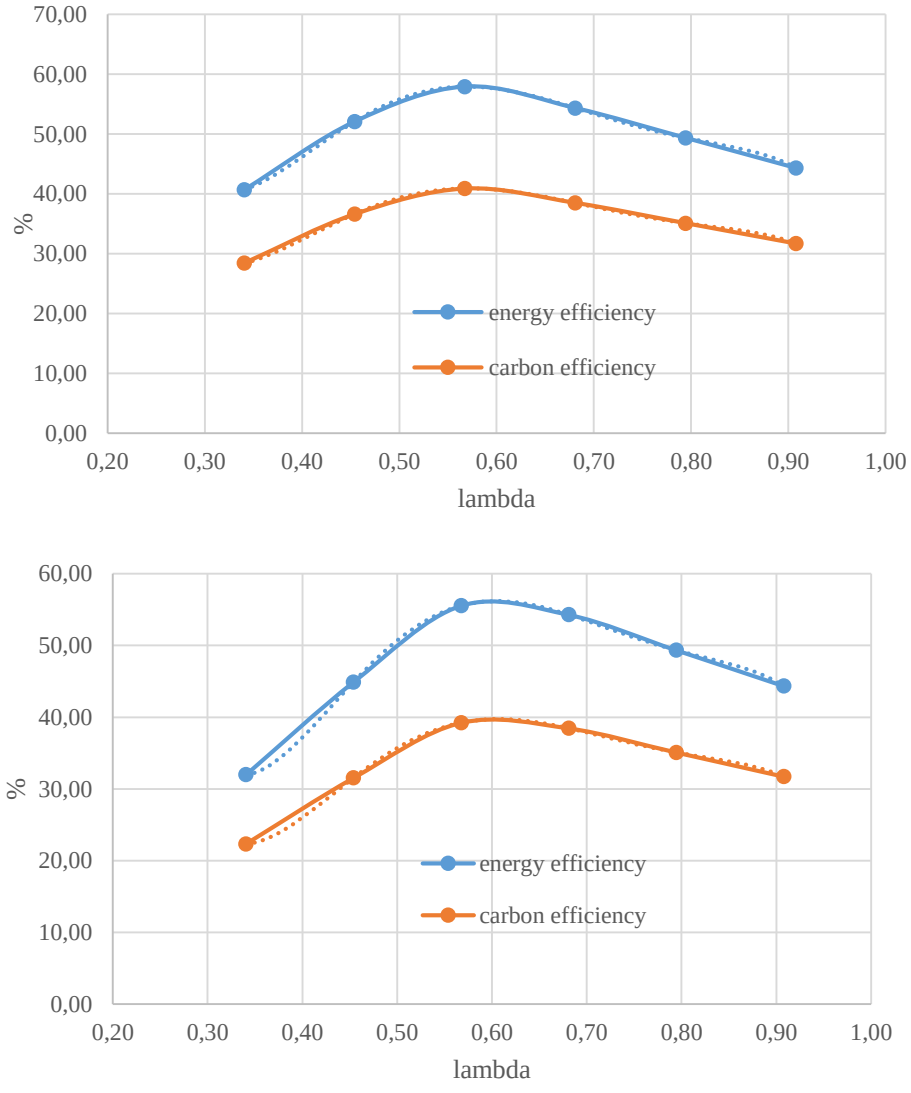

Figure 25 : Efficiencies versus lambda at 20% pure, a recycle split at 0.9, for S/C = 1.5 (upper figure) and S/C = 0.5 (lower figure)

The values of the efficiencies are similar for the two values of S/C but higher values are noticed for S/C = 0.5. It is due to the fact that less water needs to be warm up at S/C = 0.5 and then, for a same λ, the gasifier temperature is higher for S/C=0.5 than for S/C = 1.5. It is recalled that a high temperature in the gasifier favors the syngas production (see 3.3). The maximum value for the efficiencies are obtained at an optimum λ: $\lambda_{optimal}$ = 0.57 at S/C= 1.5 and $\lambda_{optimal}$ = 0.6 at S/C= 0.5 for both E_{eff} and C_{eff}. In 3.5, the optimal λ was also found at 0.57 for S/C = 0.2 anf for S/C = 1.5. The optimum lambda seems to be constant with the S/C ratio and the volumetric inlet flow (recycle). It is pointed that the actual S/C is slightly different since some water is introduced into the gasifier by the recycling loop. Because of time constraint, the experiment has not been redone. It is thought that the optimal lambda is around 0.59.

λ	O_2 inlet (kg/h)	V CSTR	T GBR (°C)	E_{eff}%	C_{eff}%	carbon loss in ERV	H_2/CO GBR	syngas (Kmole/h)
0,34	2,12E+04	378,1	722,9	40,68	28,41	-7,19	2,73	4,08E+03
0,45	2,83E+04	370,1	789	52,04	36,59	-3,74	2,28	5,19E+03
0,57	3,54E+04	348,8	903,8	57,89	40,87	3,04	1,86	5,75E+03
0,68	4,24E+04	325,9	1100	54,32	38,48	19,17	1,44	5,38E+03
0,79	4,95E+04	300,4	1307	49,34	35,08	17,74	1,17	4,89E+03
0,91	5,66E+04	273,8	1507	44,32	31,68	21,29	0,98	4,40E+03
Trend line for the energy efficiency			y = -8227,7x5 + 26340x4 - 32529x3 + 19116x2 - 5256,3x + 581,86 R^2=1					
Trend line for the carbon efficiency			y = -5821,8x5 + 18642x4 - 23027x3 + 13534x2 - 3720,9x + 411,29 R^2=1					

Table 17 : Simulation results for different lambda at S/C= 1.5, purge at 20% and recycle split at 0.9

λ	O_2 inlet (Kg/h)	V CSTR	T GBR (°C)	E_{eff}%	C_{eff}%	carbon loss in ERV	H_2/CO GBR	syngas (Kmole/h)
0,34	2,12E+04	358	739,5	31,97	22,34	12,89	1,11	3,23E+03
0,45	2,83E+04	364	808,2	44,89	31,53	17,83	1,11	4,49E+03
0,57	3,54E+04	348,5	912,3	55,53	39,22	23,30	1,07	5,52E+03
0,68	4,24E+04	325,5	1179	54,27	38,46	30,40	0,87	5,38E+03
0,79	4,95E+04	299,5	1489	49,34	35,09	34,76	0,77	4,89E+03
0,91	5,66E+04	274	1776	44,34	31,72	36,46	0,59	4,40E+03
Trend line for the energy efficiency				y = -9939,2x5 + 32681x4 - 41615x3 + 25344x2 - 7260,8x + 814,9/R^2=1				
Trend line for the carbon efficiency				y = -7114,1x5 + 23400x4 - 29811x3 + 18168x2 - 5209,9x + 584,76 /R^2=1				

Table 18 : Simulation results for different lambda at S/C= 0.5, purge at 20% and recycle split at 0.9

One of the main source of carbon loss is the necessity to have a high H_2/CO value at the FT inlet. This require the conversion of CO in the Water-gas-shift reactor. The carbon loss generates by the WGS reaction is designated by "carbon loss in ERV" and is defined by the below equation:

$$C_{loss} \text{ in ERV } (\%) = 100. \frac{FCO\ converted\ in\ CO2}{Fcarbon\ in\ biomass} \quad (30)$$

Fcarbon in biomass : Molar flow of carbon contained in the biomass inlet (Kmole/h)

F_{CO} : Molar flow of CO (Kmol/h)

In Table 17, negative value of the carbon loss in the WGS reactor is noticed. It is because the partial pressure of hydrogen is high enough to reverse the water-gas-shift reaction to produce CO instead of H_2. As expected, the methane disappears for high lambda since it is oxidized. On the contrary, CO_2 is more produced when the oxygen content increases.

λ	0,34	0,45	0,57	0,68	0,79	0,91
% CH4	46,68	25,48	0,85	0,79	0,78	0,75
%CO2	5,92	6,22	7,55	8,8	10,27	11,98

Table 19 : Inert concentration in the gasifier for different lambda at S/C= 0.5, purge at 20% and recycle split at 0.9

5.5. Influence of the steam-to-carbon ratio at constant temperature for the gasifier

The temperature of the gasifier is set at 1300°C. The purge is still at 20% and the recycle split at 0.9. The ratio S/C is changed by changing the water inlet in the gasifier. As highlights in the previous subsection, the S/C does not take into account the steam from the recycle stream but only the steam supply.

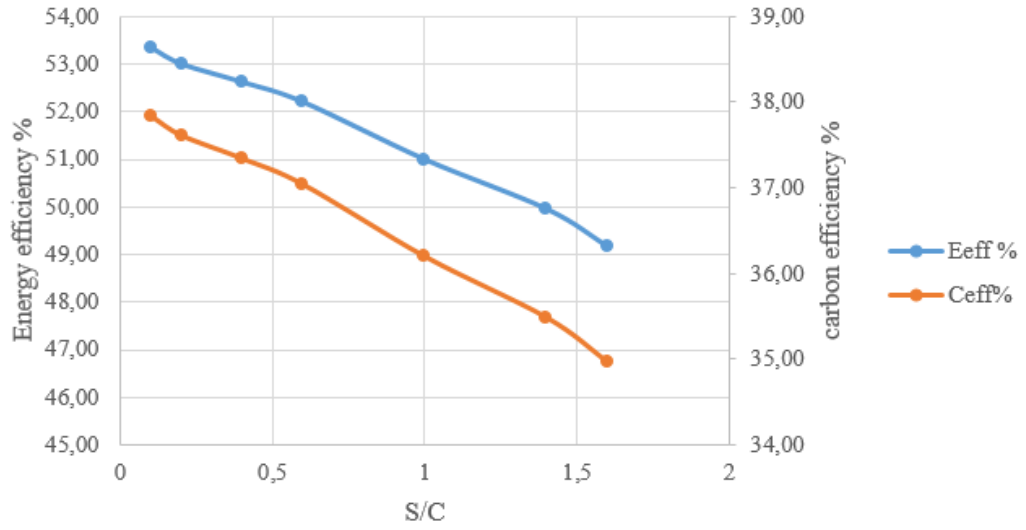

Figure 26 : Efficiencies of the BTL process for different S/C ratio at TGBR = 1300°C, purge at 20% and recycle split at 0.9

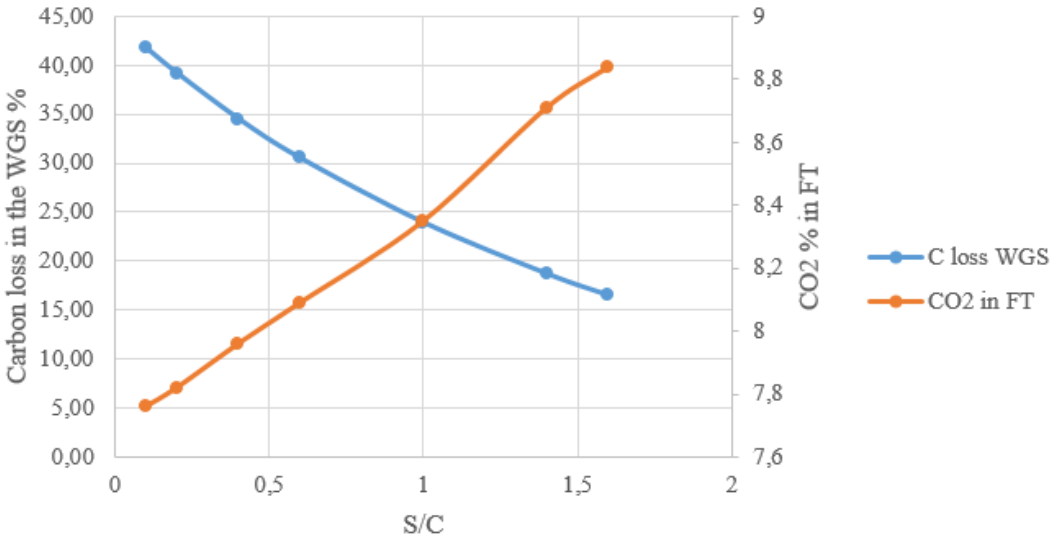

Figure 27 : Carbon loss occurring in the WGS reactor and CO_2 concentration at the FT inlet for different S/C ratio at TGBR = 1300°C, purge at 20% and recycle split at 0.9

The efficiencies decrease when the S/C increases. For S/C = 0.1, maximum values are obtained: E_{eff} = 53.4%, C_{eff} = 37.8% and drop at E_{eff} = 49.2% and C_{eff} = 35% at S/C = 1.6. Steam makes decrease the syngas production as shown in the below table. As explain in 3.7, if more steam is added into the gasifier, more oxygen is needed to maintain the temperature at 1300°C and it is the oxygen contain which governs the syngas production variation. Concretely, oxygen oxidizes CO and H_2. However, more steam makes increase the H_2/CO ratio which prevent the loss carbon in the WGS reactor. For S/C = 0.1, 41.7% of the carbon supply is converted to adjust the H_2/CO ratio. The carbon loss is reduced to only 16.5% at S/C = 1.6. Although the carbon loss is improved by adding water in the gasifier reactor, the carbon efficiency is not enhanced since H_2O and O_2 are oxidizer, thus favoring the production of CO_2 to the detriment of CO.

S/C	steam inlet (Kgmol/h)	λ	VCSTR (m3)	Eeff%	Ceff%	loss carbon in WGS %	H2/CO out GBR	syngas (Kgmol/h)	%CH4 in FT	%CO2 in FT
0,1	3,59E+02	0,62	319,20	53,35	37,85	41,71	0,63	5,29E+03	0,83	7,76
0,2	7,18E+02	0,62	317,00	53,01	37,62	39,17	0,67	5,27E+03	0,83	7,82
0,4	1,44E+03	0,63	316,00	52,63	37,35	34,50	0,76	5,22E+03	0,81	7,96
0,6	2,15E+03	0,64	314,80	52,21	37,04	30,51	0,84	5,16E+03	0,8	8,09
1	3,59E+03	0,67	308,10	51,00	36,20	23,95	1,00	5,06E+03	0,8	8,35
1,4	5,02E+03	0,69	303,00	49,95	35,49	18,73	1,14	4,93E+03	0,78	8,71
1,6	5,74E+03	0,70	298,60	49,17	34,97	16,52	1,21	4,88E+03	0,79	8,84

Table 20 : Simulation results for different S/C at Tgasifier = 1300°C, purge at 20% and recycle ratio at 0.9

5.6. Determination of the base case

The aim of the study is to maximize the energy efficiency and to minimize the carbon loss which means that the maximum of carbon from the biomass has to be transferred to the products. The wastage of the carbon elements occurs when carbon leaves the process, that means in the purge and in the acid gas removal unit which removes the byproducts.

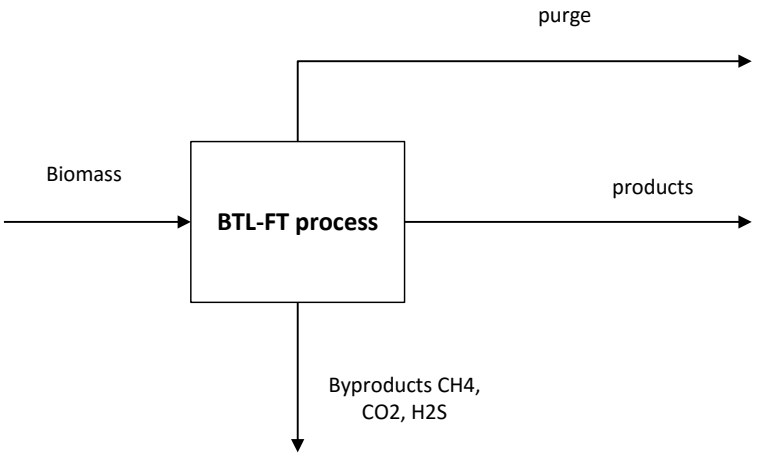

Figure 28 : Simplified diagram of the BTL process

The carbon leaves in the form of CO_2, CH_4 and light hydrocarbons. To optimize the process, the generation of methane and CO_2 shall be minimized. They are both produced during gasification, the CO_2 is also produced in the WGS reactor and CH_4 in the FT reactor. Then, three options can be exploited to fulfill the aim:

- Reduce as much as possible the purge
- Maximize the CO production in the gasifier
- Maximize the value of the H_2/CO ratio at the gasifier outlet

The two last points shall be optimized in parallel since an increase of the ratio leads to the decrease of the CO flowrate. According to the previous results, it is preferable to optimize the CO production than the ratio by adding few steam. It had then been decided to not add any extra water in the gasifier which means that the only supply of water comes from the recycling loop. The recycle split and the purge split are now modified to find the optimal configuration. The recycle split is ranged from 0.5 to 1 and the purge split from 0.17 to 0.10. The results have here been obtained using a specific area of 100 m^{-1} in the FT reactor. Even the specific area is not

equal to 40 m^{-1} as previously, the following results still allow one to find the optimal configuration.

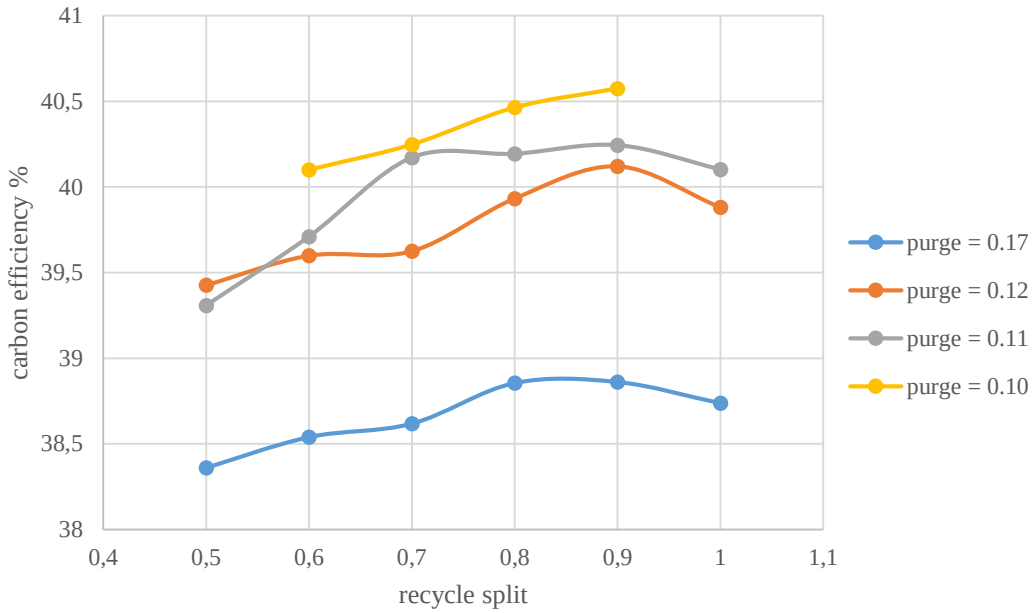

Figure 29 : Carbon efficiency versus recycle split for different purge value at S/C=0 and TGBR=1300°C

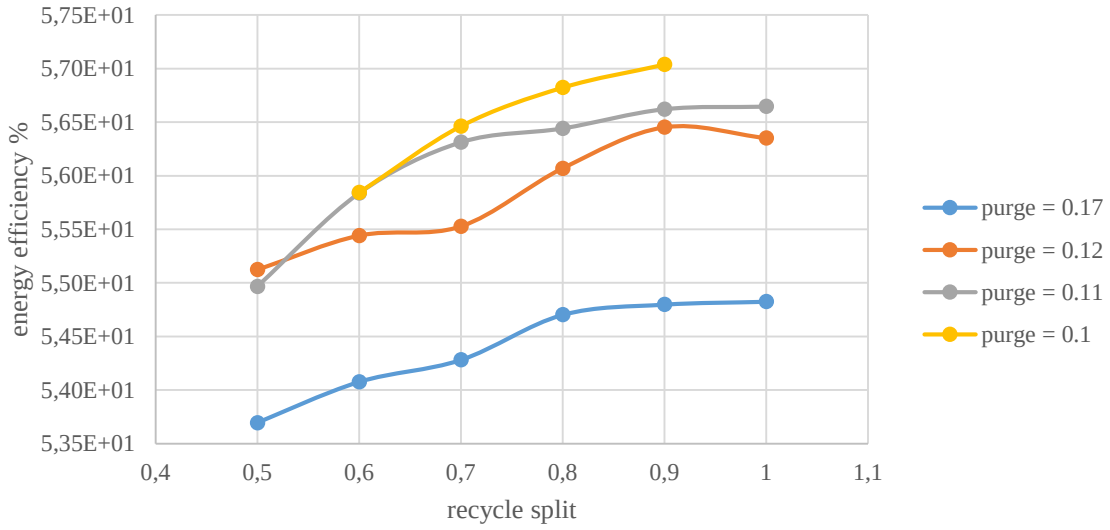

Figure 30 : Energy efficiency versus recycle split for different purge value at S/C = 0 and TGBR= 1300°C

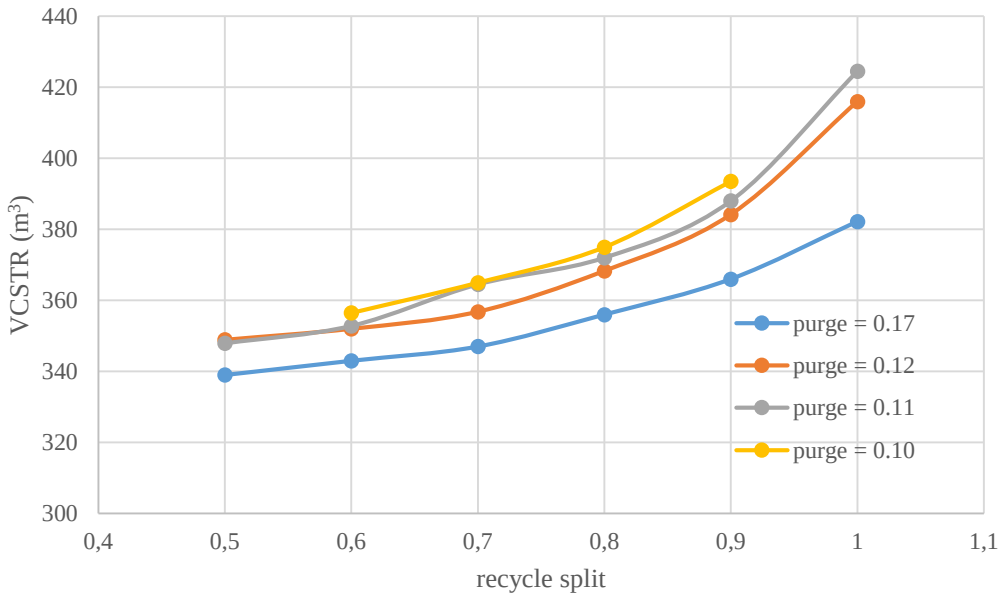

Figure 31 : Fischer-Tropsch volume versus recycle split for different purge value at S/C = 0 and TGBR = 1300°C

Lower the purge is, better are the efficiencies. A different of around 2% is noticed for the efficiencies values between the case at purge split = 0.17 and purge split = 0.10. However, below 0.10, the simulation does not converge anymore for some values of recycle split (1 and 0.5) and converge with difficulty for the others. For all purge value, the efficiencies increase with the recycle split until 0.9. Above this value, the efficiencies decrease or are stable. In parallel, the FT volume increases when more gas is recycled in it which makes rise the shell cost. The increase of the volume is not linear; the volume increase is all the more important as the recycle split is high. Then, having a split above 0.9 does not offer a benefit as the efficiencies does not increase but the shell cost does. The recycle split is then set at 0.9 and the purge at 0.11. Kreutz et al (1) (p 28) also recycle 90% of the tail gas into the Fischer-Tropsch and have a small purge to avoid the buildup of inert.

The results of the base case obtained from the workbook are presented in appendix E. The specific area in the Fischer-Tropsch was set again at 40 m^{-1} and the ACM model has been cleared and initialized again to get rid of all the previous information which could influence the results. The main data are given in the below table:

λ	0,69	**CO_2 purge (kg/h)**	1,13E+02
V_{CSTR} (m^3)	352,00	**CO_2 tot (Kg/h)**	8,24E+04
% Eeff	56,55	**actual S/C**	1,51E-04
% Ceff	40,23	**Mass density (kg/m3)**	691,10
% carbon loss WGS	44,52	**SG**	0,69
H2/CO	0,57	**API**	73,1543561
syngas (Kgmol/h)	1,34E+05	**price $/h**	8,37E+03
products (kg/h)	2,03E+04	**Price $/year**	6,70E+07
Products (bbl/d)	4.257E+03	**%CH4 in FT**	1,68
CO_2 removal (kg/h)	8,23E+04	**%CO2 in FT**	12,32
		% inerts	14,54

Table 21 : main data of the base case (purge ratio = 0.11 and recycle split = 0.9)

"CO_2 removal" and "CO_2 purge" represent respectively the CO_2 disposed by the acid gas removal unit and by the purge. "%inerts" and "%compound in FT" are taken at the inlet of the FT reactor. Table results are available in appendix G.

CO_2 formation is the main cause of carbon loss. $8.24.10^4$ Kg/h of CO_2 leave the system i.e. $1.87.10^3$ Kmole of carbon/h. Dividing by the inlet carbon stream of $3.59.10^3$ Kmole of Carbon/h, it is shown that 52.2 % of the inlet carbon are evacuated in the form of CO_2. The 8 last percent of carbon loss are caused by the elimination of CH_4, CO and light hydrocarbons in the purge.

6. Investigation of a hybrid hydrogen-carbon process

6.1. Concept of the hybrid hydrogen-carbon process

The main limitation of the BTL process is the low energetic density of the biomass, requiring high quantity of biomass to produce hydrocarbons. The Agrawal's article (5) highlights the fact that the proposed BTL process has serious limitation and can only partly contribute to the energy transition. Indeed, the article estimates that 58% of the total United States land area should be dedicated to biomass cultivation in order to support the total oil consumption in the United States (13.8 Mbbl/d). The annual available amount of biomass is estimated to 1.366 billion tons which can theoretically satisfy around 30% of the oil consumption in the USA. To improve those number, some articles like (5) propose to add hydrogen to the system. The biomass is then seen as a source of carbon and the hydrogen as the energy source. Hydrogen would be produced by a carbon-free energy source such as nuclear, solar or wind power to keep a global CO_2 balance close to zero. Hydrogen supply enables the process to transfer every carbon atom from the biomass to the products. Thus, no CO_2 can be emitted, no CO_2 removal system is required and less biomass is needed to produce the same quantity of biofuel. The addition of hydrogen would save 60% of the biomass thereby reducing the land area required close to 6.2% of the total United Sates territory.

6.2. Supply of hydrogen in the Water-gas-shift reactor case 1

Experiments with a hydrogen supply into the WGS reactor have been realized with Aspen properties. It is assumed that an unlimited quantity of hydrogen is available. The hydrogen supply is assumed to be at 1 atm and 25°C. Isothermal compression is simulated to bring hydrogen to 19.75 bar and to 800°C.

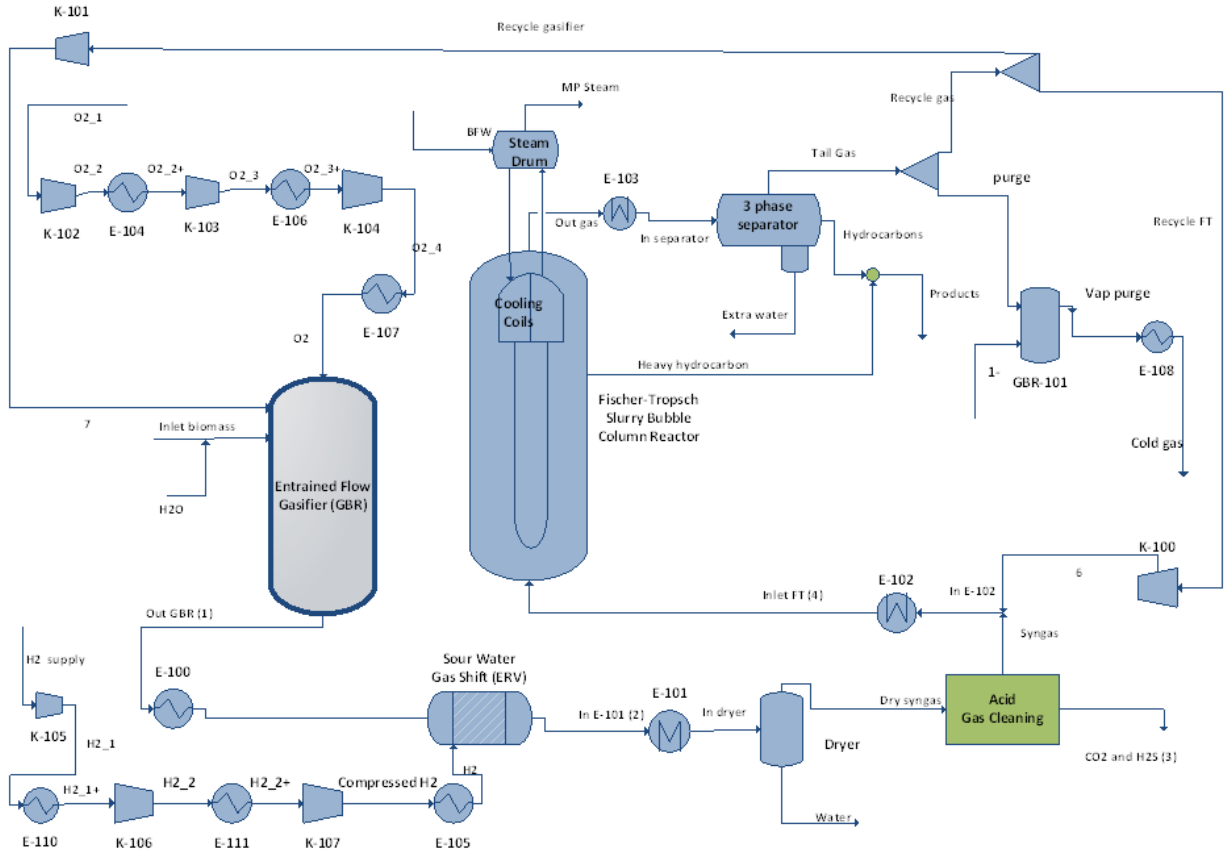

Figure 32 : Process flow diagram for the hybrid hydrogen-carbon process

It has been chosen to not warm up to higher temperature the hydrogen supply since it would lead to the purchase of a third high temperature exchanger. Two high temperature exchangers are already needed to warm up the oxygen supply to 1300°C and to cool down the syngas to 1000°C before it enters into the Water-gas shift reactor. High temperature heat exchangers are more expensive that traditional heat exchanger since they require exotic materials. An isothermal compression was simulated to compress hydrogen the supply. The 3 compressors have a pressure ratio of 2.7.

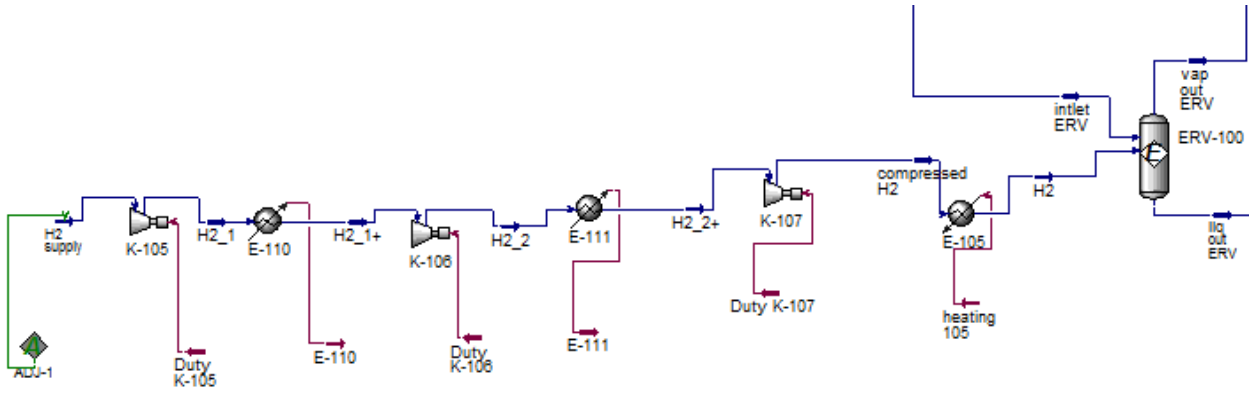

Figure 33 : Isothermal compression of hydrogen

Additional hydrogen enables one to fix the H_2/CO ratio without consuming the CO reagent. Moreover, hydrogen in the WGS reactor is used to react with CO_2 to convert it in CO by following the reverse water-gas-shift reaction. Then, less carbon loss occurs and more reagent enter into the FT reactor which leads to more hydrocarbons.

$$CO_2 + H_2 = CO + H_2O \qquad \Delta Hr = 41 \text{ KJ/mol} \qquad (31)$$

The reaction is endothermic and then high temperature is beneficial for the conversion.

T WGS (°C)	800	900	1000	1100	1300
hydrocarbons (Kg/h)	3,82E+04	3,90E+04	3,97E+04	4,05E+04	4,09E+04
H2 supply (Kg/h)	4,81E+03	5,06E+03	1,06E+04	1,09E+04	1,12E+04
CO produced (Kgmole/h)	1,91E+01	9,88E+01	1,63E+02	2,09E+02	2,61E+02

Table 22 : influencie of the WGS reactor temperature on the reverse water gas shift reaction equilibrium

The equilibrium is shifted when the temperature increases which leads to more hydrocarbons and to a high consumption of the greenhouse gas CO_2. However, above 1000°C, few example of available technologies have been found. The department of Chemical and Petroleum in Pittsburg (27) presents results obtained from a range temperature of 1148-1198 °K. A second article written by the same authors (27) presents the temperature used by different study using Quartz reactors. Without taking into account the study of Karim and Mohindra (1974) which has created disagreement within the scientific community, the highest proposed temperature for a WGS reactor is 1323 °K. Most of the studies submit WGS reactor using a temperature around 1000°C, which is the selected temperature here.

The addition of hydrogen has to be taken into account in the energy efficiency calculation. The new E_{eff} is called the "modified energy efficiency":

$$E_{eff\ mod}(\%) = \frac{LHV\ products\ (\frac{KJ}{h})}{LHV\ biomass\ (\frac{KJ}{h}) + LHV\ H2\ (\frac{KJ}{h})} \quad (32)$$

The following results are obtained keeping the same parameters used in the base case: $T_{gasifier}$ = 1300°C, S/C = 0, recycle split = 0.9, sp area = 40m^{-1}, COconv in FT reactor = 65%. However, the reverse water-gas-shift reaction occurs in the WGSR and the operating temperature is 1000°C (+/- 5°C) and the purge ratio has been raised to 20% due to convergence issues.

purge	0,2	**%C_{eff}**	78,26
recycle split	0,9	**λ**	0,69
actual S/C	1,77E-04	**products (Kg/h)**	3,97E+04
T_{WGS} (°C)	1002	**Mass density (Kg/m^3)**	752,50
H_2 supply (Kg/h)	1,06E+04	**SG**	0,75
CO_2 conv %	37,01	**API °**	56,58
CO produced WGS (Kgmol/h)	164,88	**price $/h**	1,62E+04
Vcstr (m3)	596,50	**Price $/year**	1,30E+08
%CO_2 FT	0,69	**CO_2 removal (Kg/h)**	1,12E+04
%CH_4 FT	1,22	**CO_2 purge (Kg/h)**	8,78E+02
% inerts FT	2,08	**CO_2 tot (Kg/h)**	1,21E+04
%$E_{eff\ mod}$	60,24		

Table 23 : Simulation result for the case 1

Adding H_2 greatly improves the yield. The production of hydrocarbons double, increasing from 20 tonnes for the base case to 40 tonnes, thus doubling also the income from the production. The carbon efficiency is consistent with the rise of the production and almost double going from 40.23% for the base case to 78.26%. However, it is noticed that an important amount of hydrogen is needed: 10 tonnes. This must impose substantial economic costs. Energetically speaking, the addition of hydrogen is worthwhile since $E_{eff\ mod}$ is almost 5 points higher than the E_{eff} of the base case.

6.3. Valuation of the purge by heating oxygen stream case 2 and case 3

The purge is composed of 57.9 mol% of H_2 and 31.6 mol% of CO for the case 1 which is a good fuel for burning. Besides, CO is an air pollutant, toxic by inhalation and a greenhouse gas and then should not be vented. Therefore, burning the purge gives the advantage to get rid of CO and to supply heat usable for the heat integration. The burner is simulated with an adiabatic Gibbs reactor supplied with air at 25°C. The inlet flowrate of air giving the maximum outlet temperature is determined by a case study. A maximum outlet temperature of 2157 °C is obtained for a molar flow of 3500 Kgmole/h.

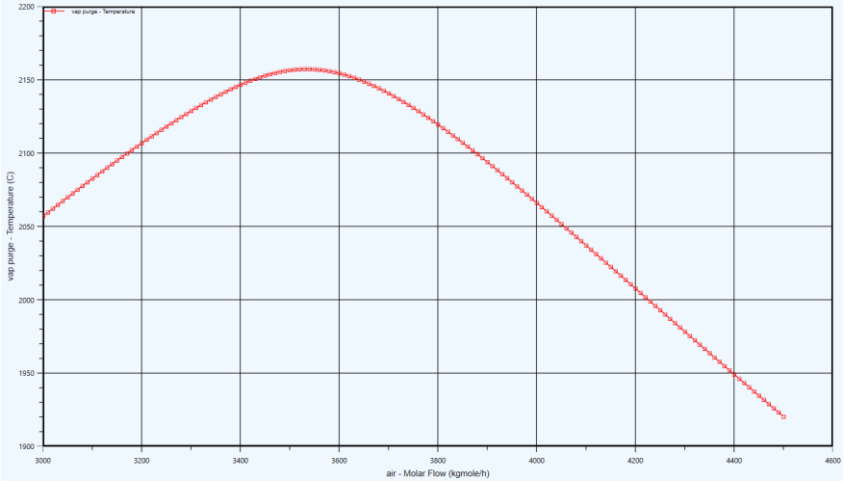

Figure 34 : case study of the purge burning case 1

However, not all CO is consumed and a significant quantity still remain after the burning. Emission limit of 100 mg/m^3 is here considered (28) and the supply of air is determined according to this criterion. The requirement is fulfilled for 5870 Kmole/h of air as 97.2 mg/m^3 of CO is released. The heat generated is evaluated by considering the outlet gas as a hot stream. The maximum recoverable heat is estimated by assuming that the gas can be cooled down to 100°C.

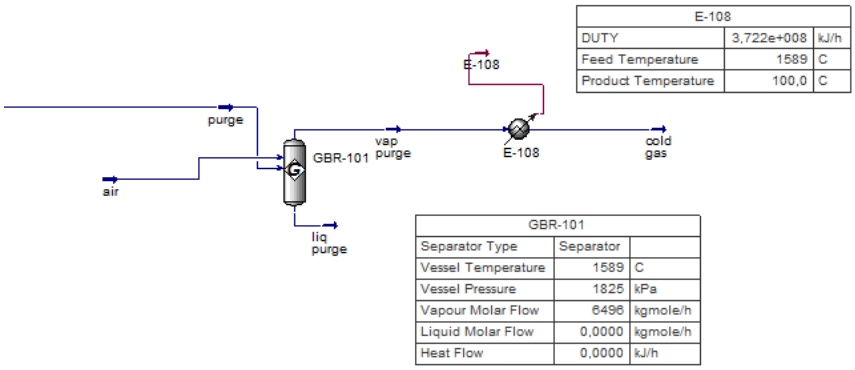

Figure 35 : Simulation of the purge burning case 1

80% of efficiency is assumed for the combustion which gives an available energy of $2.98.10^8$ KJ/h.

The heat from the purge burning is used to warm up the oxygen inlet of the gasifier. The inlet is warm up at 1350°C (case 2) and at 1600°C (case 3) for different S/C values. The S/C ratio is studied here again, because steam makes increase the H_2/CO ratio which reduces the expensive needed amount of the hydrogen supply. Previously, adding water was not beneficial because it leaded to more oxygen in order to maintain the gasifier temperature. By preheating the inlet stream, one is liberated from this obligation. By comparing with the case 1, $E_{eff\ mod}$ increases by 2%-points whereas C_{eff} is stable. The energy efficiency rises because of 2 effects: The production is higher (1%) and the supply of hydrogen in the WGSR is smaller (1%) when oxygen is preheated. This is due to the fact that less oxygen is introduced in the gasifier. Indeed, λ goes from 0.69 (base case) to 0.66-0.65. As λ is closer to the optimum (0.57 see subsection 5.4), the production is increased. Besides, small λ improves the H_2/CO value, then less hydrogen is needed.

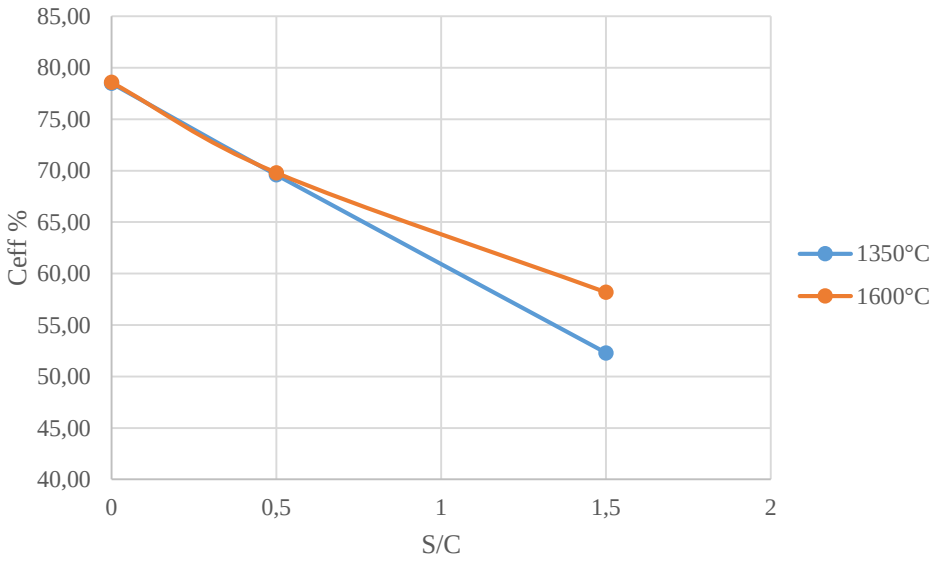

Figure 36 : Carbon efficiency versus S/C for case 2 and case 3

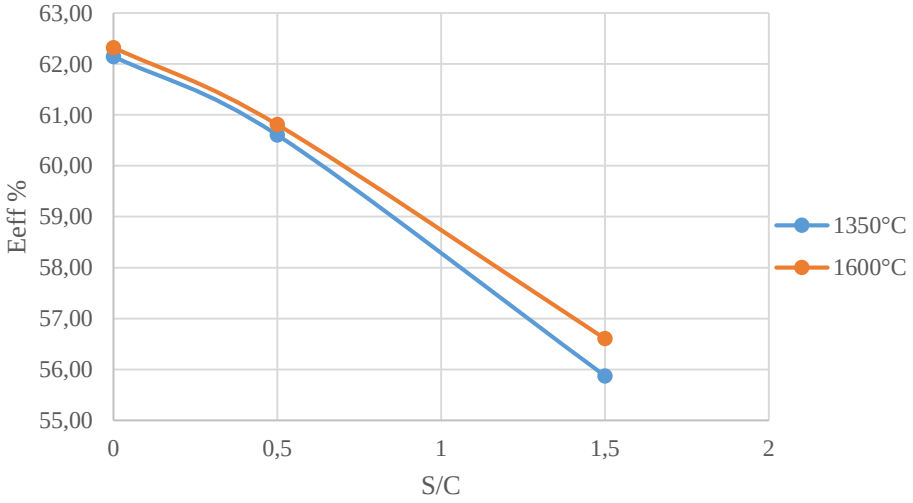

Figure 37 : Energy efficiency versus S/C for case 2 and case 3

Introducing steam makes drop the efficiencies for the same reasons than given before: more oxygen is needed to keep the gasifier temperature even if the oxygen is pre warmed and H_2O and O_2 oxidize the syngas (CO and H_2). Moreover, the ratio H_2/CO at the gasifier outlet is improved when steam is introduced. Less H_2 needs to be added to adjust the ratio which is a saving but it also means that less CO_2 is converted into CO in the WGSR. Indeed, equilibrium is assumed in the WGS reactor and then, the presence of steam shifts the reaction towards the opposite direction. It is what happened for the case 3 for S/C=2, CO_2 was produced and not consumed. To avoid that, the results for S/C=2 at TO_2=1600°C are given for a higher WGS temperature:

1100°C. Additional steam in the gasifier leads to less hydrocarbons produced, a lower carbon capture and so, lower efficiencies. Heating the oxygen at 1600°C instead of 1300°C does not show a high benefit, especially if we consider the price of ceramic heat exchanger needed to process stream in this range of temperature. The cost of hydrogen and the price of hydrocarbons are now discussed.

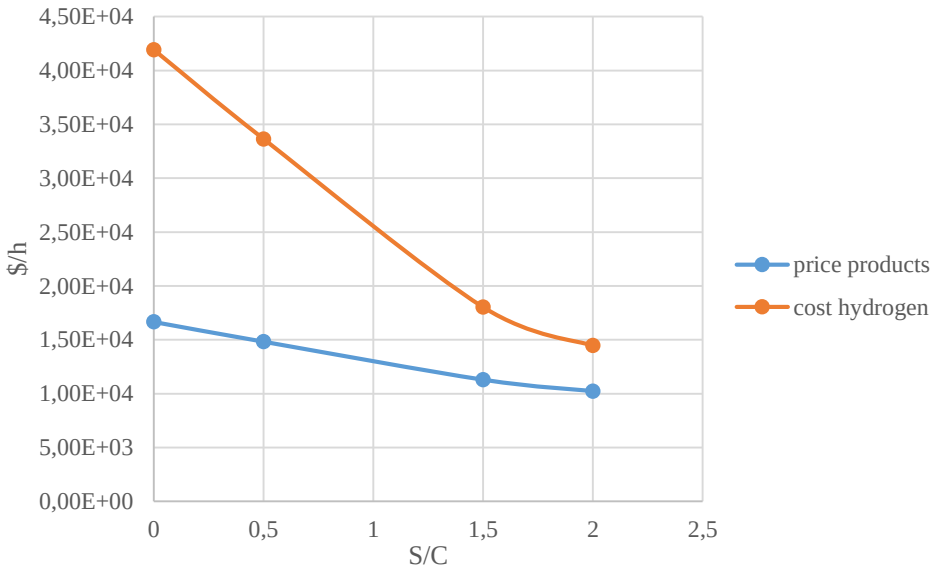

Figure 38 : Cost of hydrogen supply and price of the products in function of S/C ratio at TO_2 = 1600°C

The slopes change for the last point (S/C=2) since the temperature of the WGSR has been changed to avoid the CO_2 production in the WGSR. The cost of the hydrogen supply decreases as expected and draws near the price of the production but stays above. Although the economic aspect is improved, adding water moves one away from the main aim of a hybrid carbon-hydrogen process which is to produce fuel without releasing CO_2.

S/C	0	0,5	1,5
actual S/C	1,82E-04	5,00E-01	1,50E+00
λ	0,66	0,69	0,75
H_2 supply (Kg/h)	1,05E+04	8,46E+03	4,56E+03
CO_2 conv %	35,34	22,98	3,95
CO produced WGS (Kgmol/h)	139,23	188,78	56,17
V_{CSTR} (m3)	601,00	604,50	587,40
%CO_2 in FT	0,62	1,57	3,46
%CH_4 in FT	1,31	1,10	0,78
%C_{eff}	78,50	69,60	52,31
%$E_{eff\ mod}$	62,15	60,60	55,87
Products (Kg/h)	4,02E+04	3,57E+04	2,69E+04
Density (Kg/m3)	752,40	755,00	761,80
API °	56,48	55,83	54,16
Price products $/h	1,66E+04	1,48E+04	1,12E+04
Price hydrogen $/h	4,20E+04	3,38E+04	1,82E+04

Table 24 : Simulation results with additional hydrogen in the WGSR and heating of the oxygen supply at 1350°C (case 2) for different S/C

S/C	0	0,5	1,5	2
actual S/C	1,85E-04	5,00E-01	1,50E+00	2,00E+00
H_2 supply (Kg/h)	1,05E+04	8,41E+03	4,51E+03	3,62E+03
CO_2 conv %	34,98	22,53	3,61	4,49
CO produced WGS (Kgmol/h)	130,58	181,36	50,74	73,25
V_{CSTR} (m^3)	602,10	604,00	595,00	599,40
%CO_2 in FT	0,59	1,54	3,45	3,79
%CH_4 in FT	1,33	1,12	0,76	0,66
C_{eff}	78,59	69,81	5,82	47,63
$E_{eff\ mod}$ %	62,32	60,81	56,61	54,07
λ	0,65	0,68	0,74	13,44
Products (kg/h)	4,02E+04	3,58E+04	2,72E+04	2,46E+04
Density (Kg/m^3)	752,30	754,70	762,30	766,50
API °	56,51	55,91	54,04	53,02
Price products $/h	1,67E+04	1,48E+04	1,13E+04	1,02E+04
Price hydrogen $/h	4,19E+04	3,36E+04	1,80E+04	1,45E+04

Table 25 : Simulation results with additional hydrogen in the WGSR and heating of the oxygen supply at 1600°C (case 3) for different S/C

6.4. Valuation of the purge by heating oxygen and biomass streams case 4

The heat obtained from the burner is now used to warm up the oxygen inlet to 1600°C and the biomass to 100°C. The temperature of the WGSR is kept around 1100°C (+/- 30°C) and the results are given for different S/C ratio.

S/C	0	0,5	1,5	2
actual S/C	1,87E-04	5,00E-01	1,68E+00	2,00E+00
H_2 supply (Kg/h)	1,04E+04	8,39E+03	5,07E+03	3,53E+03
% CO_2 conv WGS	30,89	22,61	9,77	3,89
CO produced WGS (Kgmol/h)	103,49	173,58	133,90	62,12
V_{CSTR} (m^3)	602,20	607,80	606,60	605,90
%CO_2 in FT	0,55	1,45	3,01	3,73
%CH_4 in FT	1,35	1,14	0,82	0,66
C_{eff}	78,77	70,37	55,22	48,19
$E_{eff\ mod}$ %	62,74	61,45	57,41	54,90
λ	0,62	0,65	0,71	0,75
Products (kg/h)	4,03E+04	3,61E+04	2,85E+04	2,49E+04
Density (Kg/m^3)	752,30	754,70	761,30	766,90
API °	56,51	55,91	54,28	52,93
CO_2 removal (kg/h)	9,17E+03	2,35E+04	4,89E+04	6,06E+04
CO_2 in purge (kg/h)	7,18E+02	1,85E+03	3,86E+03	4,79E+03
Tot CO_2 disposal (Kg/h)	9,89E+03	2,54E+04	5,27E+04	6,54E+04
Price products ($/h)	1,67E+04	1,50E+04	1,18E+04	1,03E+04
Price hydrogen ($/h)	4,14E+04	3,36E+04	2,03E+04	1,41E+04

Table 26 : Simulation results for different S/C ratio at TO2=1600°C and Tbiomass=100°C

As previously, the best results are obtained for S/C= 0. The amount of disposed CO_2 has been collected and it is noticed that it increases considerably with high value of S/C. Heating the biomass improves slightly the performance. By comparing with the case 3, C_{eff} in between 0.2-0.5 percentage-points better in case 4 and $E_{eff\ mod}$ is between 0.4-0.8 percentage-points higher. The amount of products and of hydrogen is similar between the two cases.

The workbook for case 4 is given appendix F. Results been obtained using the following parameters: $T_{biomass}$ = 100°C, T_{oxygen} = 1600°C, T_{WGS} = 993°C, S/C= 0, CO_{conv} = 65.1%, recycle split = 0.9 and purge = 0.2.

λ	0,62	**CO_2 removal (kg/h)**	8,775E+03
V_{CSTR} (m^3)	603,9	**CO_2 purge (kg/h)**	6,97E+02
% E_{eff}	63.09	**CO_2 tot (Kg/h)**	9,472E+03
% C_{eff}	79.4	**actual S/C**	1,81E-04
% carbon loss WGS	44,52	**%CH_4 in FT**	1,34
H_2/CO	0,6405	**%CO_2 in FT**	0,54
syngas (Kg/h)	1,277E+05	**% inerts**	2,05
products (kg/h)	4,06E+04	**Products price $/year**	1,35E+08
Products (bbl/d)	8,515E+03	**Hydrogen cost $/year**	3,33E+08

Table 27: main data of the case 4 (purge ratio = 0.2 and recycle split = 0.9)

Considering the limitation of CO exhausted, it is found that $1.706.10^5$ Kg/h of air shall be introduced in the burner in this case. It is recalled that the maximum heat flow available from the burning is obtained considering 80% efficiency for the unit and considering that the outlet is cooled down to 100°C.

	Burner 80% efficency	**HX for O_2 stream**	**HX for Biomass stream**
Heat flow (KJ/h)	2.93E+08	6,176E+07	2.613E+07

Table 28 : Heat flow for case 4

Both biomass and oxygen streams can be heated up by the heat generated by the burner.

6.5. Discussion of the optimal configuration

The case 4 presents the highest yields. The biomass and the oxygen inlets are respectively warm up at 100°C and 1600°C which enables one to reduce the oxygen content in the gasifier. However, the oxygen supply does not decrease significantly in the case 4 in comparison with the base case. It is due to the fact that the recycle flowrate entering in the gasifier doubles when using hydrogen in the process. As the recycle stream is around 36°C, the more recycle gas, the more oxygen one needs to add in order to maintain the gasifier temperature at 1300°C. The main issue is that the gasification performances drop if one has oxygen and water in the gasifier. In other words, it is because oxygen is present in the gasifier that the efficiencies diminish when water is added. The consequence is no steam supply in the gasifier which leads to a really low H_2/CO at

the gasifier outlet. High amount of hydrogen is then supplied to adjust the H_2/CO ratio. Indeed, 10 tons per hour of hydrogen has to be introduced in the WGS reactor for the case 4. It is important to reduce the hydrogen supply which causes important extra cost. The case 4 is not optimal and can be improved since a lot of heat from the purge burning is available. For instance, the recycle stream can be heating to 1600°C as the oxygen inlet. 1600°C is believed to be the maximal allowed temperature for a high temperature heat exchanger. The biomass can be warm up to at least 300°C and extra heat can be used to directly warm up the vessel. If enough pre-heating is used, oxygen can be diminished and water steam can be added in the gasifier which must significantly reduce the H_2 supply as well as the operating cost. The optimal operating conditions for the process is obtained when enough water is supplied in the gasifier for approaching as much as possible the ratio value H_2/CO = 1.98 while in the same time having $\lambda = \lambda_{optimal}$. In this way, the hydrogen supply is minimized and the syngas production is maximized. Besides, the impact of the recycle has not been investigated when using the hybrid hydrogen-carbon process. It is however a relevant question since the tail gas contains some CO_2 which can be converted in the WGS reactor if recycled into the gasifier. The carbon efficiency would be then improved.

7. Heat integration

7.1. Error in Aspen Energy Analyser

Aspen EA uses the following equations to determine the total annual cost (TAC):

$$TAC = \Lambda.\sum CC + OC \quad (33)$$

$$\Lambda = \frac{\left(1+\frac{ROR}{100}\right)^{PL}}{PL} \quad (34)$$

CC : Installed capital cost

OC : Operating cost

Λ : Annualization factor

ROR : rate of return

PL : plant life

However, by using the latter expression, one can see the "Total cost" of the design increases when the plant life (PL) increases as well, contrary to what had been expected. Magne Hillestad had sent an e-mail to "AspenTech Support" at the request of a student (Tor Olav Høva Erevik) to get an opinion about this issue. "AspenTech support" recognized an error in the capital cost calculation (see e-mail in appendix M). The equation which shall be used is the one provided by Sinnott (29):

$$TAC = ACCR.\sum CC + OC \quad (35)$$

$$ACCR = \frac{i(1+i)^n}{(1+i)^n-1} \quad (36)$$

ACCR: Annual capital charge ratio

i: Interest rate

n: Number of years

In the current report, it has been chosen to calculate the capital cost using the method given by Sinnott and Towler as it is explained in the chapter 8 (the capacity "S" is in this case the total heat exchanger area) . The operating cost of the heat exchanger network given by Aspen EA is however used.

7.2. Base case

The Heat Integration (HI) has been realized by using Aspen Energy Analyser. A table summarizes the process streams in Appendix I. The global minimum approach temperature is set to 15 °C which is the average between ΔTmin for a liquid match (ΔTmin = 10°C) and a liquid gas match (ΔTmin = 20°C). The steam outlet from the FT cooling system is considered as a "utility stream" since this stream has no temperature requirement. The stream is called "FT steam" and it is specified as a MP steam at 220°C. A utility stream called "Cooling water" has been added with an original temperature at 5°C, which is realistic if the plant sets in a cold country. The composite curves are presented below:

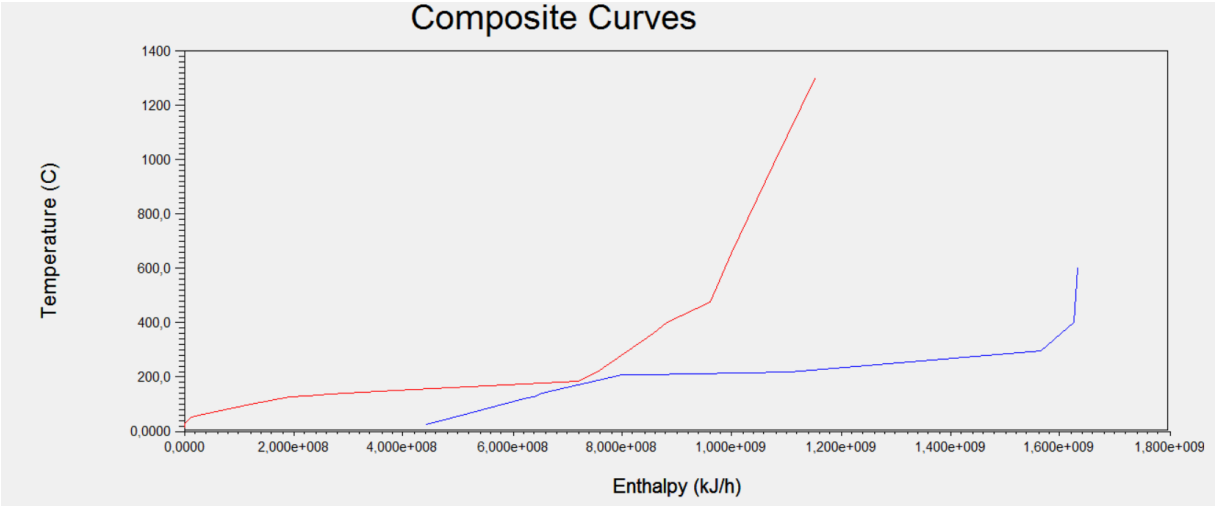

Figure 39 : Composite curves for the base case

The hot pinch temperature is obtained at 187.9°C and the cold pinch temperature at 172.9°C.

50 Heat Exchanger networks have been generated by Aspen EA using the option "Recommend designs". Only one possible design has been generated. The generation of design has been performed taking into account many utilities streams which were proposed by Aspen EA:

Name		Inlet T [C]	Outlet T [C]	Cost Index [Cost/kJ]	Segm.	HTC [kJ/h-m2-C]	Target Load [kJ/h]	Effective Cp [kJ/kg-C]	Target FlowRate [kg/h]	DT Cont. [C]
Air		30,00	35,00	1,000e-009		399,60	5,219e+007	1,000	10437514,03	10,00
Cooling water 1		20,00	25,00	2,125e-007		13500,00	3,423e+006	4,183	163679,39	5,00
Refrigerant 1		-25,00	-24,00	2,739e-006		4680,00	4,014e+005	4,000	100353,03	3,00
HP 1		250,0	249,0	2,500e-006		21600,00	3,996e+008	1703	234648,80	10,00
Hot Oil		280,0	250,0	3,500e-006		836,22	4,411e+007	3,000	490127,14	5,00
LP Steam Generation		124,0	125,0	-1,890e-00E		21600,00	3,828e+008	2196	174282,17	10,00
Cooling Water		5,000	25,00	2,125e-007		13500,00	1,606e+006	4,183	19192,55	Global
FT steam		220,0	219,0	2,200e-006		21600,00	3,578e+007	1981	18060,29	Global

Table 29 : Listing of the utility streams suggested by Aspen EA

The resulting design is presented appendix H. A refrigerant is expensive and not necessary for this process. The cooling can be guaranteed by cold water represented by the stream “Cooling Water”. Besides, the hot steam generated by the cooling system of the FT reactor “FT steam” is assumed to be partly used to warm up the water inlet of the cooling system and partly used to generate electricity:

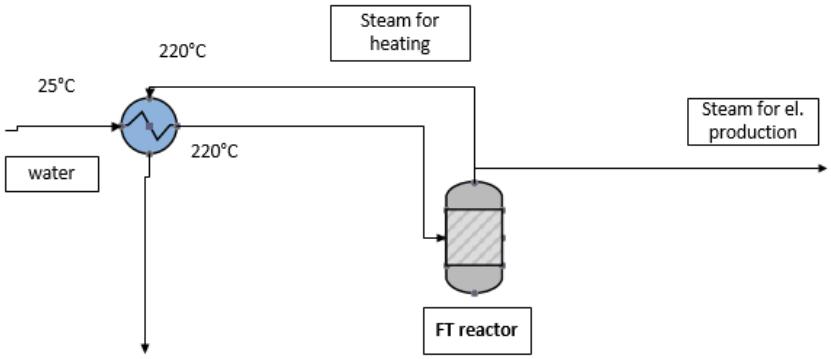

Figure 40 : Diagram of the Fischer-Tropsch cooling system

These changes leads to the heat exchanger design shown appendix I. The steam warms up the water until 210.3°C and high pressure steam brings the water to 220°C. The unused steam from the FT cooling system is used for electricity production.

The unused streams are deleted: “Air”, “Refrigerant 1” and “Hot oil” and the cost index for “FT steam” is set at 0 since the steam is available free from the FT cooling steam.

Name		Inlet T [C]	Outlet T [C]	Cost Index [Cost/kJ]	Segm.	HTC [kJ/h-m2-C]	Target Load [kJ/h]	Effective Cp [kJ/kg-C]	Target FlowRate [kg/h]	DT Cont. [C]
Cooling water 1		20,00	25,00	2,125e-007		13500,00	5,561e+007	4,183	2658901,49	5,00
HP 1		250,0	249,0	2,500e-006		21600,00	3,996e+008	1703	234648,80	10,00
LP Steam Generation		124,0	125,0	-1,890e-00E		21600,00	3,828e+008	2196	174282,17	10,00
Cooling Water		5,000	25,00	2,125e-007		13500,00	1,606e+006	4,183	19192,55	Global
FT ssteam		220,0	219,0	0,0000		21600,00	3,578e+007	1703	21011,48	Global

Table 30 : Listing of utility streams used in the heat exchanger network design for the base case

For an unknown reason, after deleting the streams, Aspen Energy Analyzer states in the tab “scenario/Summary/Targets” that the heating and cooling requirements are not fulfilled because of a lack of utility streams, even if the design is still performing. Results are available in appendix I.

7.3. Case 4

The list of process streams is available in appendix J. A hot stream at really high temperature (1572°C) is obtained in the case 4 after burning the purge. As the stream has no temperature requirement, it is considered as a utility stream and its cost index is set at 0 USD/KJ. The steam generated by the FT cooling system is completely used to generate electricity and does not take part to the heat integration in this case.

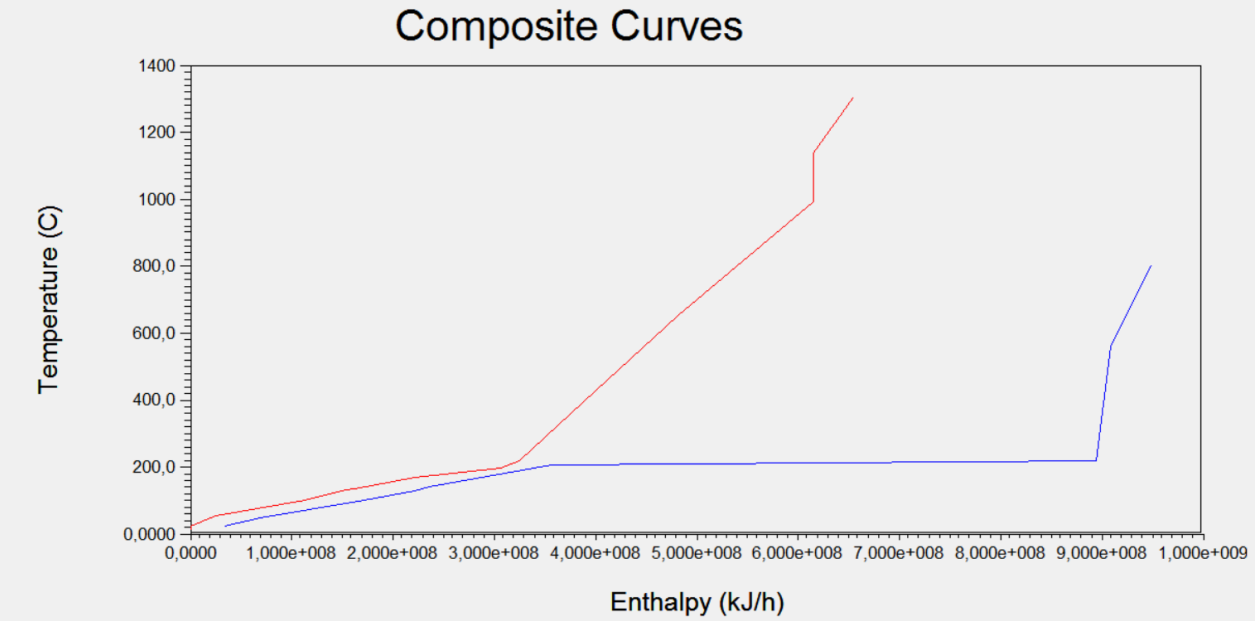

Figure 41 : Composite curves case 4

The global minimum approach temperature is set to 15 °C for the same reason than cited for the base case. The hot pinch temperature is obtained at 196.6°C and the cold pinch temperature at 181.6°C. 42 recommended design have been generating in Aspen EA and most of them presented a negative operating cost which means that the heat exchanger network produces an important amount of steam that can be sold. The design with the smallest negative operating cost has been selected. The outlet temperature of the utility stream "vap pure / cold gas" had to be set at 197°C instead of 100°C to avoid a cross pinch issue.

Name		Inlet T [C]	Outlet T [C]	Cost Index [Cost/kJ]	Segm.	HTC [kJ/h-m2-C]	Target Load [kJ/h]	Effective Cp [kJ/kg-C]	Target FlowRate [kg/h]	DT Cont. [C]
LP Steam Generation		124,0	125,0	-1,890e-00E		21600,00	2,288e+007	2196	10415,05	10,00
vap purge to cold gas		1572	197,0	0,0000		720,00	2,927e+008	1,430	148879,50	Global
Cooling Water		5,000	25,00	2,125e-007		13500,00	1,146e+007	4,183	136924,35	Global

Figure 42 : Listing of utility streams used in the heat exchanger network design for the case 4

Results are available in appendix J.

8. Costing

8.1. Sizing and costing of major equipment

The costing method given by Sinnott and Towler (29) was followed. The purchased equipment costs are determined using the Table 66 in Appendix K and the following equation:

$$Ce = a + bS^n \quad (37)$$

Ce : purchased equipment cost on a US Gulf Coast basis, Jan. 2007

a,b,n : constants in table appendix K

S : size parameter

The updated purchased cost Ce,i,2014 is found by the following equation where $CEPCI_{2015}$ and $CEPCI_{2007}$ are respectively the cost index of the purchased equipment in May 2015 (equal to 560.7) (30) and January 2007 (equal to 509.7). CEPCI is the Chemical Engineering Plant Cost Index.

$$Ce,i,2014 = Ce,i,2007.\frac{CEPCI\ 2015}{CEPCI\ 2007} \quad (38)$$

Then, the total purchase cost C is given by the below equation (p309):

$$C = \sum_{i=1}^{i=M} Ce,i.((1+fp) + (fer + fel + fi + fc + fs + fl)/fm) \quad (39)$$

M : number of equipment

fx : installation factor (cf Appendix K)

C : installed cost on a US Gulf Coast basis, Jan. 2007

The equipment of the plant are in 304 stainless steel to avoid corrosion, hence f_m=1.3. For pressure vessels, the size parameter is the shell mass. The first step is then to size the unit. The thickness is determined using the operating pressure and operating temperature:

$$t = \frac{Pi.Di}{2SE - 1.2Pi} \quad (40)$$

Pi : internal design pressure (10% greater than the operating pressure) (KPa)

Di : Internal diameter (m)

S : maximal allowable stress (KPa)

E : welded-joint efficiency (here taken equal to 1)

The maximal allowable stress is determined using the appendix K. The mass of the shell is given by the below equation:

$$m_{shell}\ (Kg) = \pi.Di.H.t.\rho_{304ss} \quad (41)$$

Di : Internal diameter (m)

H : Height (m)

ρ_{304ss} : density of 304 stainless steel (8000 Kg/m^3)

The costing can also be realized thanks to historic cost data:

$$C_2 = C_1.(\frac{S2}{S1})^n \quad (42)$$

C_i: ISBL capital cost of the plant with capacity S_i

8.1.1. Fischer-Tropsch

8.1.1.1. Sizing

The Fischer-Tropsch is sized in function of its inlet capacity q_{in} (m^3/s). It is recalled that FT reactor are thriphasic reactor. The gas velocity should be important enough for suspending the solid phase and low enough to avoid the liquid and the solid to be carried away through the outlet. A typical average superficial gas velocity is between 0.25-0.27 m/s. The cross section area is noted A (m²).

$$q_{in} = v_{sup}.A \quad (43)$$

The diameter of a cylindrical vessel is considered:

$$D = \sqrt{\frac{4.qin}{\pi.vsup}} \quad (44)$$

Knowing the diameter D (m) and the volume Vcstr (m^3) (given by the ACM model in Aspen Hysys), the height Hcstr (m) can be deduced:

$$Hcstr = \frac{4.Vcstr}{\pi.D^2} \quad (45)$$

The slurry composes 67 vol% of the volume of the equipment and 20 wt% of the slurry is the catalyst (cobalt).

	Base case	Case 4
Diameter (m)	4.92	6.546
Height (m)	20.436	17.95
Thickness (m)	0.0573	0.0764

Table 31 : Sizing Fischer-Tropsch

8.1.1.2. Costing

The FT reactor is considered as a vertical pressure vessel made of 304 stainless steel. The cobalt catalyst price is evaluated using the price of pure cobalt at 99.8% (29.4317 USD/Kg (31)) and the needed mass of catalyst is calculated in the ACM model. The price of the U-tube used to cool down the reactor as well as the price of the catalyst are added to the purchase price of the shell. The installation factor and the escalation are applied to the sum. The area of the U-tube is determined by multiplying the specific area (40 m^{-1}) with the FT volume.

Base case		Case 4	
Area U-tube (m^2)	1,55E+04	Area U-tube (m^2)	2,42E+04
Mass catalyst (ton)	43	Mass catalyst (ton)	66.9
Mass shell (ton)	5,59E+02	Mass shell (ton)	1,16E+03

Table 32 : Data for the costing of the Fischer-Tropsch

Historic data have been used to verify the accuracy of the cost result for the base case. Kreutz (1) (p 45) gives the cost of the Fischer-Tropsch reactor integrating the cost of the heat exchanger. For a capacity (S1) of 2.5 MMSCF/h, the reactor costs (C1) 13.6 $M\$_{2007}$. Using the capacity of the simulated plant for the base case (S_2 = 0.637 MMSCF/h), the equation $C_2 = C_1.(\frac{S2}{S1})^n$ (42) and after escalation, the FT cost must be 9 $M\$_{2015}$. By considering the FT reactor as a pressure vessel, it is found that the FT cost is 30 $M\$_{2015}$ (Catalyst, U tube and installation cost included). However, the price for a Fischer-Tropsh reactor that have been found in literature are closer to the highest estimation (32),

(3). Furthermore, historic estimation gives rough estimation. Thus, the FT shell cost is determined by considering it as a pressure vessel (30 M$).

8.1.2. Entrained-flow gasifier

8.1.2.1. Sizing

The entrained-flow gasifier is sized according to the residence time of solid particles and of gas. The ECN (33) and REI report (34) give one those information. 2 seconds and 1 seconds are selected as residence time for respectively the gas (τgas) and the solid particles (τsolid).

$$Vgas\ (m^3) = \tau gas.Qgas \quad (46)$$

$$Vsolid\ (m^3) = \tau solid.Qsolid \quad (47)$$

With Qgas = 1.48 m^3/s and Qsolid = $3{,}28.10^{-2}$ m^3/s (for the base case) and by summing the two volumes, the gasifier volume V is find to be 12 m^3. The ratio length over diameter is determined using data from the Chapter 8 of the book "Biomass Gasification, Pyrolysis and Torrefaction" (Table 8.9) (35) which presented data of commercial entrained-flow gasifier. The ratio L/D is taken equal to 1.75 which leads to the result in the next table.

$$D = \left(\frac{4*Vtot}{\pi*1.75}\right)^{1/3} \quad (48)$$

It is remarked that the data appendix K to determine the maximal allowable stress are given for a temperature range between 38°C and 482°C. Smax has been determined at 1300°C by extrapolation of the known values.

	Base case	**Case 4**
Diameter (m)	1.04	1.28
Height (m)	1.82	2.23
Thickness (m)	0.0238	0.0292

Table 33 : Sizing Entrained flow gasifier

NB : The sizing is reconsidered in the costing. Indeed, the cost resulting from the sizing seems not realistic. The error might come from the extrapolation of the stress value at T=1300°C.

8.1.2.2. Costing

The price has been evaluated considering the gasifier as a pressure vessel. The cost of the reactor for the base case is obtained equal to 0.147 M$. This result seems low and not realistic comparing

with results from the literature (see appendix 2 of the Holmgren's thesis (32) and Kreutz (p44)). Holmgren refers to a plant with an inlet of 483 MWth (here 433.3 MWth) which costs 173M$$_{2007}$. Using those data and a cost scaling factor n=0.5, the cost of the simulated gasifier must be 180M$$_{2015}$. Kreutz presents a plant with a capacity of 815 MWth, a cost of 198.8M$$_{2007}$ and uses a scaling factor n=0.67. By applying those data, the current reactor cost would be 143M$$_{2015}$. The results obtained with Holmgren's study (180M$) is selected because the capacities (in MWth) are similar which reduces the error. The same thinking is followed for the case 4.

The error in the sizing and the costing can have several causes. First, the table 67 gives the maximal stress for temperature between 37.7°C and 482.2°C. The maximal allowable stress for the gasifier operating at 1300°C has been extrapolated using the equation of the trend curve which might be source of inaccuracy since it is an extrapolation and not an interpolation. Secondly, the residence time are rough approximations and probably generate important imprecision.

8.1.3. Water-gas-shift reactor

8.1.3.1. Sizing

The WGS reactor is sized using an approximate residence time. Different values have been found: Callaghan (36) uses a residence time equals to 1.8 seconds for an inlet composed of around 10 mol% of CO and a concentration between 25 and 10 mol% of H_2O. Guan et al (37) gives residence time values in function of the CO conversion. For a WGS reactor at 800-850°F and for a CO conversion around 55%, Guan et al proposes residence time between 0.25 and 0.5 seconds. For the base case simulation in this study, X_{CO} = 48.37 mol%. Using the figure 4 in the last reference and the CO conversion in this study, the hold-up time should be 0.25 seconds. However, taking into account that the reactor operates at 752 °F, the residence time should be slightly higher. A hold-up time of 0.4 seconds is then chosen for the sizing. The volume occupied by the gas phase is determined using equation V_{gas} (m^3) = $\tau_{gas}.Q_{gas}$ (46) and the total volume is determined assuming that the catalyst takes 60vol% of the reactor. Using a ratio H/D of 2 (38), the diameter is calculated thanks to the equation $D = \left(\frac{4*Vtot}{\pi*1.75}\right)^{1/3}$ (48).

	Base case	Case 4
Diameter (m)	1.3	1.95
Height (m)	2.597	3.90
Thickness (m)	0.018	0.0273

Table 34 : Sizing Water-gas-shift reactor

NB : The sizing is reconsidered in the costing. Indeed, the cost resulting from the sizing seems too low comparing with prices in literature.

8.1.3.2. Costing

WGS reactor is costed as a horizontal pressure vessel. The catalyst price (Fe_2O_3-Cr_2O_3 for a high temperature water gas shift reactor) is around 10 $/Kg (39) , the bulk density is taken at 1.6 Kg/L (40) and it is estimated that 60vol% is taken by the catalyst. The WGS reactor for the case 4 is also a high temperature water-gas-shift and then uses the same catalyst.

	Base case	Case 4
Mass catalyst (ton)	4.95	16.8
Mass shell (ton)	1.54	5.24

Table 35 : Data for the Water gas shift costing

The purchased cost includes the catalyst cost. The obtained cost (including the escalation and installation costs) is 0.327 $M\$_{2015}$. The WGS reactor cost seems low. The Kreutz data (p 44) are the same as those used in Holmgren's report and makes one obtained a cost of 2.2$M\$_{2015}$ for the current study. The last is used for the final costing. The error in the costing is probably due to the utilization of an approximated retention time for the sizing of the unit.

8.1.4. Separators vertical

8.1.4.1. Sizing (41)

If the vapor fraction of a stream is high, a vertical separator is preferred to a horizontal separator. The settling velocity u_t (m/s) is the falling speed of the liquid droplets and it enables one to determine the maximal gas velocity which still enables the liquid droplet to settle in the vessel. It is determined using the following equation:

$$u_t \text{ (m/s)} = 0.07 \left(\frac{\rho L - \rho V}{\rho V}\right)^{1/2} \quad (49)$$

The presence of a demister is assumed so $v_{sup}=u_t$. The diameter is determined by the equation $D = \sqrt{\frac{4.qin}{\pi.vsup}}$ (44).

The height depends on the diameter and on the residence time of the liquid (τliq) which is around 10min.

$H(m) = 0.4 + D + D/2 + H_{liq}$ (50)

$H_{liq}\,(m) = \frac{4.Vliq}{\pi.D^2}$ (51)

$V_{liq}\,(m^3) = \tau_{liq}\,(s).Q_{liq}\,(m^3/s)$ (52)

D (m) : intern diameter

H_{liq} (m) : High of liquid in the separator

	Base case	Case 4
Diameter (m)	2.53	3.12
Height (m)	11.73	5.34
Thickness (m)	0.021	0.026

Table 36 : Sizing dryer

8.1.4.2. Costing

The dryer is costed as a pressure vessel made of 304 stainless steel.

8.1.5. Horizontal three phase separator (42)

8.1.5.1. Sizing

As for the case of the vertical separator, the liquid droplets have to settle through a gas. By equalizing the gas retention time with the settling time of droplets, the following equation (gas capacity constraint equation) is found:

$d.Leff = 420.\frac{T.Z.Qg}{P}.(\frac{CD.\rho g}{dm.(\rho l-\rho g)})^{1/2}$ (53)

d : inside vessel diameter (in)

Leff : vessel effective length (ft)

T : operating temperature (°R)

Z : gas compressibility

CD : drag coefficient (assumed equal to 2)

dm : diameter liquid droplet (μm)

ρ : density (lb/ft^3)

P : operating pressure (psia)

Qg : gas flow rate (MMscfd)

A retention time constraint equation is also set to ensure the separation between oil and water:

$$d^2.Leff = 1.42\ (Q_w.tr_w + Q_o.tr_o) \quad (54)$$

Q : flow rate (BPD)

tr : retention time (min)

As recommended in the chapter 4 of the book "Gas-Liquid and Liquid-Liquid Separators, 10min is chosen for the water retention time and 5 min for the oil phase since the oil production from the simulation belongs to very light crude oil (API° >40°). For dm=500μm, the maximum oil pad thickness results from the below equation:

$$H_{o,max}\,(m) = 320\,\frac{tro.\Delta SG}{\mu} \quad (55)$$

It is pointed that the equation (4.6b) in the book of reference (42) contains a mistake in the coefficient. For dm =500 μm, the equation should be:

$$H_{o,max}\,(m) = 825\,\frac{tro.\Delta SG}{\mu} \quad (56)$$

ΔSG : difference between specific gravity

μ : oil viscosity (cP for equation 42 and Pa.s for 43)

The fraction of the vessel cross section area which is occupied by water is given by:

$$\frac{Aw}{A} = 0.5\frac{Qw.trw}{tro.Qo+trw.Qw} \quad (57)$$

Using the graphic "4.20" from the reference, the maximal internal diameter is found:

$$d_{max} = \frac{(ho)max}{\beta} \quad (58)$$

Several diameter inferiors to d_{max} are considered. Leff is calculated for those diameter respecting the retention time constraint $d^2.Leff = 1.42\ (Q_w.tr_w + Q_o.tr_o)$

(54). The estimate seam-to-seam length is then estimated:

$$Lss = 4/3.\ Leff \quad (59)$$

The couple diameter-length is selected for a slenderness ratio SR between 3 and 5, which offer the best economical solution:

$$SR = 12\frac{Lss}{d} \quad (60)$$

Results are presented below and the selected diameter-length couple is in bold text.

d (in)	Leff (ft)	Lss (ft)	SR
40	3,91E+01	5,21E+01	1,56E+01
50	2,50E+01	3,34E+01	8,01E+00
60	**1,74E+01**	**2,32E+01**	**4,63E+00**
70	1,28E+01	1,70E+01	2,92E+00
80	9,78E+00	1,30E+01	1,96E+00

Table 37 : Determination of the couple diameter-length for 3 phases separator (base case)

d (in)	Leff (ft)	Lss	SR
40	7,89E+01	1,05E+02	3,15E+01
50	5,05E+01	6,73E+01	1,62E+01

60	3,51E+01	4,67E+01	9,35E+00
70	2,58E+01	3,43E+01	5,89E+00
80	**1,97E+01**	**2,63E+01**	**3,94E+00**
90	1,56E+01	2,08E+01	2,77E+00

Table 38 : Determination of the couple diameter-length for 3 phases separator (case4)

	Base case	**Case 4**
Diameter (m)	1.524	2.03
Height (m)	7.07	8.02
Thickness (m)	0.0109	0.0145

Table 39 : Sizing 3 phases separator

8.1.5.2. Costing

The three phase separator is costed as a horizontal pressure vessel made of 304 stainless steel.

8.1.6. Air Separation Unit

The costing is scaled from the Statoil's data given in the e-mail Appendix N and using the equation $C_2 = C_1.(\frac{S2}{S1})^n$

(42). The ISBL cost C_1 is given for 2005. The escalation for 2015 is obtained using $CEPCI_{2005}$=468.2 (43).

8.1.7. Acid gas cleaning

8.1.7.1. Sizing

A scrubber using MEA is considered. The diameter is determined by the abacus appendix L with Qgas = 8.65 MMSCFD (for the base casee) and P = 282.8 psig. The length is determined considering the ratio length-to-diameter (L/D) equal to 7 (44). The vessel for the absorption has an operating temperature of 54.43°C and the vessel for the recovery is at 120°C (45), (46) (p 41). The thicknesses are determined for this two temperatures.

Base case				Case 4			
Absorption		Regeneration		Absorption		Regeneration	
Diameter (m)	0.762	**Diameter (m)**	0.762	**Diameter (m)**	0.8382	**Diameter (m)**	0.8382
Height (m)	5.334	**Height (m)**	5.334	**Height (m)**	5.87	**Height (m)**	5.87
Thickness (m)	0.0064	**Thickness (m)**	0.0076	**Thickness (m)**	0.0071	**Thickness (m)**	0.00835
T (°C)	54.43	**T (°C)**	120	**T (°C)**	56.01	**T (°C)**	120

Table 40 : Sizing scrubber

8.1.7.2. Costing

The information given in the report (46) are used to determine the needed amount of MEA. MEA absorbs H_2S, CO_2 as well as H_2O and it is assumed that they need the same amount of MEA to be absorbed. The cost of MEA is part of the purchased cost, so both shell and MEA cost receive the escalation and are multiplied by the installation factor.

Base case				Case 4			
H_2S absorbed (Kg/h)	82.317	**Kg MEA/Kg compound captured**	1.5	**H_2S absorbed (Kg/h)**	84.65	**Kg MEA/Kg compound captured**	1.5
CO_2 absorbed (Kg/h)	82287.8	**USD/ton MEA**	1200	**CO_2 absorbed (Kg/h)**	8775.27	**USD/ton MEA**	1200
H_2O absorbed (Kg/h)	1213	**Cost MEA USD**	1,50E+05	**H_2O absorbed (Kg/h)**	1894.54	**Cost MEA USD**	1,94E+04

Table 41 : Monoethanolamine (MEA) data

8.1.8. Compressors and Heat exchangers

Centrifugal compressors are assumed in the study. The size parameter "S" for compressors is the driver power (KW) and it is the area (m²) for heat exchangers. The driver powers and the heat exchanger area are available in appendix I and J.

8.1.9. ISBL and Fixed capital costs

All of the equations used in this subsection come from the 5th edition of Towler and Sinott (29).

The inside battery limits cost is defined:

$$C_{ISBL} = \sum Ce,i \,.\, fe,i \quad (61)$$

Ce,i: purchased cost after escalation of the unit i

fe,i: installation factor for the unit i

Finally, the total fixed capital cost is calculated by the following:

$$C_{FC} = C.(1+OS).(1+D\&E+X) \quad (62)$$

C_{FC} : Total fixed capital cost on a US Gulf Coast basis, Jan. 2007

OS : Offsite investment

D&E : Design and Engineering cost

X : Contingency

For this type of process (fluid process):

Offsites (OS)	0.3
Design and Engineering (D&E)	0.3
Contingency (X)	0.1

Table 42 : Factors to define fixed capital cost (Offsites, Design and Engineering Contingency costs)

Working capital is estimated equal to 15% of the Fixed capital cost and the Investment is defined by the sum:

$$\text{Investment (USD)} = \text{Working Capital (USD)} + C_{FC}\,\text{(USD)} \quad (63)$$

	Base case (USD)	Case 4 (USD)
Installed costs		
Fischer-Tropsch	3.00E+07	5,17E+07
Gasifier	1.80E+08	1,80E+08
Water gas shift reactor	2,20E+06	2,20E+06
ASU	7,12E+07	6,70E+07
Scrubber	7,63E+05	3,37E+05
Separator horizontal	2,36E+05	3,96E+05
Dryer	9,31E+05	6,94E+05
Compressors	2,80E+07	1.73E+07
Heat exchanger	3.69E+07	2,40E+07
C_{ISBL}	**3.50E+08**	**3,84E+08**
F_{ISBL}	1.82	1.82
Fixed capital cost	**6.38+08**	**6.98E+08**
Working capital	9.57E+07	1,05E+08
Investment	**7.33E+08**	**8,03E+08**

Table 43 : ISBL and Fixed capital cost

8.2. Operating costs

8.2.1. Hydrogen

As the aim of the study is to avoid the release of greenhouse gases, the hydrogen is assumed to be produced from a carbon-free source. According to (47), hydrogen produces by non-traditional technologies costs approximatively 4USD/Kg. This price is particularly valid for conventional electrolysis and wind farm. The study forecasts a price of 1.84USD/Kg for hydrogen produced by a modular helium reactor. A second article (48) proposes the price for several renewable process: The lowest production cost estimations are 1.96$/Kg (4.9€ ct/KWh) for solar methane cracking, 2.11$/Kg (5.7 € ct/KWh) for solar hybrid Sulphur cycle, 2.21$/Kg (6 € ct/KWh) for solar Sulphur-iodine cycle and 3.88$/Kg (10.5 € ct/KWh) for solar metal/metal oxide cycle. In practice, it will likely be more expensive. The hydrogen price is here estimated at 4USD/Kg.

NB: The last prices were originally given in € ct/kWh H_2. The conversion has been made using the LHV of hydrogen (119.96 MJ/Kg H_2) and the exchange rate in May 2015 (€/USD = 1.11 (49)).

8.2.2. Biomass

Data about biomass are taken equal to those found in the NREL report (11). The estimation in the current study for dry biomass is then taken at 30 USD/dry ton. The U.S. Department of Energy (50) estimates the biomass to higher prices around 40-60$/dry ton and the prices announced by NREL, Statoil and Arlanda (14) are between 75 and 134 $/ton. 30$/dry ton is then an optimistic approximation.

8.2.3. Acid gas removal

Variable costs caused by the MEA replacement and the cost of water are neglected. Only the electricity cost is considered.

Heat consumption MJ/Kg compound removed	0.11 (51)
Electricity cost USD/Kwh	0,0681

Table 44 : Heat consumption of the acid gas removal and electricity cost

8.2.4. Heat exchanger

The operating cost represents the energy cost to run the equipment. It is determined by Aspen EA according to the following (52) (p 16):

$$OC = \sum(C_{hu}.Q_{hu,min}) + \sum(C_{cu}.Q_{cu,min}) \quad (64)$$

OC: Operating cost (USD/yr)

C_{hu}: utility cost for hot utility ($/KW.yr)

$Q_{hu,min}$: energy target of the hot utility (KW)

C_{cu}: utility cost for cold utility ($/KW.yr)

$Q_{cu,min}$: energy target of cold utility (KW)

The production and selling of steam are taken into account since “cooling cost” is a negative value. According to the Aspen Energy Analyzer Tutorial (version 8.8), the cost is given in United states dollar. As the tutorial is dated May 2015, it is assumed that no escalation is needed.

8.2.5. Labor

Number of operators per shift can be correlated to the number of major processing units (41).

$$N_{operators} = (6.29 + 0.23.N_{units})^{0.5} \quad (65)$$

The major processing units include reactors, columns, compressors and heat exchangers. 20 units have been enumerated for the base case which gives 3.3 operators i.e. 4 operators per shift. For the case 4, 27 units have been enumerated which gives one also 4 operators per shift. Considering 5 shifts per day, 20 operators would be needed. The total labor is assumed to be the double of the operators number and the average wage is taken equal to 64 690 USD/year (53).

8.2.6. Water

Water in the process is in contact with hydrocarbons whose solubility is non-negligible. The water from the dryer and the 3-phases separator has to be treated. The cost of wastewater treatment is approximated by 6 USD/1000 gal (41). The FT reactor produces water which satisfy the water supply of the WGS reactor. It is assumed that the cooling water of the FT reactor circulates in a closed loop and then, no water loss is considered.

out		in	
3 phase separator (Kg/h)	2,77E+04	WGS (Kg/h)	1,33E+04
Dryer (Kg/h)	2,24E+05		
Balance (out-in)	**2,38E+05**		

Table 45 : Water balance for the base case

out		in	
3 phase separator (Kg/h)	5.572E+04	WGS (Kg/h)	0
Dryer (Kg/h)	1.158E+04		
Balance (out-in)	**6.73E+04**		

Table 46 : Water balance for the case 4

8.2.7. Total operating costs

Costs generated by catalyst and MEA renewal are neglected. Estimations are made (41) : Supervision = 25%.Labor ; Maintenance = 40%.C_{ISBL} ; Plant_overhead=65%(Labor+Maintenance) and Taxes, insurance = 2%.Fixed capital. The number of hours of operation is set at 8000 h/y.

The following table gives details of the total variable cost calculation.

	Base case (USD/year)	Case 4 (USD/year)
Biomass	2,00E+07	2,00E+07
O_2 production	9,37E+06	8,47E+06
CO_2 capture	1,41E+06	1.82E+05
Wastewater treatment	4,65E+07	1,23E+07
Compressor	2,37E+06	1,12E+07
HX network	2,81E+06	-7.38E+06
H_2 supply	-	3,33E+08
Labor	2,59E+06	2,59E+06
Supervision	6,47E+05	6,47E+05
Maintenance	1,40E+08	1,53E+08
Overhead	9,28E+07	1,01E+08
Taxes, insurance	1,28E+08	1,40E+08
Total operating costs	**4,46E+08**	**5,26E+08**

Table 47 : Total variable costs

Operating costs are compared with those obtained in Penniall's thesis (54) (p65). In the thesis, the biomass represents 30% of the total operating costs contrary to the current study, where the biomass participates only for 4.5%. The comparison with the capital cost highlights even more the difference. Indeed, the operating cost represents only 12.6% of the capital cost in the Penniall's thesis. In the current paper, the operating cost is 70% of the capital cost. The operating cost result contains some errors. Achieved results are keeping because of the time limitation but a revaluation is needed. The errors are likely due to the high cost estimations of the wastewater treatment, the maintenance and the taxes. Besides, taking into account taxes is questionable since the plant is a renewable technology and by that, the taxes might be relaxed.

8.3. Revenues

The price of the products has been evaluated knowing the price of a barrel and the average thermal energetic content of a barrel.

$$\text{Price (\$/h)} = \frac{\text{Price barrel (\$/bbl)}}{\text{Energetic content (MBTU/bbl)}}.F_{products}(\text{Kmol/h}).LHV_{products}(\text{MBTU/Kmol}) \quad (66)$$

The price of the barrel is set at 60 USD (price for May 2015) to be consistent with the costing which uses the CEPCI from May 2015 (55), (56). More recent data give the price barrel around 40 USD referring to the number of 2016 on the eia web site (57). The average thermal energetic content of a barrel is evaluated at 6 million BTU (58). Steam is also an income source. The FT cooling water is boiling water at 20 bar and 220°C. The needed amount of cooling water is determined using the heat of reaction per volume (sumdeltaH= 193.318 KJ/m^3.s (base case) and the volume of the reactor (Vcstr = 352 m^3 (base case)) given by the ACM model. $M_{cooling\ water}$ =132 tonnes/h has been found using the following equation:

$$\Delta Hr\ (\text{KJ/h}) = M_{cooling\ water}\ (\text{Kg/h}).\ \Delta H_{vap\ (220°C)}\ (\text{KJ/Kg}) \quad (67)$$

$$\Delta H_{vap\ (220°C)} = 1856.23\ KJ/Kg \quad (59)$$

The outlet steam is partly integrated to the heat integration. According to Aspen Energy Analyser (for the base case), 96.1 tonnes/h of steam is used for heating of process streams. The rest is used to generate electricity, i.e. 122 tonnes/h of steam. Some steam is also produced using the extra heat of the heat integration which is equal to $Heat_{extra} = 3.91.10^7$ KJ/h. By simulating a heater fulfilling the condition duty= $Heat_{extra}$, T_{out}=212°C and P=20bar, one determines that 13.7 tonnes/h of steam can be generated. The steam price given by Sinnott is used.
For the case 4, the steam produced by the cooling system of the Fischer-Tropsch is completely used for electricity production and does not take part of the heat integration. The hot stream obtained after burning the purge handles the needed extra heating for the heat exchanger network. It is determined that 266 tonnes/h water is needed to cool down the FT reactor, which gives 266 tonnes of steam.

	Base case	Case 4
Heat of reaction in FT reactor ΔHr (KJ/s)	6,80E+04	1,37E+05
Extra heat from HI (KJ/h)	3,86E+07	6,56E+08
Total steam production used for el. Production (Kg/h)	1,36E+05	4,99E+05

Table 48 : steam production used for electricity generation

	Values	Notes
£$_{2009}$/ton of steam	8.76	(29) (p338)
USD$_{2009}$/ton of steam	14.016	(60)
USD$_{2015}$/ton of steam	15.058	CEPCI$_{2009}$=521.9 (61)

Table 49 : Price of MP steam

	Base case	Case 4
Hydrocarbons	6,70E+07	1,35E+08
MP steam from FT	1,47E+07	3,21E+07
MP steam from HI	1,65E+06	2,80E+07
MP steam total	1,63E+07	6,01E+07
Revenues	**8,33E+07**	**1,95E+08**
Operating cost	4,46E+08	7,76E+08
Profit	**-3,63E+08**	**-5.81E+08**

Table 50 : Revenues and profit in USD/year for the different cases

In both case, the process does not make profits. The loss is higher when using the hybrid hydrogen-carbon process. Although the production in case 4 is twice more than in the base case, the profit is not improved. The economic results are discussed in the following subsection.

8.4. Discussion

The hybrid carbon-hydrogen process greatly reduces greenhouse gas emission and increase the crude oil production. Thus, the cost for removing CO_2 is significantly reduced and the revenues are enhanced. However, it is seen from the economic study that more losses are generated in the case 4 than in the base case. This result is due to the important amount of hydrogen required and the high cost of hydrogen which compensates the gain generated by the increase in the production and the saving in the CO_2 removal. A sensitive study has been made for the base case and the case 4.

Price barrel (USD/bbl)	60	100	120	140	160
profit (USD/y)	-3,63E+08	-3,34E+08	-3,12E+08	-2,90E+08	-2,67E+08

Table 51 : Variation in profit for different prices of crude oil barrel for the base case

		price of H2 USD/kg			
		4	**3**	**2**	**1**
cost crude oil USD/barrel	**60**	-5,81E+08	-4,98E+08	-4,15E+08	-3,31E+08
	100	-4,92E+08	-4,08E+08	-3,25E+08	-2,42E+08
	120	-4,47E+08	-3,63E+08	-2,80E+08	-1,97E+08
	140	-4,02E+08	-3,19E+08	-2,35E+08	-1,52E+08
	160	-3,57E+08	-2,74E+08	-1,91E+08	-1,07E+08

Table 52 : Sensitivity analysis

None of the above combination has a positive profit. The results are now compared with the literature. Several value of breakeven price has been found for a non-hybrid BtL process. Kreutz (1) (p58) found a breakeven price of 127$/barrel for a BtL process with recycle. Chris Penniall (54) proposes 118$/barrel. The polymerization takes place in a Microchannel reactor at 10 bar and at 240°C. Syed (2) found similar breakeven price around 120$/bbl. The economic study in the current report seems not realistic when compared with literature. The operating costs are too important for both cases which is likely due to an error in the estimation of the wastewater treatment cost, the maintenance cost and the taxes cost.

However, the fact that the case 4 causes more deficits than the base case comes from the

simulation results. Indeed, the needed supply of hydrogen and oxygen are too important which results in considerable costs. The problem that remains is the need of oxygen to maintain the gasifier temperature. In the case 4, the biomass and the oxygen inlet are respectively warm up at 100°C and 1600°C to make reduced the oxygen content in the gasifier since the oxygen makes drop the syngas production. But the impact is weak and an important amount of oxygen is still needed. The hybrid hydrogen-carbon process has not been optimized. It is possible to reduce the hydrogen supply by increasing the pre-warming and by injecting steam in the gasifier as explained in the subsection 6.5.

9. Conclusion

In this report, the Biomass-To-Liquid-Fischer-Tropsch process has been simulated and optimized on Aspen Hysys and Aspen Properties with a biomass feedstock equals to 20 000 tonnes per day. Kinetic model suggested by Ma et al (22) and Hillestad (21) was used for the Fischer-Tropsch synthesis. First, the gasification performances have been investigated for various operating conditions. It has been found that the syngas production reaches a maximum when λ is equal to 0.57, which corresponds to an oxygen inlet of 42.4 tonnes per hour. The oxygen supply is however set to get a gasifier temperature at 1300°C in order to avoid tar formation. Best results were found no steam is supplied.

The Biomass-To-Liquid-Fischer-Tropsch process has been optimized by maximizing the carbon and energy efficiencies of the simulated plant. The optimal configuration gives an energy efficiency of 56.55% and a carbon efficiency of 40.23% with a production of 4257 barrel per day. It has been obtained by purging 11% of the tail gas and by injecting 90% of the recycled tail gas into the Fischer-Tropsch reactor for a gasifier temperature equal to 1300°C.

A hybrid hydrogen-carbon BTL process has been simulated in order to improve the efficiencies and in particular to reduce the carbon loss. The highest performances have been found for the case 4 which gives an energy efficiency of 63.09% and a carbon efficiency of 79.4%. It has been obtained by warming up the gasifier inlets: the feedstock is pre-heated at 100°C and the oxygen supply at 1600°C. 20% of the tail gas is purged and 90% of the recycled tail gas is injected into the Fischer-Tropsch reactor. Greenhouse emissions have been divided by 12 and the production has doubled when using a hybrid hydrogen-carbon BTL process. Although case 4 presents the best results in the study, it is not the optimal configuration for the process and it can be improved in many ways.

An economical evaluation was performed for BTL and the hybrid process. It results that any of the process make profit. A sensitivity analysis has been made for the both processes. The barrel price was increased up to 160$/bbl and the hydrogen cost was reduced to 1$/Kg. However, even in the most advantageous situation, the study does not show any profit. The results from the economic study are unrealistic and are significantly different from the literature data. The error is found in the too high estimation of the operating costs. Wastewater, maintenance and taxes costs are likely responsible of the error and should be reviewed.

10. Further Work

The simulated processes are supplied by a hypothetical dry biomass that contain no ash. The BTL process shall be realized considering a moisture and ash content to get more realistic results.
It has been noticed that the length of the hydrocarbons decrease when one recycle more tail gas into the Fischer-Tropsch reactor. The composition of the Fischer-Tropsch inlet is modified when the recycling rate varies which changes the probability of growth α. The quality of crude oil partly depends on the rate of heavy hydrocarbons. The investigation on the parameters which influence the average carbon number of the product is relevant.
The hybrid hydrogen-carbon BTL process has not been optimized. Feedstocks, recycle stream and the gasifier vessel can be pre-heated to higher temperature which will reduce the required oxygen supply. The optimal configuration is obtained when enough water is supplied in the gasifier for approaching as much as possible the ratio $H_2/CO = 1.98$ while in the same time having $\lambda = \lambda_{optimal}$. It is beneficial for the carbon efficiency to increase the recycle rate into the gasifier.
Finally, results from the economic study are unrealistic due to an error in the operating estimation. Consequently, the accurate manufacturing breakeven price could not be determined. A review of the cost estimation is needed.

Bibliographie

1. **Thomas Kreutz, Eric Larson, Guangjian Liu, Robert Williams.** ***Fischer-Tropsch fuels from coal and biomass, 25th Annual International Pittsburgh coal Conference.*** **Pittsburgh : s.n., 2008. 08544 .**

2. **Gardezi, Syed Ali, Babu Joseph, Faustino Prado, Alejandro Barbosa. Thermochemical biomass to liquid process : bench-scale experimental results and projected process economics of a commercial scale process.** ***Biomass and Bioenergy.*** **Tampa : Elsevier, 2013, Vol. 59, pp. 168-186.**

3. Gerald N. Choi, Sheldon I. Kramer and Samuel S. Tam. DESIGN AND ECONOMICS OF A FISCHER-TROPSCH PLANT FOR CONVERTING NATURAL GAS TO LIQUID TRANSPORTATION FUELS. [Online] https://web.anl.gov/PCS/acsfuel/preprint%20archive/Files/42_2_SAN%20FRANCISCO_04-97_0667.pdf.

4. **OPEC's World Oil Outlook to be launched 23 December 2015.** ***Organization of the Petroleum Exporting Countries.*** **[Online] 2016. http://www.opec.org/opec_web/en/press_room/3393.htm.**

5. ***Sustainable fuel for the transportation sector.*** **Agrawal, Rakesh. 12, s.l. : CrossMark, 2007, Vol. 104. 4828-4833.**

6. ***Application of Fischer–Tropsch Synthesis in Biomass to Liquid Conversion.*** **Jin Hu, Fei Yu. 2, Mississippi : Catalysts, 2012. 303-326.**

7. Boerrigter, H. ***Economy of Biomass-to-Liquids (BtL) plants.*** **s.l. : The Netherlands: Energy Research Center of The Netherlands, 2006. Report-ECN-C-06-019.**

8. Forum, The International Transport. Reducing transport greenhouse gas emissions. [Online] 2010. http://www.internationaltransportforum.org/Pub/pdf/10GHGTrends.pdf.

9. Bank, The World. ***Municipal Solid Waste Incineration.*** **Washington D.C. 20433 U.S.A. : s.n., 1999.**

10. Daniela Jölli, Stefan Giljum. ***Unused biomass extraction in agriculture, forestry and fishery.*** **Vienna : Sustainable Europe Research Institute (SERI), 2005.**

11. P. Spath, A. Aden, T. Eggeman, M. Ringer, B. Wallace, and J. Jechura. ***Biomass to Hydrogen Production Detailed Design and Economics Utilizing the Battelle Columbus Laboratory Indirectly-Heated Gasifier.*** **s.l. : National Renewable Energy Laboratory, 2005. Technical Report NREL/TP-510-37408.**

12. Prins, Mark Jan. ***Thermodynamic analysis of biomass gasification and torrefaction.*** **EINDHOVEN : Technische Universiteit Eindhoven, 2005. 90-386-2886-2.**

13. Linghong Zhang, Chunbao (Charles) Xu, Pascale Champagne. Overview of recent advances in thermo-chemical conversion of biomass. ***Energy Conversion and Management.*** **Kingston, Thunder bay : Elsevier, 2009, Vol. 51.**

14. Erling Rytter, Esther Ochoa-Fernandez, Adil Fahmi. ***Biomass-to-Liquids by the Fischer-Tropsch process.*** **Germany : Catalytic Process Development for Renewable Materials, 2013. 978-3-527-33169-7.**

15. Tremal A, Becherer D, Fendt S, Gaderer M, Spliethoff H. Performance of entrained flow and fluidised bed biomass gasifiers on different scales. ***Energy Convers Manage.*** **2013, Vol. 69, 95-106.**

16. ***Model development for biomass gasification in an entrained flow gasifier using intrinsic reaction rate submodel.*** **Xiaoyan Gao, Yaning Zhang. Harbin : Elsevier, 2016, Vol. 108, pp. 120-131.**

17. Weiland, Fredrik. Influence of process parameters on the performance of an oxygen blown entrained flow biomass gasifier. ***FUEL.*** **Piteå, Luleå : Elsevier, 2015, Vol. 153, pp. 510-519.**

18. Bhawasut Chutichai, Yaneeporn Patcharavorachot, Suttichai Assabumrungrat, Amornchai Arpornwichanop. Parametric analysis of a circulating fluidized bed biomass gasifier for hydrogen production. ***Energy.*** **Bangkok : Elsevier, 2015, Vol. 82, pp. 406-413.**

19. Vannier, Damien. ***Kinetic study of high temperature water gas shift reaction (Master Thesis).*** **Trondheim : NTNU, 2011. 6445.**

20. Nathan A. Fine, Gary Rochelle. Absorption of Nitrogen Oxides in Aqueous Amines, 12th International Conference on Greenhouse Gas Control Technologies. ***Energy Procedia.*** **Austin : Elsevier, 2014, Vol. 63.**

21. ***Modeling the Fischer-Tropsch Product Distribution and Model Implementation.*** **Hillestad, Magne. 3, Trondheim : De Gruyter, 2015, Vol. 10. 2194-6159.**

22. Wenping Ma, Gary Jacobs, Dennis E. Sparks, Robert spicer, Burtron Davis. Fischer-Tropsch synthesis : kinetics and water efect study over 25%CO/Al2O3 catalysts. ***Catalysis Today.*** **Lexington : Elsevier, 2013, Vol. 228.**

23. ***Evidence for two chain growth probabilities on iron catalysts in the Fischer-Tropsch synthesis.*** **Georges A. Huff, Charles N. Satterfield. 2, Cambridge : Elsevier, 1983, Jourbal of catalysis, Vol. 85.**

24. ***Kinetic Model of Product Distribution over Fe Catalyst for Fischer-Tropsch Synthesis.*** **Zhang, Rongle. 4740–4747, Singapore : s.n., 2009, Energy and fuels, Vol. 23.**

25. ***On the selectivity to higher hydrocarbons in Co-based Fischer–Tropsch synthesis.*** **Erling Rytter, Nikolaos E. Tsakoumis, Anders Holmen. p 3-16, Trondheim : Recent Advances in F-T Synthesis and Fuel Processing Catalysis, 2016, Vol. 261.**

26. ***Biomass gasification behavior in an entrained flow reactor: gas product distribution and soot formation.*** **Qin K, Jensen P, Lin W, Jensen A. s.l. : Energy Fuels, 2012.**

27. ***High-temperature kinetics of the homogeneous reverse water–gas shift reaction.*** **F. Bustamante, R. M. Enick, A. V. Cugini, R. P. Killmeyer, B. H. Howard, K. S. Rothenberger, M. V. Ciocco, B. D. Morreale, S. Chattopadhay, S. Shi. 5, s.l. : AIChe, 2004, Vol. 50.**

28. DIRECTIVE 2010/75/EU OF THE EUROPEAN PARLIAMENT AND OF THE COUNCIL. ***Official Journal of the European Union.*** **[Online] http://eur-lex.europa.eu/legal-content/EN/TXT/HTML/?uri=CELEX:32010L0075&from=EN.**

29. Sinott, Ray K, Towler, Gavin. ***Chemical Engineering Design - 5th Edition.*** **s.l. : Elsevier, 2009. 9780750685511.**

30. Economic indicators. ***Scribd.*** **[Online] https://fr.scribd.com/doc/277921333/CEPCI-2015.**

31. Metal index. ***Metal Prices.*** **[Online] http://www.metalprices.com/p/Metal_Index.**

32. HOLMGREN, KRISTINA M. ***Integration Aspects of Biomass Gasification in Large Industrial or Regional Energy Systems – Consequences for Greenhouse Gas Emissions and Economic Performance.*** **Göteborg : Industrial Energy Systems and Technologies, Department of Energy and Environment , 2015.**

33. A. van der Drift H, Boerrigter, B. Coda, M.K. Cieplik, K. Hemmes. ***Entrained flow gasification of biomass.*** **s.l. : ECN, 2004. ECN-C--04-039.**

34. Michael Bockelie, Martin Denison, Zumao Chen, Temi Linjewile, Constance Senior, Adel Sarofim. ***CFD Modeling for entrained flow gasifiers.*** **Alto : s.n., 2011.**

35. Basu, Prabir. ***Biomass Gasification, Pyrolysis and Torrefaction (Second Edition).*** **s.l. : Elsevier, 2013. 978-0-12-396488-5.**

36. Callaghan, Caitlin A. ***Kinetics and Catalysis of the Water-Gas-Shift Reaction: A Microkinetic and Graph Theoretic Approach.*** **s.l. : WORCESTER POLYTECHNIC INSTITUTE, Department of Chemical Engineering , 2006.**

37. Xiaofeng Guan, Pannalal Vimalchand, Alexander Bonsu, Subhash Datta, and Wanwang Peng. ***DEVELOPMENT AND TESTING OF A WATER-GAS SHIFT REACTION CATALYTIC FILTER ELEMENT IN GASIFICATION PROCESS*** **. Wilsonville : s.n.**

38. Water Gas Shift Reactor Design. ***SlideShare.*** **[Online] http://fr.slideshare.net/l16cn/water-gas-shift-reactor-design.**

39. HT-B113-2 Low Water/carbon Shift Catalyst. ***Alibaba.com.*** **[Online] https://www.alibaba.com/product-detail/HT-B113-2-Low-Water-carbon_298766219.html?spm=a2700.7724857.29.46.6qnf1d.**

40. Co., Anhui Imp. & Exp. MEDIUM TEMPERATURE CO SHIFT CATALYST. [Online] 2014. http://www.aniec.com/PRODUCTS/chemical/C-SPEC1.htm.

41. Hillestad, Magne. Lecture Notes TKP4165 Process Design. 2016.

42. Stewart, Maurice. Gas-Liquid And Liquid-Liquid Separators. [book auth.] Maurice, Ken Arnold Stewart. 4, pp. 131-174.

43. Economic Indicators. [Online] http://www.engr.uconn.edu/~ewanders/Design/Chemical%20Engineering%20Cost%20Indices%20Jan%202008.pdf.

44. ***Technical manual : Design guidelines for carbon dioxide scrubbers.*** **M. L. Nuckols, A. Purer, G. A. Deason. AD-A160 181, Panama city : The Defense Technical Information Center, 1985. 1-800-225-3842.**

45. The Capture and Sequestration of Carbon Dioxide. [Online] http://www.esru.strath.ac.uk/EandE/Web_sites/02-03/carbon_sequestration/Carbon%20Sequestration-423.htm.

46. Berkenpas, Anand B. Rao Edward S. Rubin Michael B. ***AN INTEGRATED MODELING FRAMEWORK FOR CARBON MANAGEMENT TECHNOLOGIES.*** **Pittsburgh : Carnegie Mellon University, 2004. DE-FC26-00NT40935 .**

47. Jeffrey R. Bartels, Michael B. Pate, Norman K. Olson. An economic survey of hydrogen production from conventional and alternative energy sources. ***International Journal of Hydrogen Energy.*** **s.l. : Elsevier, 2010, Vol. 35.**

48. ***Prospects of solar thermal hydrogen production processes.*** **Thomas Pregger, Daniela Graf, Wolfram Krewitt, Christian Sattler, Martin Roeb, Stephan Möller. 10, Stuttgart, Cologne : Elsevier, 2009, Vol. 34.**

49. L'histoire de la taux de change Euro (EUR) et Dollar américain (USD) pour 2015. [Online] http://freecurrencyrates.com/fr/exchange-rate-history/EUR-USD/2015.

50. Energy, U.S. Department of. U.S. Billion-Ton Update: Biomass Supply for a Bioenergy and Bioproducts Industry. [Online] 2011. http://www.energy.gov/sites/prod/files/2015/01/f19/billion_ton_update_0.pdf.

51. *COMPARISON OF TWO CO2 REMOVAL OPTIONS IN COMBINED CYCLE POWER PLANTS.* OLAV BOLLAND, PHILIPPE MATHIEU. Trondheim : Elsevier Science , 1998. S0196-8904(98)00078-8.

52. Aspentech. *Aspen Energy Analyzer, reference guide.* 2015.

53. Occupational Employment Statistics. *Bureau of Labor Statistics.* [Online] may 2015. http://www.bls.gov/oes/current/oes518091.htm.

54. Penniall, Chris. *Fischer-Tropsch Based Biomass to Liquid Fuel Plants in the New Zealand Wood Processing Industry Based on Microchannel Reactor Technology (thesis).* s.l. : University of Canterbury Christchurch, New Zealand, 2013.

55. Journal, The Wall Street. U.S. Oil Prices Rise Above $60 a Barrel. [Online] May 2015. http://www.wsj.com/articles/oil-prices-rise-ahead-of-inventory-data-1430818316.

56. Average Crude Oil Spot Price. *YCHARTS.* [Online] https://ycharts.com/indicators/average_crude_oil_spot_price.

57. Administration, U.S. Energy Information. SHORT-TERM ENERGY OUTLOOK. [Online] https://www.eia.gov/forecasts/steo/report/prices.cfm.

58. Measurement Units and Conversion Factors. *IHRDC.* [Online] https://www.ihrdc.com/els/po-demo/module01/mod_001_03.htm.

59. Jean-Noël Jaubert, Professor at ENSIC. Thermodynamique Tables et diagrammes.

60. Monthly Average. *X-rates.* [Online] 2009. http://www.x-rates.com/average/?from=GBP&to=USD&amount=1&year=2009.

61. Chemical Engineering Plant Cost Index (averaged over year). [Online] http://www.nt.ntnu.no/users/magnehi/cepci_2011_py.pdf.

62. B, Jenkins. Biomass Energy Data Book. [Online] 2011. http://cta.ornl.gov/bedb/pdf/BEDB4_Appendices.pdf.

63. *Basic Design and Cost Data on MEA Treating units.* Perry Pyote, Charles R. Odessa : s.n.

64. Center, Biomass Energy. [Online] http://www.biomassenergycentre.org.uk/portal/page?_pageid=73,1&_dad=portal&_schema=PORTAL.

65. *F. Bustamante, R. M. Enick, Cugini, Killmeyer, B.H. Howard, K. S. Rothenberger, Ciocco, Morreale, Chattopadhyay, Shi.* Reaction, High-Temperature Kinetics of the Homogeneous Reverse Water–Gas Shift. 2004.

A Heat Content Ranges for Various Biomass Fuels (dry weight basis) with English and Metric Units (62)

Fuel type & source	English			Metric[b]			
	Higher Heating Value			Higher Heating Value		Lower Heating Value	
	Btu/lb[c]	Btu/lb	MBtu/ton	kJ/kg	MJ/kg	kJ/kg	MJ/kg
Agricultural Residues							
Corn stalks/stover (1,2,6)	7,487	7,587 - 7,967	15.2 - 15.9	*17,636 - 18,519*	*17.6 - 18.5*	16,849 - 17,690	16.8 - 18.1
Sugarcane bagasse (1,2,6)	7,031	7,450 - 8,349	14.9 - 16.7	*17,317 - 19,407*	*17.3 - 19.4*	17,713 - 17,860	17.7 - 17.9
Wheat straw (1,2,6)		*6,964 - 8,148*	13.9 - 16.3	16,188 - 18,940	16.1 - 18.9	15,082 - 17,659	15.1 - 17.7
Hulls, shells, prunings (2,3)		6,811 - 8,838	13.6 - 17.7	*15,831 - 20,543*	*15.8 - 20.5*		
Fruit pits (2-3)		8,950 - 10,000	17.9 - 20.0				
Herbaceous Crops	7,791						
Miscanthus (6)				18,100 - 19,580	18.1 - 19.6	17,818 - 18,097	17.8 - 18.1
switchgrass (1,3,6)		7,754 - 8,233	15.5 - 16.5	*18,024 - 19,137*	*18.0 - 19.1*	16,767 - 17,294	16.8 - 18.6
Other grasses (6)				18,185 - 18,570	18.2 - 18.6	16,909 - 17,348	16.9 - 17.3
Bamboo (6)				19,000 - 19,750	19.0 - 19.8		
Woody Crops	8,852						
Black locust (1,6)		8,409 - 8,582	16.8 - 17.2	*19,546 - 19,948*	*19.5 - 19.9*	18,464	18.5
Eucalyptus (1,2,6)		*8,174* - 8,432	16.3 - 16.9	19,000 - *19,599*	*19.0 - 19.6*	17,963	18.0
Hybrid poplar (1,3,6)		*8,183* - 8,491	*16.4* - 17.0	19,022 - *19,737*	*19.0 - 19.7*	17,700	17.7
Willow (2,3,6)		7,983 - 8,497	16.0 - 17.0	18,556 - 19,750	18.6 - 19.7	16,734 - 18,419	16.7 - 18.4
Forest Residues	7,082						
Hardwood wood (2,6)		8,017 - 8,920	16.0 - 17.5	*18,635 - 20,734*	*18.6 - 20.7*		
Softwood wood (1,2,3,4,5,6)		8,000 - 9,120	16.0 - 18.24	*18,595 - 21,119*	*18.6 - 21.1*	17,514 - 20,768	17.5 - 20.8
Urban Residues							
MSW (2,6)		5,644 - 8,542	11.2 - 17.0	*13,119 - 19,855*	*13.1 - 19.9*	11,990 - 18,561	12.0 - 18.6
RDF (2,6)		*6,683 - 8,563*	*13.4 - 17.1*	15,535 - 19,904	15.5 - 19.9	14,274 - 18,609	14.3 - 18.6
Newspaper (2,6)		8,477 - 9,550	17 - 19.1	*19,704 - 22,199*	19.7 - 22.2	18,389 - 20,702	18.4 - 20.7
Corrugated paper (2,6)		7,428 -7,939	14.9 - 15.9	17,265 - 18,453	17.3 - 18.5	17,012	
Waxed cartons (2)		11,727 - 11,736	23.5 - 23.5	*27,258 - 27,280*	*27.3*	25,261	

Sources:

1 http://www1.eere.energy.gov/biomass/feedstock_databases.html

2 Jenkins, B., *Properties of Biomass*, Appendix to *Biomass Energy Fundamentals*, EPRI Report TR-102107, January, 1993.

3 Jenkins, B., Baxter, L., Miles, T. Jr., and Miles, T., *Combustion Properties of Biomass*, Fuel Processing Technology 54, pg. 17-46, 1998.

4 Tillman, David, *Wood as an Energy Resource*, Academic Press, New York, 1978

5 Bushnell, D., *Biomass Fuel Characterization: Testing and Evaluating the Combustion Characteristics of Selected Biomass Fuels*, BPA report, 1989

6 http://www.ecn.nl/phyllis
Original references are provided in the Phyllis database for biomass and waste of the Energy Research Centre of the Netherlands.

[a] This table attempts to capture the variation in reported heat content values (on a dry weight basis) in the US and European literature based on values in the Phyllis database, the US DOE/EERE feedstock database, and selected literature sources. Table A.3 of this document provides information on heat contents of materials "as received" with varying moisture contents.

[b] Metric values include both HHV and LHV since Europeans normally report the LHV (or net calorific values) of biomass fuels.

[c] HHV assumed by GREET model given in Table A.1 of this document

B Results table for the Water Gas Shift reactor investigation (cf:4.1)

S/C in GBR	MH2O in GBR	MH2O in ERV	MH2O tot	Stot/C	MCO out_ERV	MCO over Mcarbon in biomass	MCO2 dry syngas	T GBR (°C)	%mol CO2	%mol CH4	%mol carbon loss
0,01	5,00E+01	1,16E+04	1,17E+04	3,255618	1,71E+03	0,48	1848,771	1072	26,27	0,25	1,17
0,04	1,50E+02	1,15E+04	1,16E+04	3,244469	1,71E+03	0,48	1849,0563	1071	26,27	0,25	1,17
0,06	2,00E+02	1,14E+04	1,16E+04	3,241682	1,71E+03	0,48	1848,4193	1071	26,25	0,24	1,17
0,07	2,50E+02	1,14E+04	1,16E+04	3,238894	1,71E+03	0,48	1848,1503	1070	26,24	0,23	1,17
0,08	3,00E+02	1,13E+04	1,16E+04	3,230532	1,71E+03	0,48	1848,1806	1069	26,24	0,22	1,17
0,10	3,50E+02	1,12E+04	1,16E+04	3,230532	1,71E+03	0,48	1847,9338	1069	26,23	0,22	1,17
0,11	4,00E+02	1,12E+04	1,16E+04	3,227745	1,71E+03	0,48	1847,9721	1068	26,23	0,21	1,17
0,13	4,50E+02	1,11E+04	1,16E+04	3,224958	1,71E+03	0,48	1847,7233	1067	26,22	0,21	1,17
0,14	5,00E+02	1,11E+04	1,16E+04	3,219383	1,71E+03	0,48	1847,733	1067	26,22	0,2	1,17
0,15	5,50E+02	1,10E+04	1,15E+04	3,216596	1,71E+03	0,48	1847,5013	1066	26,21	0,2	1,17
0,17	6,00E+02	1,09E+04	1,15E+04	3,213808	1,71E+03	0,48	1847,5556	1066	26,21	0,19	1,17
0,18	6,50E+02	1,09E+04	1,15E+04	3,208234	1,71E+03	0,48	1847,3771	1065	26,2	0,19	1,17
0,20	7,00E+02	1,08E+04	1,15E+04	3,205446	1,71E+03	0,48	1847,5527	1064	26,2	0,18	1,17
0,21	7,50E+02	1,07E+04	1,15E+04	3,199872	1,71E+03	0,48	1847,193	1064	26,19	0,18	1,17
0,22	8,00E+02	1,07E+04	1,15E+04	3,199872	1,71E+03	0,48	1847,2681	1063	26,19	0,17	1,17
0,24	8,50E+02	1,06E+04	1,15E+04	3,194297	1,71E+03	0,48	1847,0553	1063	26,18	0,17	1,17
0,25	9,00E+02	1,06E+04	1,15E+04	3,19151	1,71E+03	0,48	1847,126	1062	26,18	0,17	1,17
0,26	9,50E+02	1,05E+04	1,14E+04	3,188722	1,72E+03	0,48	1847,1337	1061	26,18	0,16	1,17
0,28	1,00E+03	1,04E+04	1,14E+04	3,185935	1,72E+03	0,48	1847,396	1061	26,18	0,16	1,17
0,42	1,50E+03	9,80E+03	1,13E+04	3,150814	1,72E+03	0,48	1846,3035	1055	26,15	0,13	1,17
0,56	2,00E+03	9,21E+03	1,12E+04	3,123777	1,72E+03	0,48	1845,6593	1049	26,18	0,12	1,17
0,70	2,50E+03	8,61E+03	1,11E+04	3,097576	1,72E+03	0,48	1845,5102	1043	26,17	0,1	1,17
0,84	3,00E+03	8,03E+03	1,10E+04	3,073047	1,72E+03	0,48	1845,3608	1037	26,16	0,09	1,17
0,98	3,50E+03	7,44E+03	1,09E+04	3,050191	1,72E+03	0,48	1845,2808	1031	26,15	0,08	1,17
1,11	4,00E+03	6,87E+03	1,09E+04	3,028729	1,72E+03	0,48	1845,1843	1026	26,14	0,08	1,17
1,39	5,00E+03	5,73E+03	1,07E+04	2,989985	1,72E+03	0,48	1845,1824	1015	26,14	0,07	1,17
1,67	6,00E+03	4,61E+03	1,06E+04	2,956815	1,72E+03	0,48	1845,5435	1005	26,13	0,06	1,17
1,95	7,00E+03	3,48E+03	1,05E+04	2,921973	1,73E+03	0,48	1844,6704	996,2	26,12	0,05	1,17
2,23	8,00E+03	2,38E+03	1,04E+04	2,893821	1,73E+03	0,48	1844,6673	987,7	26,11	0,05	1,17

Notes:

All the flowrate are given in Kgmole/h.

The percentage of Carbon loss is calculated neglecting the methane.

The percentage of methane and carbon monoxide are evaluated after drying the syngas. 1% of water is tolerated in the dry syngas

C Element of the Process Flow Diagram of the Biomass-to-Liquid process (base case)

The simulation flowsheet has been divided in 3 areas for greater readability.

Gasification

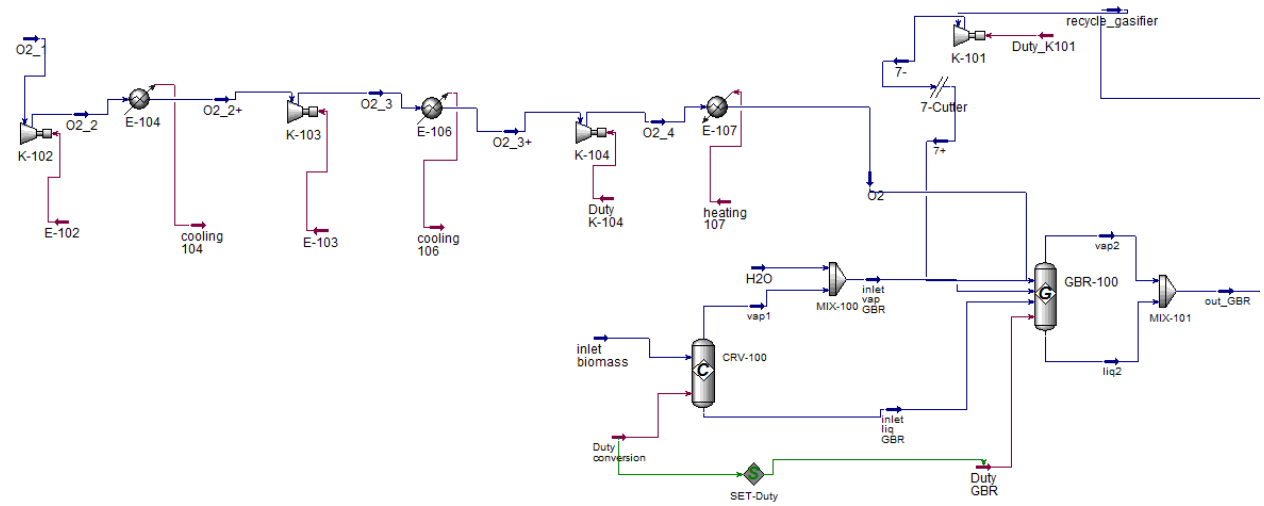

Syngas treatment (WGS reactor, Dryer, Acid gas removal)

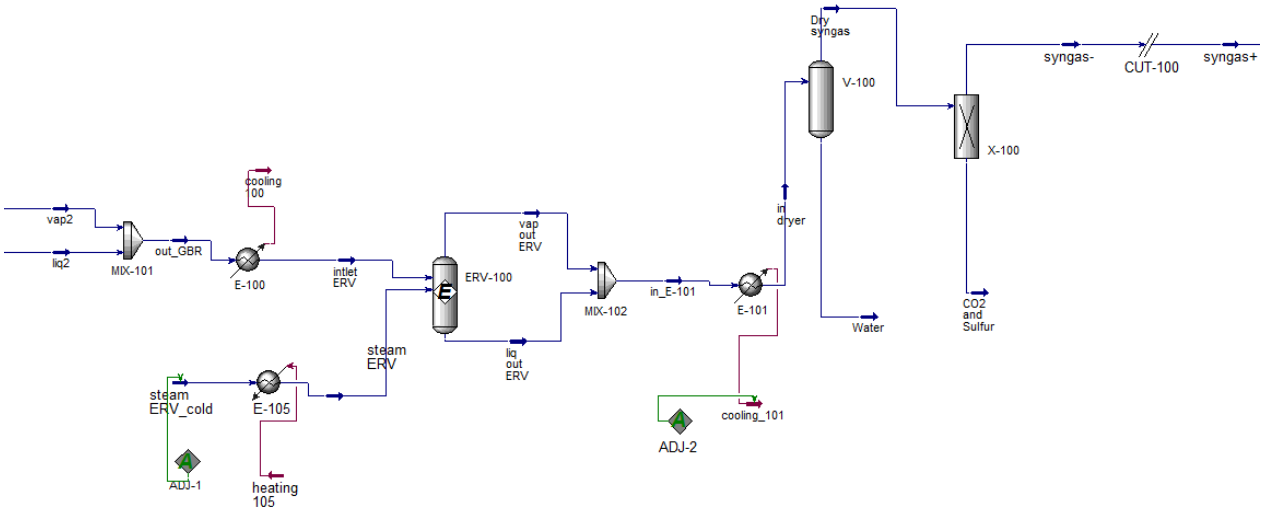

Polymerization and separation

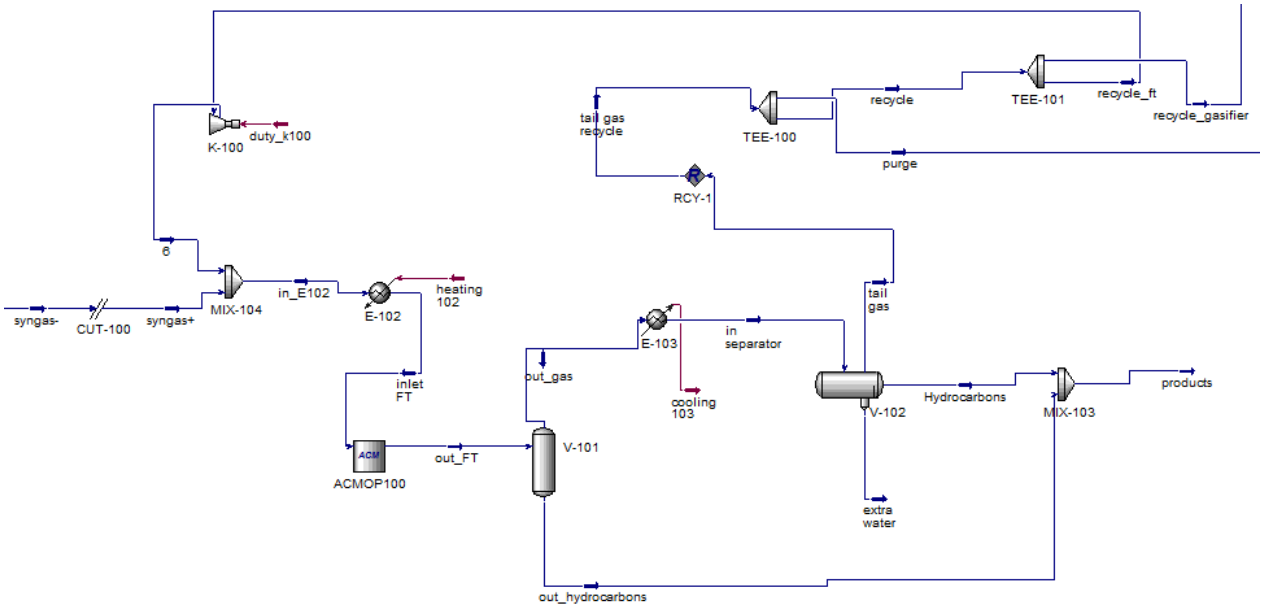

Name	Function
Set-duty	Set the duty of the gibbs reactor “GBR-100” equal to the duty of the conversion reactor “CRV-100” in order to represent the adiabatic aspect of the gasifier
ADJ-1	Adjust the amount of steam at the WGS reactor inlet to reach $H_2/CO=1.98$ at the FT inlet called “inlet FT”
ADJ-2	Adjust the duty of the cooler E-101 to remove 99% of the water in the dryer (H_2O content in dry syngas < 1%)

Table 53 : Utilization of the tools "SET" and "ADJUST" in Aspen Hysys

D Element of the Process Flow Diagram of the hybrid Biomass-to-Liquid process (case 4)

The gasification and the polymerization are not different from the base case. Only the syngas treatment system and the combustion of the purge are presented for the case 4.

Syngas treatment (WGS reactor, Dryer, Acid gas removal)

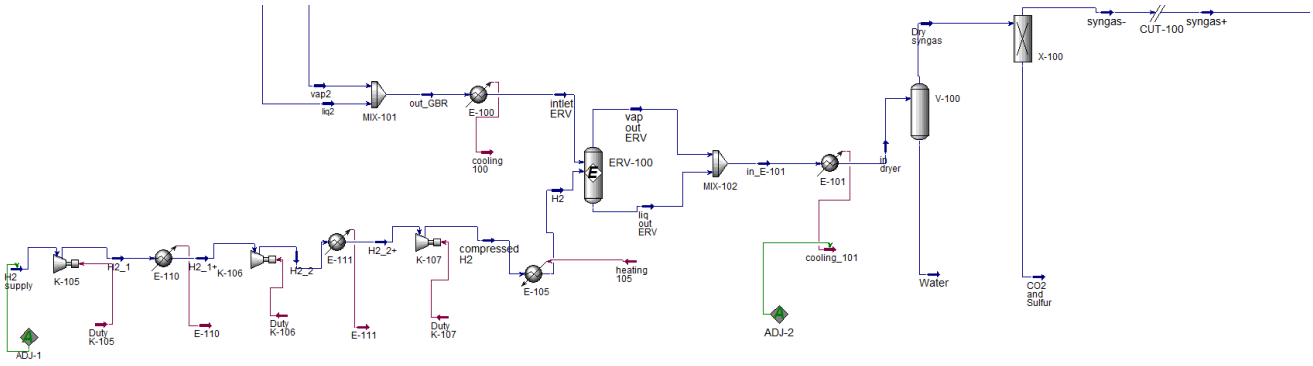

Combustion of the purge

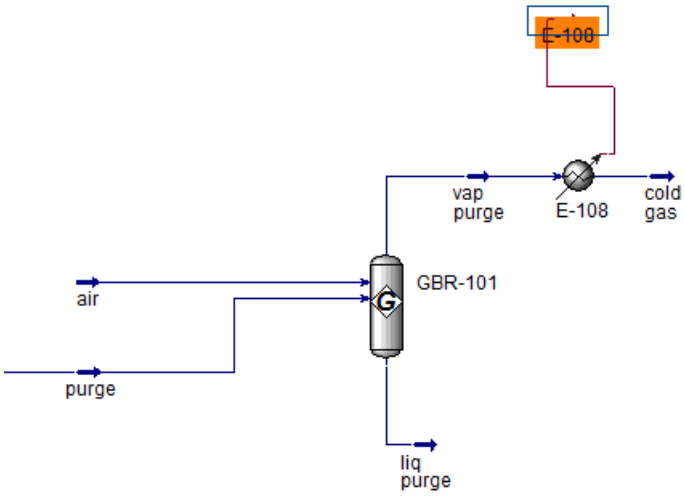

E Workbook Base case

	Vapour Fraction	Temperature	Pressure	Molar Flow	Mass Flow	Liquid Volume Flow	Heat Flow
Unit		*C*	*kPa*	*kgmole/h*	*kg/h*	*m3/h*	*kJ/h*
inlet biomass	0,00	2,50E+01	2,00E+03	8,32E+02	8,33E+04	1,18E+02	-4,55E+08
vap1	1,00	8,00E+02	2,00E+03	3,61E+03	4,02E+04	1,03E+02	8,53E+07
inlet liq GBR	0,00	8,00E+02	2,00E+03	3,59E+03	4,32E+04	2,63E+01	4,84E+07
inlet vap GBR	1,00	8,00E+02	2,00E+03	3,61E+03	4,02E+04	1,03E+02	8,53E+07
vap2	1,00	1,30E+03	2,00E+03	6,53E+03	1,34E+05	2,12E+02	-4,77E+08
liq2	0,00	1,30E+03	2,00E+03	0,00E+00	0,00E+00	0,00E+00	0,00E+00
H2O	1,00	8,00E+02	2,00E+03	0,00E+00	0,00E+00	0,00E+00	0,00E+00
intlet ERV	1,00	4,00E+02	1,98E+03	6,53E+03	1,34E+05	2,12E+02	-6,86E+08
vap out ERV	1,00	4,80E+02	1,98E+03	1,98E+04	3,73E+05	4,98E+02	-3,73E+09
steam ERV_cold	0,00	2,50E+01	1,98E+03	1,33E+04	2,39E+05	2,39E+02	-3,80E+09
out_GBR	1,00	1,30E+03	2,00E+03	6,53E+03	1,34E+05	2,12E+02	-4,77E+08
liq out ERV	0,00	4,80E+02	1,98E+03	0,00E+00	0,00E+00	0,00E+00	0,00E+00
Dry syngas	1,00	5,42E+01	1,95E+03	7,34E+03	1,48E+05	2,73E+02	-1,02E+09
Water	0,00	5,42E+01	1,95E+03	1,25E+04	2,25E+05	2,25E+02	-3,54E+09
in_E-101	1,00	4,80E+02	1,98E+03	1,98E+04	3,73E+05	4,98E+02	-3,73E+09
in dryer	0,37	5,42E+01	1,95E+03	1,98E+04	3,73E+05	4,98E+02	-4,55E+09
CO2 and Sulfur	1,00	8,40E+01	1,95E+03	1,94E+03	8,36E+04	1,01E+02	-7,49E+08
in separator	0,71	3,00E+01	1,83E+03	5,29E+03	1,11E+05	2,35E+02	-9,60E+08
Hydrocarbons	0,00	3,00E+01	1,83E+03	1,99E+01	2,02E+03	2,80E+00	-4,78E+06
extra water	0,00	3,00E+01	1,83E+03	1,54E+03	2,77E+04	2,77E+01	-4,38E+08
tail gas	1,00	3,00E+01	1,83E+03	3,74E+03	8,16E+04	2,05E+02	-5,17E+08
out_hydrocarbons	0,00	2,23E+02	1,93E+03	3,54E+01	1,83E+04	1,96E+01	-2,89E+07
out_gas	1,00	2,23E+02	1,93E+03	5,29E+03	1,11E+05	2,35E+02	-8,56E+08
out_FT	0,99	2,23E+02	1,93E+03	5,33E+03	1,30E+05	2,55E+02	-8,85E+08
tail gas recycle	1,00	3,00E+01	1,83E+03	3,74E+03	8,16E+04	2,05E+02	-5,17E+08
purge	1,00	3,00E+01	1,83E+03	4,11E+02	8,98E+03	2,25E+01	-5,69E+07
recycle_ft	1,00	3,00E+01	1,83E+03	2,99E+03	6,54E+04	1,64E+02	-4,14E+08

6	1,00	3,68E+01	1,95E+03	2,99E+03	6,54E+04	1,64E+02	-4,13E+08
syngas-	1,00	4,25E+01	1,95E+03	5,40E+03	6,42E+04	1,72E+02	-2,68E+08
inlet FT	1,00	2,20E+02	1,93E+03	8,39E+03	1,30E+05	4,53E+02	-6,33E+08
in_E102	1,00	3,99E+01	1,95E+03	8,39E+03	1,30E+05	4,53E+02	-6,81E+08
syngas+	1,00	4,25E+01	1,95E+03	5,40E+03	6,42E+04	2,89E+02	-2,68E+08
recycle_gasifier	1,00	3,00E+01	1,83E+03	3,32E+02	7,26E+03	1,82E+01	-4,60E+07
7-	1,00	3,94E+01	2,00E+03	3,32E+02	7,26E+03	1,82E+01	-4,59E+07
7+	1,00	4,07E+01	2,00E+03	3,32E+02	7,21E+03	1,33E+01	-4,58E+07
recycle gas	1,00	3,00E+01	1,83E+03	3,32E+03	7,26E+04	1,82E+02	-4,60E+08
products	0,03	2,04E+02	1,83E+03	5,52E+01	2,03E+04	2,24E+01	-3,37E+07
steam ERV	1,00	4,00E+02	1,98E+03	1,33E+04	2,39E+05	2,39E+02	-3,04E+09
O2_1	1,00	1,50E+01	1,00E+02	1,34E+03	4,30E+04	3,78E+01	-4,05E+05
O2_2	1,00	1,39E+02	2,72E+02	1,34E+03	4,30E+04	3,78E+01	4,56E+06
O2_2+	1,00	1,50E+01	2,72E+02	1,34E+03	4,30E+04	3,78E+01	-4,28E+05
O2_3	1,00	1,40E+02	7,40E+02	1,34E+03	4,30E+04	3,78E+01	4,54E+06
O2_3+	1,00	1,50E+01	7,40E+02	1,34E+03	4,30E+04	3,78E+01	-4,90E+05
O2_4	1,00	1,40E+02	2,03E+03	1,34E+03	4,30E+04	3,78E+01	4,49E+06
O2	1,00	6,00E+02	2,00E+03	1,34E+03	4,30E+04	3,78E+01	2,46E+07

	Mole Frac (H2)	**Mole Frac (CO)**	**Mole Frac (CO2)**	**Mole Frac (Methane)**
inlet biomass	0,00	0,00	0,00	0,00
vap1	0,70	0,00	0,00	0,00
inlet liq GBR	0,00	0,00	0,00	0,00
inlet vap GBR	0,70	0,00	0,00	0,00
vap2	0,29	0,51	0,08	0,00
liq2	0,29	0,51	0,08	0,00
H2O	0,00	0,00	0,00	0,00
intlet ERV	0,29	0,51	0,08	0,00
vap out ERV	0,18	0,09	0,11	0,00
steam ERV_cold	0,00	0,00	0,00	0,00
out_GBR	0,29	0,51	0,08	0,00

liq out ERV	0,18	0,09	0,11	0,00
Dry syngas	0,47	0,23	0,28	0,00
Water	0,00	0,00	0,00	0,00
in_E-101	0,18	0,09	0,11	0,00
in dryer	0,18	0,00	0,11	0,00
CO2 and Sulfur	0,00	0,00	0,96	0,00
in separator	0,29	0,16	0,20	0,03
Hydrocarbons	0,00	0,01	0,09	0,00
extra water	0,00	0,00	0,00	0,00
tail gas	0,41	0,22	0,28	0,05
out_hydrocarbons	0,01	0,01	0,02	0,00
out_gas	0,29	0,16	0,20	0,03
out_FT	0,29	0,16	0,19	0,03
tail gas recycle	0,41	0,22	0,28	0,05
purge	0,41	0,22	0,28	0,05
recycle_ft	0,41	0,22	0,28	0,05
6	0,41	0,22	0,28	0,05
syngas-	0,64	0,32	0,04	0,00
inlet FT	0,56	0,28	0,12	0,02
in_E102	0,56	0,28	0,12	0,02
syngas+	0,64	0,32	0,04	0,00
recycle_gasifier	0,41	0,22	0,28	0,05
7-	0,41	0,22	0,28	0,05
7+	0,41	0,22	0,28	0,05
recycle gas	0,41	0,22	0,28	0,05
products	0,01	0,01	0,04	0,00
steam ERV	0,00	0,00	0,00	0,00
O2_1	0,00	0,00	0,00	0,00
O2_2	0,00	0,00	0,00	0,00
O2_2+	0,00	0,00	0,00	0,00
O2_3	0,00	0,00	0,00	0,00

O2_3+	0,00	0,00	0,00	0,00
O2_4	0,00	0,00	0,00	0,00
O2	0,00	0,00	0,00	0,00

	Heat Flow
Unit	***kJ/h***
Duty conversion	5,89E+08
Duty GBR	-5,89E+08
cooling 100	2,09E+08
cooling_101	8,28E+08
heating 102	4,86E+07
cooling 103	1,04E+08
duty_k100	6,62E+05
Duty_K101	1,02E+05
heating 105	7,57E+08
E-102	4,96E+06
cooling 104	4,99E+06
E-103	4,96E+06
cooling 106	5,03E+06
Duty K-104	4,98E+06
heating 107	2,01E+07

F Workbook case 4

	Vapour Fraction	Temperature	Pressure	Molar Flow	Mass Flow	Liquid Volume Flow	Heat Flow
Unit		*C*	*kPa*	*kgmole/h*	*kg/h*	*m3/h*	*kJ/h*
inlet biomass	0,00	1,00E+02	2,00E+03	8,32E+02	8,33E+04	1,18E+02	-4,29E+08
vap1	1,00	8,00E+02	2,00E+03	3,61E+03	4,02E+04	1,03E+02	8,53E+07
inlet liq GBR	0,00	8,00E+02	2,00E+03	3,59E+03	4,32E+04	2,63E+01	4,84E+07
inlet vap GBR	1,00	8,00E+02	2,00E+03	3,61E+03	4,02E+04	1,03E+02	8,53E+07
vap2	1,00	1,30E+03	2,00E+03	6,65E+03	1,28E+05	2,15E+02	-3,83E+08
liq2	0,00	1,30E+03	2,00E+03	0,00E+00	0,00E+00	0,00E+00	0,00E+00
H2O	1,00	8,00E+02	2,00E+03	0,00E+00	0,00E+00	0,00E+00	0,00E+00
intlet ERV	1,00	1,14E+03	1,98E+03	6,65E+03	1,28E+05	2,15E+02	-4,22E+08
vap out ERV	1,00	9,94E+02	1,97E+03	1,18E+04	1,38E+05	3,60E+02	-3,04E+08
H2 supply	1,00	2,50E+01	1,00E+02	5,17E+03	1,04E+04	1,49E+02	-5,56E+02
out_GBR	1,00	1,30E+03	2,00E+03	6,65E+03	1,28E+05	2,15E+02	-3,83E+08
liq out ERV	0,00	9,94E+02	1,97E+03	0,00E+00	0,00E+00	0,00E+00	0,00E+00
Dry syngas	1,00	5,60E+01	1,95E+03	1,12E+04	1,27E+05	3,49E+02	-4,98E+08
Water	0,00	5,60E+01	1,95E+03	6,43E+02	1,16E+04	1,16E+01	-1,82E+08
in_E-101	1,00	9,94E+02	1,97E+03	1,18E+04	1,38E+05	3,60E+02	-3,04E+08
in dryer	0,95	5,60E+01	1,95E+03	1,18E+04	1,38E+05	3,60E+02	-6,80E+08
CO2 and Sulfur	1,00	1,60E+02	1,95E+03	3,08E+02	1,08E+04	1,27E+01	-1,03E+08
in separator	0,63	3,00E+01	1,82E+03	8,41E+03	1,30E+05	3,51E+02	-1,14E+09
Hydrocarbons	0,00	3,00E+01	1,82E+03	3,90E+01	4,15E+03	5,80E+00	-8,77E+06
extra water	0,00	3,00E+01	1,82E+03	3,09E+03	5,57E+04	5,58E+01	-8,83E+08
tail gas	1,00	3,00E+01	1,82E+03	5,28E+03	6,98E+04	2,90E+02	-2,44E+08
out_hydrocarbons	0,00	2,24E+02	1,92E+03	7,19E+01	3,65E+04	3,92E+01	-5,78E+07
out_gas	1,00	2,24E+02	1,92E+03	8,41E+03	1,30E+05	3,51E+02	-9,45E+08
out_FT	0,99	2,24E+02	1,92E+03	8,49E+03	1,66E+05	3,91E+02	-1,00E+09
tail gas recycle	1,00	3,00E+01	1,82E+03	5,29E+03	6,99E+04	2,90E+02	-2,44E+08
purge	1,00	3,00E+01	1,82E+03	1,06E+03	1,40E+04	5,80E+01	-4,88E+07
recycle_ft	1,00	3,00E+01	1,82E+03	3,81E+03	5,03E+04	2,09E+02	-1,76E+08
6	1,00	3,72E+01	1,95E+03	3,81E+03	5,03E+04	2,09E+02	-1,75E+08
syngas-	1,00	5,23E+01	1,95E+03	1,09E+04	1,16E+05	3,36E+02	-3,95E+08
inlet FT	1,00	2,20E+02	1,92E+03	1,47E+04	1,66E+05	7,91E+02	-4,94E+08
in_E102	1,00	4,81E+01	1,95E+03	1,47E+04	1,66E+05	7,91E+02	-5,70E+08
syngas+	1,00	5,23E+01	1,95E+03	1,09E+04	1,16E+05	5,82E+02	-3,95E+08
recycle_gasifier	1,00	3,00E+01	1,82E+03	4,23E+02	5,59E+03	2,32E+01	-1,95E+07
7-	1,00	4,00E+01	2,00E+03	4,23E+02	5,59E+03	2,32E+01	-1,94E+07
7+	1,00	3,60E+01	2,00E+03	4,23E+02	5,54E+03	1,45E+01	-1,94E+07
recycle	1,00	3,00E+01	1,82E+03	4,23E+03	5,59E+04	2,32E+02	-1,95E+08
products	0,01	2,04E+02	1,82E+03	1,11E+02	4,06E+04	4,50E+01	-6,65E+07
O2_1	1,00	1,50E+01	1,00E+02	1,22E+03	3,89E+04	3,42E+01	-3,66E+05

O2_2	1,00	1,39E+02	2,72E+02	1,22E+03	3,89E+04	3,42E+01	4,12E+06
O2_2+	1,00	1,50E+01	2,72E+02	1,22E+03	3,89E+04	3,42E+01	-3,87E+05
O2_3	1,00	1,40E+02	7,40E+02	1,22E+03	3,89E+04	3,42E+01	4,10E+06
O2_3+	1,00	1,50E+01	7,40E+02	1,22E+03	3,89E+04	3,42E+01	-4,43E+05
O2_4	1,00	1,40E+02	2,03E+03	1,22E+03	3,89E+04	3,42E+01	4,06E+06
O2	1,00	1,60E+03	2,00E+03	1,22E+03	3,89E+04	3,42E+01	6,58E+07
compressed H2	1,00	1,59E+02	1,98E+03	5,17E+03	1,04E+04	1,49E+02	1,98E+07
H2	1,00	8,00E+02	1,97E+03	5,17E+03	1,04E+04	1,49E+02	1,18E+08
vap purge	1,00	1,57E+03	1,82E+03	6,49E+03	1,85E+05	3,18E+02	-7,28E+07
liq purge	0,00	1,57E+03	1,82E+03	0,00E+00	0,00E+00	0,00E+00	0,00E+00
air	1,00	2,50E+01	1,83E+03	5,88E+03	1,71E+05	3,15E+02	-2,40E+07
cold gas	0,92	1,00E+02	1,82E+03	6,49E+03	1,85E+05	3,18E+02	-4,39E+08
cold biomass*	0,00	2,50E+01	2,00E+03	8,32E+02	8,33E+04	1,18E+02	-4,55E+08
hot biomass*	0,00	1,00E+02	2,00E+03	8,32E+02	8,33E+04	1,18E+02	-4,29E+08
H2_1	1,00	1,58E+02	2,70E+02	5,17E+03	1,04E+04	1,49E+02	1,97E+07
H2_1+	1,00	2,50E+01	2,70E+02	5,17E+03	1,04E+04	1,49E+02	-1,45E+03
H2_2	1,00	1,58E+02	7,29E+02	5,17E+03	1,04E+04	1,49E+02	1,97E+07
H2_2+	1,00	2,50E+01	7,29E+02	5,17E+03	1,04E+04	1,49E+02	-3,56E+03

	Mole Frac (CO)	Mole Frac (CO2)	Mole Frac (H2)	Molar Flow (CH4)
inlet biomass	0,000	0,000	0,000	0,000
vap1	0,000	0,000	0,696	0,000
inlet liq GBR	0,000	0,000	0,000	0,000
inlet vap GBR	0,000	0,000	0,696	0,000
vap2	0,520	0,050	0,333	1,032
liq2	0,520	0,050	0,333	0,000
H2O	0,000	0,000	0,000	0,000
intlet ERV	0,520	0,050	0,333	1,032
vap out ERV	0,302	0,019	0,615	1,032
H2 supply	0,000	0,000	1,000	0,000
out_GBR	0,520	0,050	0,333	1,032
liq out ERV	0,302	0,019	0,615	0,000
Dry syngas	0,320	0,020	0,650	1,032
Water	0,000	0,000	0,000	0,000
in_E-101	0,302	0,019	0,615	1,032
in dryer	0,302	0,019	0,615	1,032
CO2 and Sulfur	0,000	0,647	0,000	1,032
in separator	0,197	0,009	0,364	0,033
Hydrocarbons	0,011	0,005	0,007	0,005
extra water	0,000	0,000	0,000	0,000

tail gas	0,314	0,015	0,580	0,052
out_hydrocarbons	0,007	0,001	0,009	0,002
out_gas	0,197	0,009	0,364	0,033
out_FT	0,196	0,009	0,361	0,032
tail gas recycle	0,314	0,015	0,580	0,052
purge	0,314	0,015	0,580	0,052
recycle_ft	0,314	0,015	0,580	0,052
6,000	0,314	0,015	0,580	0,052
syngas-	0,329	0,002	0,669	0,000
inlet FT	0,325	0,005	0,646	0,013
in_E102	0,325	0,005	0,646	0,013
syngas+	0,329	0,002	0,669	0,000
recycle_gasifier	0,314	0,015	0,580	0,052
7-	0,314	0,015	0,580	0,052
7+	0,314	0,015	0,580	21,902
recycle	0,314	0,015	0,580	0,052
products	0,008	0,002	0,008	0,003
O2_1	0,000	0,000	0,000	0,000
O2_2	0,000	0,000	0,000	0,000
O2_2+	0,000	0,000	0,000	0,000
O2_3	0,000	0,000	0,000	0,000
O2_3+	0,000	0,000	0,000	0,000
O2_4	0,000	0,000	0,000	0,000
O2	0,000	0,000	0,000	0,000
compressed H2	0,000	0,000	1,000	0,000
H2	0,000	0,000	1,000	0,000
vap purge	0,000	0,089	0,000	0,000
liq purge	0,000	0,086	0,000	0,000
air	0,000	0,010	0,000	0,000
cold gas	0,000	0,089	0,000	0,000
H2_1	0,000	0,000	1,000	0,000
H2_1+	0,000	0,000	1,000	0,000
H2_2	0,000	0,000	1,000	0,000
H2_2+	0,000	0,000	1,000	0,000

	Heat Flow
Unit	*kJ/h*
Duty conversion	5,63E+08
Duty GBR	-5,63E+08
cooling 100	3,95E+07
cooling_101	3,76E+08
heating 102	7,64E+07
cooling 103	1,91E+08
duty_k100	8,60E+05
Duty_K101	1,32E+05
heating 105	9,84E+07
E-102	4,49E+06
cooling 104	4,51E+06
E-103	4,49E+06
cooling 106	4,54E+06
Duty K-104	4,50E+06
heating 107	6,18E+07
E-108	3,67E+08
Duty biomass	2,61E+07
E-110	1,97E+07
Duty K-105	1,97E+07
Duty K-106	1,97E+07
E-111	1,97E+07
Duty K-107	1,98E+07

G Results table for the base case investigation

recycle split	1	0,9	0,8	0,7	0,6	0,5
λ	0,66	0,68	0,70	0,71	0,72	0,73
V_{CSTR} (m^3)	382,20	366,00	356,00	347,00	343,00	339,00
% Eeff	54,82	54,80	54,70	54,28	54,08	53,69
% Ceff	38,74	38,86	38,86	38,62	38,54	38,36
% carbon loss WGS	42,56	43,90	44,73	45,42	45,87	46,28
H2/CO	0,56	0,57	0,58	0,60	0,61	0,62
syngas (Kmol/h)	4,93E+03	5,14E+03	5,33E+03	5,52E+03	5,67E+03	5,83E+03
%CH4 in FT	1,92	1,25	0,87	0,64	0,46	0,34
%CO2 in FT	13,83	10,22	8,17	6,81	5,89	5,20
% inerts	16,11	11,84	9,42	7,84	6,75	5,94
actual S/C	0,00E+00	1,22E-04	2,23E-04	3,19E-04	4,03E-04	4,83E-04
price $/h	8,12E+03	8,11E+03	8,10E+03	8,04E+03	8,01E+03	7,95E+03

Table 54 : simulation results for different recycle split at purge = 0.17, S/C = 0 and TGBR = 1300°C

recycle split	1	0,9	0,8	0,7	0,6	0,5
λ	0,6613162	0,686998	0,70626	0,7223114	0,73194222	0,7407705
V_{CSTR} (m^3)	416	384,2	368,3	356,8	352	348,9
% Eeff	56,35058	56,45123	56,06854	55,5266974	55,4410319	55,122386
% Ceff	39,8808	40,1197	39,9322	39,6248	39,5986	39,4263
% carbon loss WGS	43,1299	44,3309	45,3152	46,0569	46,447	46,7505
H_2/CO	0,5647	0,5715	0,5824	0,596	0,6078	0,6226
syngas (Kgmol/h)	4925,0772	5181,222	5387,427	5583,1578	5744,3738	5928,9006
%CH4 in FT	2,61	1,57	1,05	0,75	0,53	0,37
%CO2 in FT	17,85	11,91	9	7,27	6,17	5,32
% inerts	20,92	13,98	10,57	8,55	7,25	6,24
actual S/C	0	8,24E-06	1,48E-05	2,0788E-05	2,5594E-05	3,088E-05
price $/h	8344,7137	8359,619	8302,948	8222,70845	8210,02261	8162,8357

Table 55 : simulation results for different recycle split at purge = 0.12, S/C = 0 and TGBR = 1300°C

recycle split	1	0,9	0,8	0,7	0,6	0,5
λ	0,66	0,69	0,71	0,72	0,73	0,74
VCSTR (m3)	424,50	388,00	372,00	364,50	352,80	347,90
% Eeff	56,65	56,62	56,44	56,31	55,84	54,97

% Ceff	40,10	40,24	40,19	40,17	39,71	39,31
% carbon loss WGS	42,63	44,50	45,42	45,93	46,36	46,85
H2/CO syngas	0,56	0,57	0,58	0,59	0,61	0,62
(Kgmol/h)	4,93E+03	5,19E+03	5,39E+03	5,58E+03	5,75E+03	5,92E+03
%CH4 in FT	2,82	1,65	1,08	0,73	0,53	0,37
%CO2 in FT	18,98	12,30	9,23	7,42	6,16	5,34
% inerts	22,29	14,49	10,87	8,73	7,23	6,26
actual S/C	0	8,63E-06	1,51E-05	2,0615E-05	2,0615E-05	3,098E-05
price $/h	8,39E+03	8,38E+03	8,36E+03	8,34E+03	8,27E+03	8,14E+03

Table 56 : simulation results for different recycle split at purge = 0.11, S/C = 0 and TGBR = 1300°C

recycle split	**1**	**0,9**	**0,8**	**0,7**	**0,6**	**0,5**
λ	-	0,69	0,71	0,72	0,74	-
VCSTR (m3)	-	393,50	375,00	365,00	356,50	-
% Eeff	-	57,04	56,82	56,46	55,84	-
% Ceff	-	40,58	40,46	40,25	40,10	-
% carbon loss WGS	-	44,61	45,58	46,18	46,72	-
H2/CO	-	0,57	0,58	0,59	0,61	-
syngas						
(Kgmol/h)	-	5,19E+03	5,40E+03	5,60E+03	5,79E+03	-
%CH4 in FT	-	1,72	1,12	0,77	0,55	-
%CO2 in FT	-	12,82	9,46	7,51	6,26	-
% inerts	-	15,12	11,19	8,91	7,45	-
actual S/C	-	8,85E-06	1,54E-05	2,14E-05	2,71E-05	-
price $/h	-	8,45E+03	8,41E+03	8,36E+03	8,27E+03	-

Table 57 : simulation results for different recycle split at purge = 0.10, S/C = 0 and TGBR = 1300°C

Note :

The actual S/C takes into account the steam contained in the gasifier recycle stream.

The H_2/CO ratio in the above tables is taken at the gasifier outlet.

Sp area in FT reactor = 100 m^{-1}

H Original design proposed by Aspen Energy Analazyer for the base case

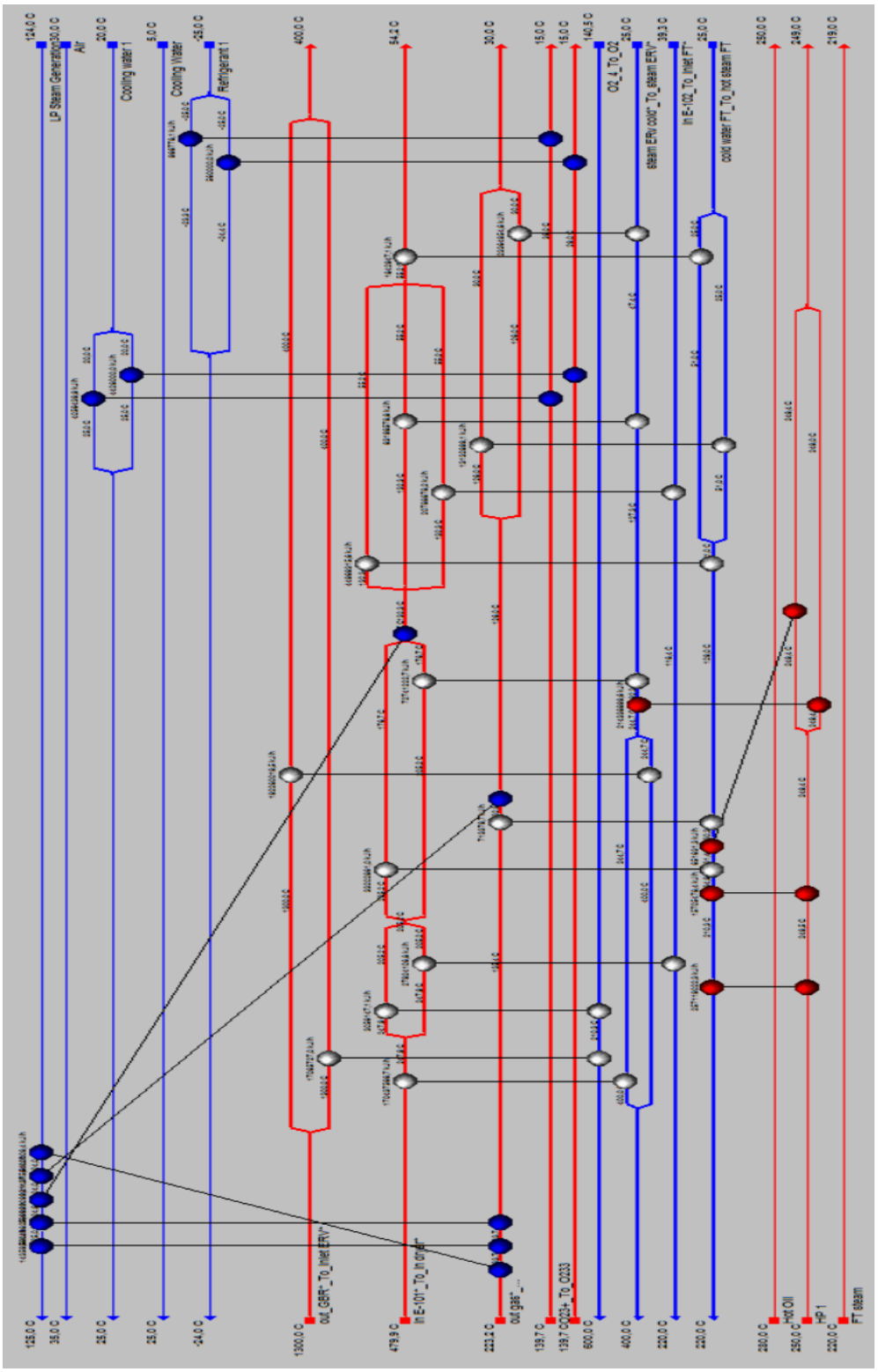

I Heat Integration results for the base case

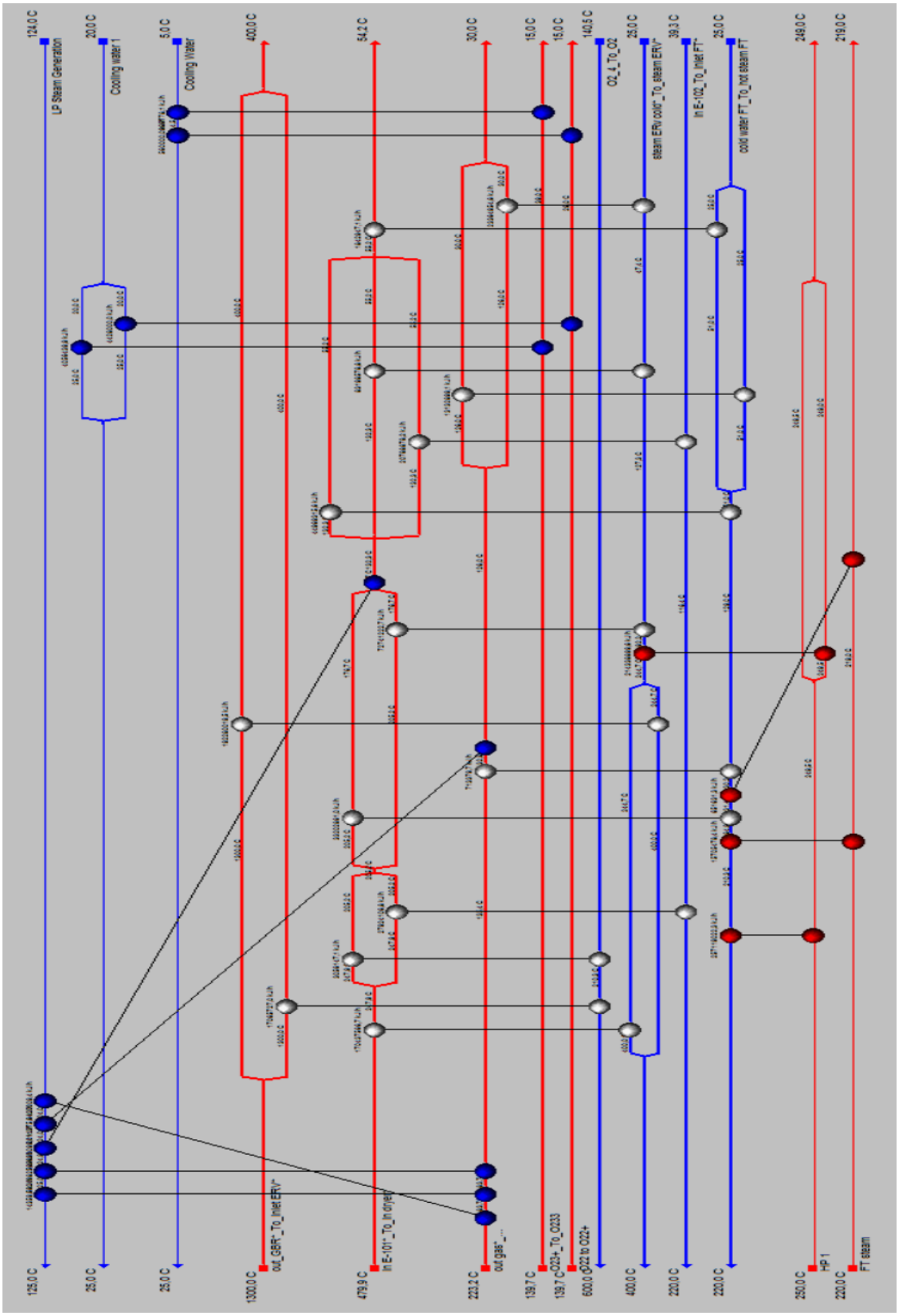

Name		Inlet T [C]	Outlet T [C]	MCp [kJ/C-h]	Enthalpy [kJ/h]	Segm.	HTC [kJ/h-m2-C]	Flowrate [kg/h]	Effective Cp [kJ/kg-C]	DT Cont. [C]
out gas*_To_in separator 2*		223,2	30,0	---	1,059e+008		----	1,160e+005	----	Global
in E-101*_To_in dryer*		479,9	54,2	---	8,282e+008		----	3,724e+005	----	Global
out_GBR*_To_inlet ERV*		1300,0	400,0	---	2,093e+008		----	1,335e+005	----	Global
cold water FT_To_hot steam		25,0	220,0	---	3,673e+008		----	1,320e+005	----	Global
steam ERv cold*_To_steam		25,0	400,0	---	7,564e+008		----	2,389e+005	----	Global
O23+_To_O233		139,7	15,0	4,028e+004	5,023e+006		207,36	4,301e+004	0,937	Global
O2_4_To_O2		140,5	600,0	4,379e+004	2,012e+007		226,58	4,301e+004	1,018	Global
in E-102_To_inlet FT*		39,3	220,0	2,696e+005	4,871e+007		475,93	1,295e+005	2,081	Global
O22 to O22+		139,7	15,0	4,000e+004	4,988e+006		720,00	4,301e+004	0,930	Global

Table 58 : Process streams of the heat integration for the base case

Streams	**HX in flowsheet**	**Q (KW)**
Out gas / in separator	E-103	$2{,}888.10^{4}$
In E-101 / in dryer	E-101	$2{,}301.10^{5}$
Out GBR / inlet ERV	E-100	$5{,}818.10^{4}$
Cold water FT / Hot steam FT	Not simulated	$6{,}8047.10^{4}$
Steam ERV cold / steam ERV	E-105	$2{,}1.10^{5}$
O2_3 / O2_3+	E-106	$1{,}396.10^{3}$
O2_4 / O2	E-107	$5{,}589.10^{3}$
In E-102 / inlet FT	E-102	$1{,}349.10^{4}$
O2_2 / O2_2+	E-104	$1{,}385.10^{3}$

Table 59 : Process streams and the associated heat exchanger units (base case)

Area (m^2)	**Units**	**Shells**	**Heating (KJ/h)**	**Cooling (KJ/h)**	**Operating cost (USD/s)**
$3{,}475.10^{4}$	27	135	$4{,}878.10^{8}$	$4{,}492.10^{8}$	0.09771

Table 60 : Costing data of the base case design

Heat Exchanger	Load [kJ/h]	Cost Index [Cost]	Area [m2]	Shells	LMTD [C]	Overall U [kJ/h-m2-C]	FFactor	Fouling [C-h-m2/kJ]	Hot Stream	Hot T in [C]	Hot T out [C]	Cold Stream	Cold T in [C]	Cold T out [C]	dT Min Hot [C]	dT Min Cold [C]
E-135	6,516e+00	1,095e+004	1,232	1	88,21	5995,0	1,0000	0,0000	FT steam	219,0	219,0	cold water FT_To_hot steam FT	130,2	131,4	87,67	88,76
E-137	3,700e+00	5,016e+005	2046	5	23,70	7731,8	0,9867	0,0000	in E-101* _To_in dryer*	176,7	132,3	LP Steam Generation	124,0	124,9	51,82	8,241
E-141	2,011e+00	4,591e+004	116,2	1	4,596	3767,5	0,9997	0,0000	out gas* _To_in separator 2*	132,9	126,0	LP Steam Generation	124,0	124,0	8,899	1,971
E-129	2,143e+00	2,885e+005	1063	4	21,00	11981,6	0,9329	0,0000	HP 1	249,5	249,0	steam ERv cold* _To_steam ERv*	192,2	244,7	4,776	56,76
E-119	1,923e+00	3,260e+005	1245	4	423,9	373,5	0,9009	0,0000	out_GBR* _To_inlet ERv*	1300,0	400,0	steam ERv cold* _To_steam ERv*	244,7	400,0	900,0	155,3
E-123	8,420e+00	6,646e+004	204,6	1	77,81	529,0	1,0000	0,0000	out gas* _To_in separator 2*	223,2	183,7	LP Steam Generation	124,0	124,0	99,18	59,75
E-142	1,843e+00	2,018e+004	20,22	2	12,85	7294,0	0,9725	0,0000	in E-101* _To_in dryer*	55,2	54,2	cold water FT_To_hot steam FT	25,0	51,0	4,170	29,17
E-144	2,336e+00	9,451e+004	257,3	3	26,71	3718,2	0,8781	0,0000	out gas* _To_in separator 2*	126,0	30,0	steam ERv cold* _To_steam ERv*	25,0	47,4	78,57	5,000
E-136	7,134e+00	2,685e+004	45,13	1	4,501	3604,4	0,9743	0,0000	out gas* _To_in separator 2*	135,4	132,9	cold water FT_To_hot steam FT	129,0	130,2	5,139	3,918
E-140	2,079e+00	8,505e+005	3363	10	15,84	458,7	0,7945	0,0000	in E-101* _To_in dryer*	132,3	55,2	in E-102_To_inlet FT*	39,3	116,4	15,84	15,84
E-138	4,497e+00	5,515e+005	1613	21	3,696	7284,3	0,7945	0,0000	in E-101* _To_in dryer*	132,3	55,2	cold water FT_To_hot steam FT	51,0	129,0	3,260	4,170
E-130	1,436e+00	1,010e+004	7,160e-002	1	58,74	3414,2	1,0000	0,0000	out gas* _To_in separator 2*	183,7	183,7	LP Steam Generation	125,0	125,0	58,75	58,74
E-128	1,571e+00	4,614e+004	117,1	1	19,41	6989,7	0,9882	0,0000	FT steam	220,0	219,0	cold water FT_To_hot steam FT	184,9	210,3	9,710	34,09
E-143	1,313e+00	6,523e+004	151,2	3	25,85	3721,6	0,8664	0,0000	out gas* _To_in separator 2*	126,0	30,0	cold water FT_To_hot steam FT	25,0	51,0	75,01	5,000
E-133	7,274e+00	8,792e+005	3709	8	27,28	1607,3	0,8286	0,0000	in E-101* _To_in dryer*	205,2	176,7	steam ERv cold* _To_steam ERv*	127,3	192,2	13,01	49,41
E-139	8,320e+00	5,761e+005	1922	13	6,261	7277,1	0,7946	0,0000	in E-101* _To_in dryer*	132,3	55,2	steam ERv cold* _To_steam ERv*	47,4	127,3	4,982	7,729
E-131	5,600e+00	1,210e+005	336,5	4	2,909	683,5	0,8367	0,0000	O22 to O22+	29,0	15,0	Cooling Water	14,5	20,0	8,974	0,4851
E-121	4,056e+00	1,180e+005	386,8	2	53,23	204,2	0,9647	0,0000	O23+ To_O233	139,7	39,0	Cooling water 1	20,0	25,0	114,7	19,00
E-125	3,056e+00	1,419e+005	497,0	2	49,96	152,4	0,8077	0,0000	in E-101* _To_in dryer*	247,9	205,2	O2_4_To_O2	140,5	210,3	37,64	64,71
E-127	9,668e+00	1,097e+005	350,0	2	16,18	204,2	0,8362	0,0000	O23+ To_O233	39,0	15,0	Cooling Water	5,0	14,5	24,49	10,00
E-132	3,320e+00	2,285e+005	933,7	2	31,13	2057,0	0,8156	0,0000	in E-101* _To_in dryer*	205,2	176,7	cold water FT_To_hot steam FT	131,4	184,9	20,27	45,31
E-134	5,825e+00	1,216e+005	479,4	1	28,03	3866,2	0,9984	0,0000	out gas* _To_in separator 2*	183,7	135,4	LP Steam Generation	124,9	125,0	58,74	10,51
E-118	1,704e+00	2,982e+006	1,225e+004	32	23,94	407,5	0,8035	0,0000	in E-101* _To_in dryer*	479,9	247,9	steam ERv cold* _To_steam ERv*	244,7	400,0	79,90	3,249
E-120	1,707e+00	1,087e+005	345,9	2	390,9	148,7	0,8296	0,0000	out_GBR* _To_inlet ERv*	1300,0	400,0	O2_4_To_O2	210,3	600,0	700,0	188,7
E-122	2,571e+00	1,224e+005	483,9	1	34,38	15467,4	0,9993	0,0000	HP 1	250,0	249,5	cold water FT_To_hot steam FT	210,3	220,0	30,00	39,16
E-124	4,428e+00	6,360e+004	161,2	2	41,53	683,5	0,9677	0,0000	O22 to O22+	139,7	29,0	Cooling water 1	20,0	25,0	114,7	9,000
E-126	2,792e+00	6,478e+005	2707	6	52,62	235,3	0,8332	0,0000	in E-101* _To_in dryer*	247,9	205,2	in E-102_To_inlet FT*	116,4	220,0	27,93	88,79

Table 61 : Data of the heat integration for the base case

J Heat Integration results for the case 4

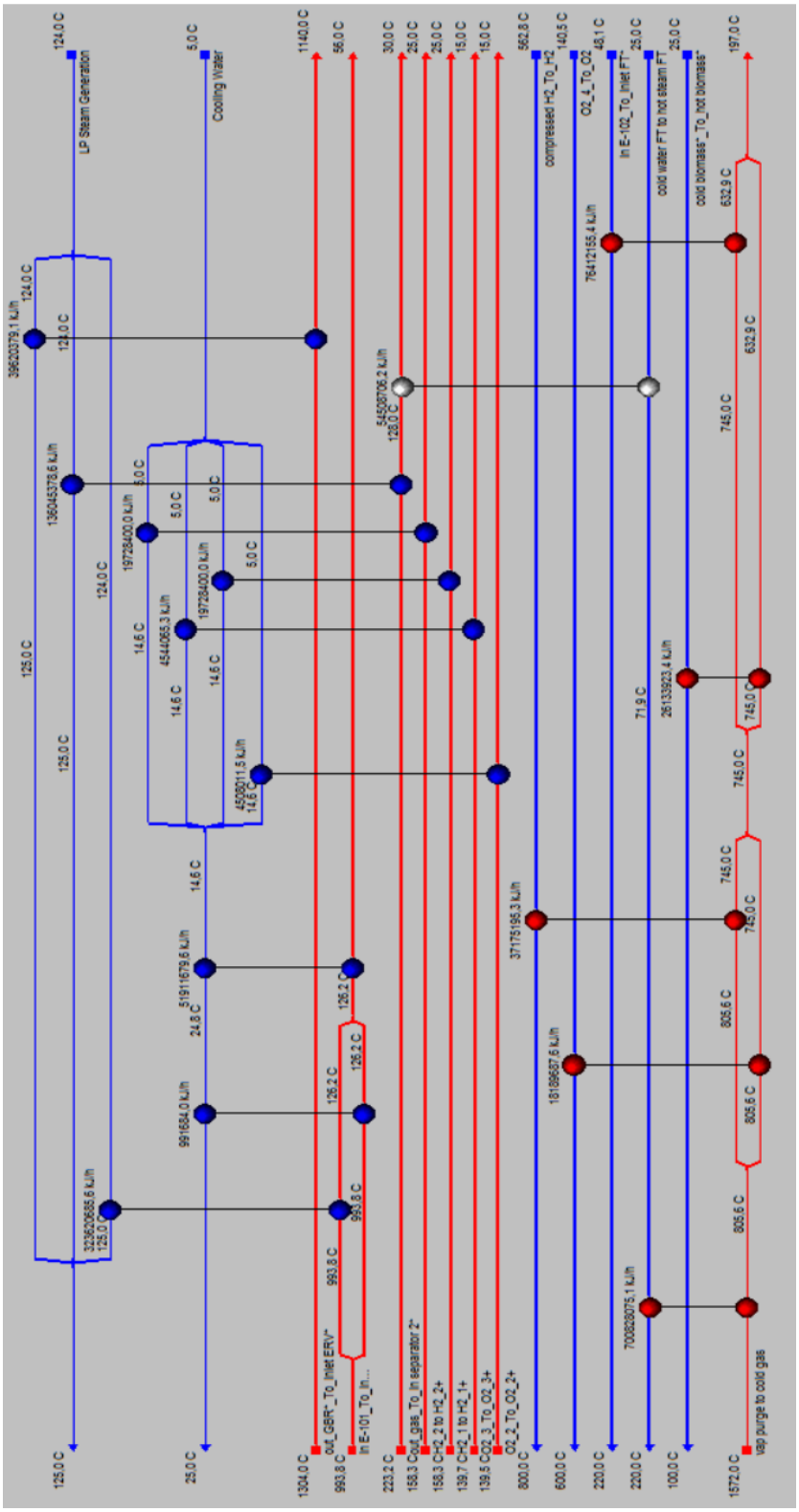

Name		Inlet T [C]	Outlet T [C]	MCp [kJ/C-h]	Enthalpy [kJ/h]	Segm.	HTC [kJ/h-m2-C]	Flowrate [kg/h]	Effective Cp [kJ/kg-C]
compressed H2_To_H2		562,8	800,0	1,567e+005	3,718e+007		196,21	1,041e+004	15,055
in E-101_To_in dryer		993,8	56,0	---	3,765e+008		----	1,382e+005	----
out_GBR*_To_inlet ERV*		1304,0	1140,0	2,416e+005	3,962e+007		416,95	1,276e+005	1,894
in E-102_To_inlet FT*		48,1	220,0	4,445e+005	7,641e+007		456,60	1,663e+005	2,674
O2_3_To_O2_3+		139,7	15,0	3,644e+004	4,544e+006		209,73	3,888e+004	0,937
O2_2_To_O2_2+		139,5	15,0	3,621e+004	4,508e+006		120,04	3,888e+004	0,931
O2_4_To_O2		140,5	600,0	3,959e+004	1,819e+007		226,58	3,888e+004	1,018
out_gas_To_in separator 2*		223,2	30,0	---	1,906e+008		----	1,297e+005	----
cold biomass*_To_hot biom		25,0	100,0	3,485e+005	2,613e+007		720,00	8,333e+004	4,182
H2_1 to H2_1+		158,3	25,0	1,480e+005	1,973e+007		196,21	1,041e+004	14,217
H2_2 to H2_2+		158,3	25,0	1,480e+005	1,973e+007		196,21	1,041e+004	14,217
cold water FT to hot steam F		25,0	220,0	---	7,553e+008		----	2,660e+005	----

Table 62: Process streams of the heat integration for the case 4

Streams	**HX in flowsheet**	**Q (KW)**
Compressed H2 / H2	E-105	$2{,}734.10^{4}$
In E-101 / in dryer	E-101	$1{,}045.10^{5}$
Out GBR / inlet ERV	E-100	$1{,}099.10^{4}$
In E-102 / inlet FT	E-102	$2{,}122.10^{4}$
O2_3 / O2_3+	E-106	$1{,}262.10^{3}$
O2_2 / O2_2+	E-104	$1{,}252.10^{3}$
O2_4 / O2	E-107	$1{,}716.10^{3}$
Out gas / in separator	E-103	$5{,}297.10^{4}$
Cold biomass / hot biomass	E-109	$7{,}259.10^{3}$
H2_1 / H2_1+	E-110	$5{,}467.10^{3}$
H2_2 / H2_2+	E-111	$5{,}473.10^{3}$
Cold water FT / hot steam	Not simulated	$1{,}37.10^{5}$

Table 63 : Process streams and the associated heat exchanger units (case 4)

Area (m^2)	**Units**	**Shells**	**Heating (KJ/h)**	**Cooling (KJ/h)**	**Operating cost (USD/s)**
$1{,}783.10^{4}$	15	49	$1{,}257.10^{9}$	$6{,}007.10^{8}$	-0.2561

Table 64 : Costing data for the design of the case 4

Heat Exchanger	Load [kJ/h]	Cost Index [Cost]	Area [m2]	Shells	LMTD [C]	Overall U [kJ/h-m2-C]	FFactor	Fouling [C-h-m2/kJ]	Hot Stream	Hot T in [C]	Hot T out [C]	Cold Stream	Cold T in [C]	Cold T out [C]	dT Min Hot [C]	dT Min Cold [C]
E-110	1,360e+00	1,972e+005	769,6	2	29,43	5115,6	0,9920	0,0000	out_gas_To_in separator 2	223,2	128,0	LP Steam Generation	124,0	125,0	98,20	4,000
E-123	4,508e+00	2,180e+005	878,0	2	45,51	119,0	0,9481	0,0000	O2_2_To_O2_2+	139,5	15,0	Cooling Water	5,0	14,6	124,9	10,00
E-115	5,451e+00	2,104e+005	704,9	4	21,13	4449,8	0,8225	0,0000	out_gas_To_in separator 2	128,0	30,0	cold water FT to hot steam FT	25,0	71,9	56,07	5,000
E-111	3,236e+00	8,282e+005	3439	8	145,2	627,0	0,9891	0,0000	in E-101_To_in dryer	993,8	126,2	LP Steam Generation	124,0	125,0	868,8	2,226
E-109	3,962e+00	3,886e+004	88,42	1	1095	409,1	1,0000	0,0000	out_GBR* To_inlet ERV*	1304,0	1140,0	LP Steam Generation	124,0	125,0	1179	1016
E-112	9,917e+00	1,292e+004	4,250	2	384,3	595,4	0,9998	0,0000	in E-101_To_in dryer	993,8	126,2	Cooling Water	24,8	25,0	968,8	101,4
E-114	5,191e+00	1,448e+005	510,5	2	67,02	1685,1	0,9716	0,0000	in E-101_To_in dryer	126,2	56,0	Cooling Water	14,6	24,8	101,4	41,44
E-116	3,718e+00	1,296e+006	5469	12	50,60	154,2	0,8711	0,0000	vap purge to cold gas	805,6	745,0	compressed H2_To_H2	562,8	800,0	5,553	182,2
E-118	7,641e+00	1,252e+005	498,6	1	554,3	279,4	0,9894	0,0000	vap purge to cold gas	745,0	632,9	in E-102_To_inlet FT*	48,1	220,0	525,0	584,8
E-113	7,008e+00	2,946e+005	1123	3	1012	667,7	0,9809	0,0000	vap purge to cold gas	1572,0	805,6	cold water FT to hot steam FT	71,9	220,0	1352	733,6
E-119	2,613e+00	4,595e+004	116,3	1	626,2	360,0	0,9964	0,0000	vap purge to cold gas	745,0	632,9	cold biomass* To_hot biomass*	25,0	100,0	645,0	607,9
E-117	1,819e+00	8,595e+004	296,4	1	369,8	172,3	0,9629	0,0000	vap purge to cold gas	805,6	745,0	O2_4_To_O2	140,5	600,0	205,6	604,5
E-121	4,544e+00	1,445e+005	509,3	2	45,56	206,5	0,9482	0,0000	O2_3_To_O2_3+	139,7	15,0	Cooling Water	5,0	14,6	125,1	10,00
E-122	1,973e+00	4,172e+005	1710	4	62,74	193,4	0,9511	0,0000	H2_1 to H2_1+	158,3	25,0	Cooling Water	5,0	14,6	143,7	20,00
E-120	1,973e+00	4,172e+005	1710	4	62,74	193,4	0,9511	0,0000	H2_2 to H2_2+	158,3	25,0	Cooling Water	5,0	14,6	143,7	20,00

Table 65 : Data of the heat integration for the case 4

K Costing data for the factorial method (29)

Equipment	Units for size, S	S_{lower}	S_{upper}	a	b	n	Note
Agitators & mixers							
Propeller	driver power, kW	5.0	75	15,000	990	1.05	
Spiral ribbon mixer	driver power, kW	5.0	35	27,000	110	2.0	
Static mixer	L/s	1.0	50	500	1030	0.4	
Boilers							
Packaged, 15 to 40 bar	kg/h steam	5000	200,000	106,000	8.7	1.0	
Field erected, 10 to 70 bar	kg/h steam	20,000	800,000	110,000	45	0.9	
Centrifuges							
High-speed disk	diameter, m	0.26	0.49	50,000	423,000	0.7	
Atmospheric suspended basket	power, kW	2.0	20	57,000	660	1.5	
Compressors							
Blower	m^3/h	200	5000	3800	49	0.8	
Centrifugal	driver power, kW	75	30,000	490,000	16,800	0.6	
Reciprocating	driver power, kW	93	16,800	220,000	2300	0.75	
Conveyors							
Belt, 0.5 m wide	length, m	10	500	36,000	640	1.0	
Belt, 1.0 m wide	length, m	10	500	40,000	1160	1.0	
Bucket elevator, 0.5 m bucket	height, m	10	30	15,000	2300	1.0	
Crushers							
Reversible hammer mill	t/h	30	400	60,000	640	1.0	
Pulverisers	kg/h	200	4000	14,000	590	0.5	
Crystallizers							
Scraped surface crystallizer	length, m	7	280	8400	11,300	0.8	
Distillation columns See pressure vessels, packing and trays							
Dryers							
Direct contact rotary	area, m^2	11	180	13,000	9100	0.9	1
Atmospheric tray batch	area, m^2	3.0	20	8700	6800	0.5	2
Spray dryer	evap. rate, kg/h	400	4,000	350,000	1900	0.7	
Evaporators							
Vertical tube	area, m^2	11	640	280	30,500	0.55	
Agitated falling film	area, m^2	0.5	12	75,000	56,000	0.75	
Exchangers							
U-tube shell and tube	area, m^2	10	1000	24,000	46	1.2	
Double pipe	area, m^2	1.0	80	1600	2100	1.0	
Thermosyphon reboiler	area, m^2	10	500	26,000	104	1.1	
U-tube kettle reboiler	area, m^2	10	500	25,000	340	0.9	
Plate and frame	area, m^2	1.0	500	1350	180	0.95	3
Filters							
Plate and frame	capacity, m^3	0.4	1.4	110,000	77,000	0.5	
Vacuum drum	area, m^2	10	180	−63,000	80,000	0.3	
Furnaces							
Cylindrical	duty, MW	0.2	60	68,500	93,000	0.8	
Box	duty, MW	30	120	37,000	95,000	0.8	

Equipment	Units for size, S	S_{lower}	S_{upper}	a	b	n	Note
Packings							
304 ss Raschig rings	m^3			0	7300	1.0	
Ceramic intalox saddles	m^3			0	1800	1.0	
304 ss Pall rings	m^3			0	7700	1.0	
PVC structured packing	m^3			0	500	1.0	
304 ss structured packing	m^3			0	6900	1.0	4
Pressure vessels							
Vertical, cs	shell mass, kg	160	250,000	10,000	29	0.85	5
Horizontal, cs	shell mass, kg	160	50,000	8800	27	0.85	
Vertical, 304 ss	shell mass, kg	120	250,000	15,000	68	0.85	5
Horizontal, 304 ss	shell mass, kg	120	50,000	11,000	63	0.85	
Pumps and drivers							
Single-stage centrifugal	flow, L/s	0.2	126	6900	206	0.9	
Explosion proof motor	power, kW	1.0	2500	-950	1770	0.6	
Condensing steam turbine	power, kW	100	20,000	-12,000	1630	0.75	
Reactors							
Jacketed, agitated	volume, m^3	0.5	100	53,000	28,000	0.8	3
Jacketed, agitated, glass lined	volume, m^3	0.5	25	11,000	76,000	0.4	
Tanks							
Floating roof	capacity, m^3	100	10,000	97,000	2800	0.65	
Cone roof	capacity, m^3	10	4000	5000	1400	0.7	
Trays							
Sieve trays	diameter, m	0.5	5.0	110	380	1.8	6
Valve trays	diameter, m	0.5	5.0	180	340	1.9	6
Bubble cap trays	diameter, m	0.5	5.0	290	550	1.9	6
Utilities							
Cooling tower & pumps	flow, L/s	100	10,000	150,000	1300	0.9	7
Packaged mechanical refrigerator	evaporator duty, kW	50	1500	21,000	3100	0.9	
Water ion exchange plant	flow, m^3/h	1	50	12,000	5400	0.75	

Notes

1. Direct heated.
2. Gas fired.
3. Type 304 stainless steel.
4. With surface area 350 m^2/m^3.
5. Not including heads, ports, brackets, internals, etc. (see Chapter 13 for how to calculate wall thickness).
6. Cost per tray, based on a stack of 30 trays.
7. Field assembly.
8. All costs are U.S. Gulf Coast basis, Jan. 2007 (CE index (CEPCI) = 509.7, NF refinery inflation index = 2059.1).

Table 66 : Purchased equipment cost for common plant equipment

Item	Process type Fluids	Fluids – Solids	Solids
Major equipment, total purchase cost	C_e	C_e	C_e
f_{er} Equipment erection	0.3	0.5	0.6
f_p Piping	0.8	0.6	0.2
f_i Instrumentation and control	0.3	0.3	0.2
f_{el} Electrical	0.2	0.2	0.15
f_c Civil	0.3	0.3	0.2
f_s Structures and buildings	0.2	0.2	0.1
f_l Lagging and paint	0.1	0.1	0.05
ISBL cost, $C = \Sigma C_e \times$	3.3	3.2	2.5
Offsites (OS)	0.3	0.4	0.4
Design and Engineering (D&E)	0.3	0.25	0.2
Contingency (X)	0.1	0.1	0.1
Total fixed capital cost $C_{FC} = C\,(1 + \text{OS})(1 + \text{D\&E} + \text{X})$			
$= C \times$	1.82	1.89	1.82
$= \Sigma C_e \times$	6.00	6.05	4.55

Table 67 : Typical factors for estimation of project fixed capital cost

T (°F)	Smax [ksi]
100	20
300	15
500	12.9
700	11.7
900	10.8
Trend curve for x=T(°C) and y=Smax(KPa)	y = -25007ln(x) + 228565 R² = 0,9998

Table 68 : Maximal allowable stress (Ksi) at different temperature (°F) for 304 stainless steel (29) (p 1001)

L Abacus of scrubber diameter in function of the capacity and the operating pressure (63)

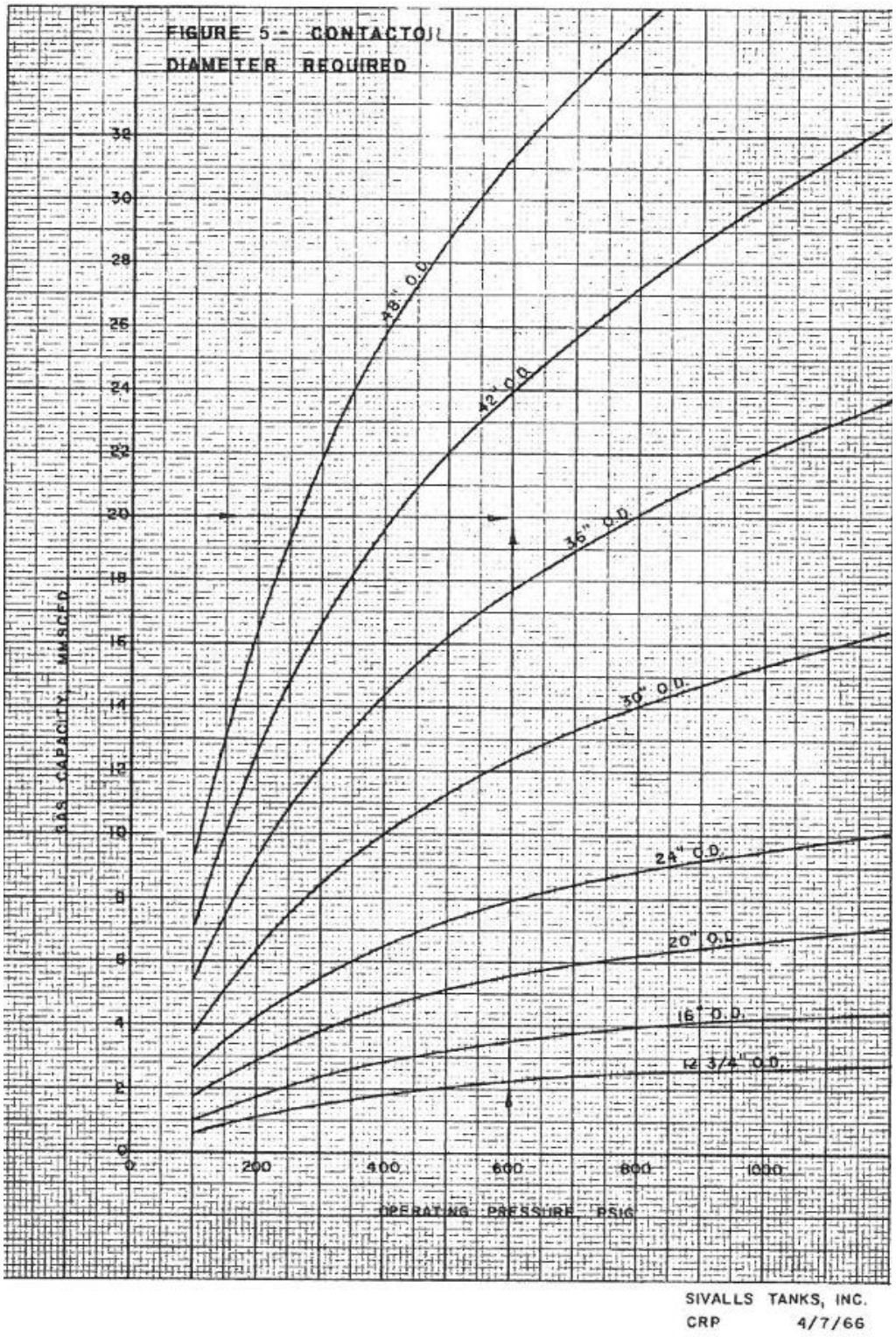

M Data from Statoil for Air Separation Unit

1. Air Separation Unit (ASU)

- Capacity : 3800 MTPD (Metric Ton Per Day)
- Power consumption : 0.40 kWh/kg oxygen produced
- Cooling duty : 0.40 kWh/kg oxygen produced
- Installed cost : ~ US$130 million Cost basis year: 2005

Jostein Sogge
Specialist Process Technology Downstream Gas processing & LNG
UNC NVC GTL
Statoil ASA

Mobile: +47 99163113
Email: jso@statoil.com

Visitor address: Arkitekt Ebbells veg 10, Rotvoll, Norway
Incorporation number: NO 923 609 016 MVA
www.statoil.com

N E-mail from AspenTech Support

From: AES Support [mailto:AES.Support@aspentech.com]
Sent: Wednesday, May 18, 2016 2:22 PM
To: Magne Hillestad
Subject: [1576066] Calculation of anualized capital cost

Hello Magne,

Thank you for contacting AspenTech Support. I am the Technical Support Consultant who will be the primary contact for this incident.

Yes, the query you have reported is an known issue. We have corrected the cost equation in a coming version V9 where the equation (2.3) is used. Many thanks for highlighting this issue. I'll keep you updated once the version is released.
Regards,
Jing
Jing Liu
||| Technical Support Consultant
Aspen Technology, Inc. ||| +44 (0)1189226555 ||| fax: 1-781-564-5100 ||| www.aspentech.com

Easily Monitor and Update this Incident Through Our Web Site

You can view this incident and send us real-time updates at: http://support.aspentech.com/webteamasp/Incident.asp?area=CORP&ID=1576066

If you are not satisfied with this support experience you may contact our regional Support Managers at
http://support.aspentech.com/SupportPublic/SupportManagers.html